WSRC-TR-2003-00126, Rev. 0

Keywords: DWPF, Sludge Batch 3, Coal, Oxalate, Formate, Nitrate, Oxidation, Reduction

Retention: Permanent

TTR No.: HLW/DWPF/TTR-02-0017

ELECTRON EQUIVALENTS MODEL FOR CONTROLLING REDUCTION-OXIDATION (REDOX) EQUILIBRIUM DURING HIGH LEVEL WASTE (HLW) VITRIFICATION

C. M. Jantzen
J. R. Zamecnik
D.C. Koopman
C.C. Herman
J. B. Pickett*

Publication Date: May 9, 2003

Approved by:

E.W. Holtzscheiter, Research Manager
Immobilization Technology Section

Westinghouse Savannah River Company
Savannah River Site
Aiken, SC 29808

Savannah River Technology Center
SRTC
We Put Science to Work

PREPARED FOR THE U.S. DEPARTMENT OF ENERGY UNDER CONTRACT NO. DE-AC09-96SR18500

* Retired from Westinghouse Savannah River Co.

DISCLAIMER

WSRC-TR-2003-00126, Rev. 0

Keywords: DWPF, Sludge Batch 3, Coal, Oxalate, Formate, Nitrate, Oxidation, Reduction

Retention: Permanent

TTR No.: HLW/DWPF/TTR-02-0017

ELECTRON EQUIVALENTS MODEL FOR CONTROLLING REDUCTION-OXIDATION (REDOX) EQUILIBRIUM DURING HIGH LEVEL WASTE (HLW) VITRIFICATION

C. M. Jantzen
J. R. Zamecnik
D.C. Koopman
C.C. Herman
J. B. Pickett*

Publication Date: May 9, 2003

Approved by:

E.W. Holtzscheiter, Research Manager
Immobilization Technology Section

Westinghouse Savannah River Company
Savannah River Site
Aiken, SC 29808

Savannah River Technology Center
SRTC
We Put Science to Work

PREPARED FOR THE U.S. DEPARTMENT OF ENERGY UNDER CONTRACT NO. DE-AC09-96SR18500

* Retired from Westinghouse Savannah River Co.

Approvals

C. M. Jantzen, Author, Immobilization Technology Section	Date
D. K. Peeler, Technical Reviewer, Immobilization Technology Section	Date
A. D. Cozzi, Technical Reviewer, Immobilization Technology Section	Date
M. A. Rios-Armstrong, Reviewer, DWPF Process Engineering	Date
T. B. Edwards, Design Check, Statistical Consulting	Date
J. E. Occhipinti, Manager, DWPF Process Engineering	Date
S. L. Marra, Manager, Immobilization Technology Section	Date
E. W. Holtzscheiter, Manager, Immobilization Technology Section	Date

EXECUTIVE SUMMARY

High-level nuclear waste is being immobilized at the Savannah River Site (SRS) by vitrification into borosilicate glass at the Defense Waste Processing Facility (DWPF). Control of the REDuction/OXidation (REDOX) equilibrium in the DWPF melter is critical for processing high level liquid wastes. Based upon the development of an electomotive force (EMF) series for DWPF glasses and melter experience at Pacific Northwest National Laboratory, an acceptable iron REDOX ratio was defined for the DWPF melts as $0.09 \le Fe^{2+}/\Sigma Fe \le 0.33$. Controlling the DWPF melter at a REDuction/OXidation (REDOX) equilibrium of $Fe^{+2}/\Sigma Fe \le 0.33$ prevents the potential for conversion of $NiO \rightarrow Ni°$, $RuO_2 \rightarrow Ru°$, and $2SO_4^{=} \rightarrow S_2 + 4O_2$ during vitrification; such that metallic and sulfide rich species do not form and accumulate on the floor of the melter. Control of foaming due to deoxygenation of manganic species is achieved by having 66-100% of the MnO_2 or Mn_2O_3 species converted to MnO during SRAT refluxing. At the lower redox limit of $Fe^{+2}/\Sigma Fe \sim 0.09$ about 99% of the Mn^{+4}/Mn^{+3} is converted to Mn^{+2}. Therefore, the lower REDOX limit eliminates melter foaming from deoxygenation.

Organic and nitrate concentrations in the DWPF melter feed are the major parameters influencing melt REDOX. Organics such as formates act as reductants while nitrates, nitrites, and manganic (Mn^{+4} and Mn^{+3}) species act as oxidants.

Sludge from Tank 7 is being processed for inclusion in the next DWPF Sludge Batch (SB-3). Tank 7 contains several organic components that are considered non-typical of DWPF sludge to date, e.g. oxalates and coal. During melting, the REDOX of the melt pool cannot be measured. Therefore, the $Fe^{+2}/\Sigma Fe$ ratio in the glass poured from the melter must be related to melter feed organic and oxidant concentrations to ensure production of a high quality glass without impacting production rate (e.g., from foaming) or melter life (e.g., from metal formation and accumulation).

In previous REDOX studies, attempts were made to control melt REDOX using models that only included formate and nitrate concentrations in the DWPF melter feeds. In this study, the effects of all the organics (formate, oxalate, and coal) were investigated as well as the role of the oxidizers (nitrates and manganic species). A REDOX model was developed that generalized the product and reactant species from the 4-stages of the DWPF cold cap reaction model so that the impact on melt REDOX could be represented by REDuction/OXidation equations such as the following for organics and oxidizers:

$$\underset{feed}{Fe_2O_3} + 5\underset{feed}{SiO_2} + 6\underset{organic}{NaCOOH} + 2\underset{oxidizer}{NaNO_3} \rightarrow \underset{glass}{Fe_2SiO_4} + 6\underset{offgas}{CO_2} + \underset{offgas}{N_2} + 4\underset{glass}{Na_2SiO_3} + 3\underset{offgas}{H_2O}$$

The generalized cold cap reaction assumes that Fe^{3+} enters the melter as Fe_2O_3 and that $COOH^-$ and NO_3^- both enter as properly formated and nitrated sodium compounds. The formated and nitrated salts react with glass formers such as SiO_2 to form Fe^{+2} and

Na_2SiO_3 components in the glass and liberate CO_2, N_2 and H_2O vapors to the melter plenum. Similar reactions can be written for the remaining organics, oxalate and coal.

Chemical reduction is defined as making an atom or molecule less positive by electron transfer, while oxidation is defined as making an atom or molecule more positive by electron transfer. Therefore, the number of electrons transferred for each REDuction/OXidation reaction can be summed and an Electron Equivalents term for each organic and oxidant species defined. In the REDuction/OXidation equilibrium between nitrate and formate salts, one mole of nitrate gains 5 electrons when it is reduced to N_2, while one mole of carbon in formate loses 2 electrons during oxidation to CO_2. Thus the Electron Equivalents term for formate is 2 while the term for nitrate is 5. In a similar manner, one mole of carbon in coal loses 4 electrons during oxidation to CO_2 so its electron equivalent term is 4. For sugar, one mole of carbon in sugar loses 4 electrons during oxidation to CO_2. For manganese, one mole of Mn^{+4} gains 2 electrons during reduction to Mn^{+2}. The pertinent electron equivalent terms are 4 for sugar and 2 for manganese.

Theoretically, one mole of carbon in oxalate should lose 1 mole of electrons during oxidation to CO_2 or one mole of oxalate should transfer 2 moles of electrons during oxidation to CO_2 since there are 2 moles of carbon in one mole of oxalate. Therefore, the Electron Equivalents term for oxalate is expected to be 2. However, REDOX modeling indicated that oxalate was twice as effective a reductant as would be anticipated from the simple electron transfer model applied to the other organic species, e.g. the Electron Equivalents term should be 4. Data from SRAT processing indicated that 8-37% of the oxalate salts convert to oxalic acid, which then disproportionates to formic acid and CO_2. Therefore, it was assumed that disproportionation also occurs in the cold cap when the liquid slurry impacts the melt pool surface. Since only half of the oxalate is acting as a reductant, the reduction potential of oxalate is doubled. Therefore, the number of electrons gained during reduction or lost during oxidation are the following:

- $[NO_3]$ = +5
- [Mn] = +2
- $[C]_{formate}$ = -2
- $[C]_{coal}$ = -4
- $[C]_{oxalate}$ = -4
- $[C]_{sugar}$ = -4

The water content of a melter feed alters the species concentrations of the [reductants] and [oxidants] and can influence the equilibrium oxygen fugacity (f_{O_2}) in a melter during vitrification. Since the effects of water on oxygen fugacity are small relative to the impact of dilution on feed concentrations, the molar concentrations were transformed to a 45% solids basis as was done in previous REDOX modeling.

The overall relationship between the REDOX ratio and the Electron Equivalents, ξ, can then be expressed as:

$$\frac{Fe^{2+}}{\Sigma Fe} = f\left[\left(2[F]+4[C]+4[\mathrm{O_T}]-5[N]-2[Mn]\right)\frac{45}{T}\right] = f[\xi]$$

where f = indicates a function
[F] = formate (mol/kg feed)
[C] = coal (carbon) (mol/kg feed)
[O_T] = $oxalate_{Total}$ (soluble and insoluble) (mol/kg feed)
[N] = nitrate + nitrite (mol/kg feed)
[Mn] = manganese (mol/kg feed)
T = total solids (wt%)

and ξ (mol/kg feed at 45 wt% solids) = $\left(2[F]+4[C]+4[\mathrm{O_T}]-5[N]-2[Mn]\right)\frac{45}{T}$

In the presence of sugar, [S], the Electron Equivalents term becomes

ξ (mol/kg feed at 45 wt% solids) = $\left(2[F]+4[C]+4[S]+4[\mathrm{O_T}]-5[N]-2[Mn]\right)\frac{45}{T}$

Note that the Electron Equivalents model has an {[F]–2.5[N]} dependency in the absence of coal, total oxalate, sugar, and manganese.

The REDOX data generated in the current study were pooled with the REDOX data used to generate the DWPF {[F]-3[N]} model. This was accomplished after the archival data for the manganese concentrations were determined. The pooled model data were fit as a linear function of ξ:

$\frac{Fe^{2+}}{\Sigma Fe} = b + m\xi$ or $\frac{Fe^{2+}}{\Sigma Fe} = 0.1942 + 0.1910\xi$ with an $R^2 = 0.81$ and a RMSE = 0.069.

The fit of the Electron Equivalents model for the 120 data points is about the same as the DWPF {[F]-3[N]} and {[F]- [N]} REDOX models which had R^2 values of 0.88 and 0.80, respectively.

The $\frac{Fe^{2+}}{\Sigma Fe}$ predictions from the Electron Equivalents model given above were fitted to measured REDOX data generated from the DWPF melter from SME Batch 224, to data generated by the SRTC mini-melter, and to data from the SRTC Slurry-fed Melt Rate Furnace (SMRF). All the data from these melters fell within the 95% confidence bands of the Electron Equivalents model. Additional validation data from SRS pilot scale melter, Pacific Northwest National Laboratory testing, and West Valley Nuclear Services testing agreed with the Electron Equivalents model better than the {[F]-3[N]} REDOX model.

TABLE OF CONTENTS

LIST OF TABLES

LIST OF FIGURES

LIST OF ACRONYMS

ACT-C	Activated Carbon
ACTL	Aiken County Technical Laboratory
CC	Coarse Coal
DSC	Differential Scanning Calorimetry
DWPF	Defense Waste Processing Facility
EDAX	Energy Dispersive Analysis by X-ray
EE	Electron Equivalents
EMF	ElectroMotive Force
HAN	Hydroxyl Amine Nitrate
HLW	High Level Waste
HWVP	Hanford Waste Vitrification Project
IC	Ion Chromatography
ICP-ES	Inductively Coupled Plasma – Emission Spectroscopy
IDMS	Integrated DWPF Melter System
ML	Mobile Laboratory
OLS	Ordinary Least Squares
PHEF	Precipitate Hydrolysis Experimental Facility
PNNL	Pacific Northwest National Laboratory
REDOX	REDuction/OXidation
RMSE	Root Mean Square Error
SB-1	Sludge Batch -1
SB-2	Sludge Batch-2
SB-3	Sludge Batch-3
SCF	Shielded Cell Facility
SEM	Scanning Electron Microscopy
SGM	Scale Glass Melter
SME	Slurry Mix Evaporator
SMRF	Slurry-Fed Melt Rate Furnace
SRAT	Sludge Receipt and Adjustment Tank
SRS	Savannah River Site
SRTC	Savannah River Technology Center
TPB	Tetraphenylborate
WGSR	Water Gas Shift Reaction
WSRC	Westinghouse Savannah River Co.
WVNS	West Valley Nuclear Services
XRD	X-ray Diffraction

This page intentionally left blank.

ELECTRON EQUIVALENTS MODEL FOR CONTROLLING REDUCTION-OXIDATION (REDOX) EQUILIBRIUM DURING HIGH LEVEL WASTE (HLW) VITRIFICATION

C. M. Jantzen, J. R. Zamecnik, D.C. Koopman, C.C. Herman, and J. B. Pickett*

Westinghouse Savannah River Company
Savannah River Site
Aiken, South Carolina 29808

1.0 INTRODUCTION

1.1 DWPF PROCESS CONSTRAINTS

High-level nuclear waste is being immobilized at the Savannah River Site (SRS) by vitrification into borosilicate glass at the Defense Waste Processing Facility (DWPF). In the DWPF Sludge Receipt and Adjustment Tank (SRAT), the insoluble fraction of the waste sludge is refluxed with acid [1] for the following reasons:

- control potential foaming by gaseous species in the melter by:
  - converting NO_3 (entering as nitrate species in the feed) to NO_2, NO, and/or N_2,
  - converting carbonates in the feed to CO_2, and
  - converting >66% of the oxidized Mn^{+4} or Mn^{+3} present as MnO_2, Mn_2O_3, and Mn_3O_4 and/or hydrous complexes in the feed to MnO, liberating O_2;
- steam strip mercury for subsequent removal, $HgO \rightarrow Hg^0$; and
- improve slurry rheology by neutralizing excess hyrdroxide (OH^-) in the feed.

The SRAT product is then fed to the DWPF Slurry Mix Evaporator (SME), where a borosilicate glass frit slurry is added to produce the melter feed slurry. The melter feed slurry is typically concentrated to 45-50 wt% total solids in the SME and then fed to the DWPF joule-heated melter where it is fused into glass (vitrified) at 1150°C.

Prior to 1982, the DWPF reference flowsheet prescribed that 28 wt% sludge oxides (on a dry calcine basis) from the SRAT be combined with 72 wt% frit oxides in the SME. Formic acid was the only acid added during SRAT processing. Most glasses produced from this "sludge-only" and "formic acid-only" flowsheet were highly reduced, e.g. $>>0.33\ Fe^{+2}/\Sigma Fe$. Any carbon containing species in melter feeds (coal, oxalate, formic acid, sugar) cause reduction of transition metal species such as Fe^{+3} and Mn^{+4} at the elevated melter temperatures [2,3,4]. The interaction of the carbon with the transition metal species in the waste feed occurs primarily in the melter cold cap [5,6].

Excess reduction of transition metal species in the melter can cause the following to occur:

- liberation of oxygen which can cause foaming from decomposition of Mn^{+4} or Mn^{+3} species if they were not previously reduced during SRAT processing
- reduction of metallic species such as $NiO \rightarrow Ni°$ and $RuO_2 \rightarrow Ru°$ which may fall to the melter floor and cause shorting of electrical pathways in the melt and accumulations which may hinder glass pouring
- reduction of sulfate ($SO_4^{=}$) to sulfide ($S^{=}$) which can complex with Ni° and/or Fe° to form metal sulfides which can fall to the melter floor and cause shorting of electrical pathways and/or hinder glass pouring
- reduced glasses which can be less durable than their oxidized equivalents [7].

Controlling the DWPF melter at a REDuction/OXidation (REDOX) equilibrium of $Fe^{+2}/\Sigma Fe \leq 0.33$ [2, 8] prevents the potential for conversion of $NiO \rightarrow Ni°$, $RuO_2 \rightarrow Ru°$, and $2SO_4^{=} \rightarrow S_2 + 4O_2$ during vitrification. Control of foaming due to deoxygenation of manganic species is achieved by having 66-100% of the MnO_2 or Mn_2O_3 species converted to MnO [9] during SRAT refluxing. At the lower redox limit of $Fe^{+2}/\Sigma Fe \sim 0.09$ about 99% of the Mn^{+3} is converted to Mn^{+2} [2, 8]. Therefore, the lower REDOX limit eliminates melter foaming from deoxygenation.

While nitric acid can be used to control feed rheology and destroy carbonates, only a reducing acid such as formic acid can convert $HgO \rightarrow Hg^0$ when it is present in a feed and convert $MnO_2 \rightarrow MnO + ½\ O_2$ in the SRAT. Currently, the REDOX equilibrium in DWPF is controlled by balancing formic acid (a reductant) and nitric acid (an oxidizer) additions to the SRAT.

1.2 HISTORICAL CHANGES IN DWPF FLOWSHEET REDUCTANTS AND OXIDANTS

In late 1982, an in-tank process for the removal of cesium, strontium, and plutonium from the aqueous fraction of the waste was developed [10]. The separated radioactive components could then be combined with high level waste (HLW) sludge for processing in DWPF while the decontaminated aqueous fraction could be disposed of in Saltstone. In the SRS Tank Farm, sodium tetraphenylborate (TPB) was added to precipitate out cesium, and sodium titanate was added to adsorb residual strontium and plutonium. During Salt Cell processing, additional formic acid and copper (as a catalyst) were added during hydrolysis of the TPB slurry so that TPB (and phenylboric acid) would hydrolyze completely to mitigate the production of high-boiling organic compounds and tars [11]. This flowsheet change caused the melter feeds to be even more reducing ($Fe^{+2}/\Sigma Fe$ of 0.7 to 0.8) due to the presence of the high-boiling organics and tars.

In 1986 it was decided that sodium nitrite would be added to the precipitate slurry in the SRS Tank Farm to inhibit corrosion of the waste processing and storage vessels [12] despite the recognition that the required inhibitor concentration would hinder TPB

hydrolysis chemistry in DWPF. Late washing of the precipitate feed (i.e., washing the feed prior to entering DWPF) to remove the added nitrite and the addition of hydroxylamine nitrate (HAN) to reduce nitrite to nitrous oxide (as well as mitigate formation of high-boiling organic compounds and tars) were seen as likely solutions. During pilot-scale testing in the Precipitate Hydrolysis Experimental Facility (PHEF) the results of the HAN process were shown to be unsatisfactory for long-term DWPF use due to insufficient mitigation of high-boiling organic compounds and introduction of excessive nitrate, a melt oxidizer. Most glasses produced from these "coupled" flowsheets were highly oxidized due to the high nitrite and nitrate concentrations relative to the amount of formate and the other reductants in the “coupled” flowsheet.

During 1991, it was determined that late washing of the precipitate feed to remove nitrite (and, in turn, eliminating the need for HAN addition) was a technical solution. However, late washing the precipitate feed to remove nitrite also removed nitrate; this, in addition to the omission of the nitrate produced from HAN, upset the formate/nitrate balance in the DWPF melter feed to the extent that resulting melts would likely be excessively reduced, e.g. $Fe^{+2}/\Sigma Fe > 0.33$. Pilot-scale testing of non-radioactive sludge containing noble metals in the Integrated DWPF Melter System (IDMS), demonstrated that formic acid underwent a catalytic decomposition in the SRAT producing hydrogen gas; this reaction also caused the SRAT slurry to become more basic allowing evolution of ammonia. This ammonia formed ammonium nitrate (i.e., an explosive compound) in the IDMS Process Vessel Vent System. The formation of both hydrogen gas and ammonium nitrate during waste processing led to both flammability and operational issues that had to be resolved with this flowsheet.

A flowsheet calling for the substitution of nitric acid for a portion of the formic acid during SRAT processing reduced the hydrogen evolution. This “nitric acid” flowsheet also reestablished the formate/nitrate (REDOX) balance in the resulting melter feed [13]. Thus to maintain reliable and efficient feed preparation and melter operation, DWPF waste processing requires that both an oxidizing acid (i.e., nitric acid) and a reducing acid (i.e., formic acid) be added in the proper balance.

During the first four years of DWPF operation (1996-2000), e.g. processing of Sludge Batch 1A, nitric acid in excess of that required for waste processing [14, 15] was added to DWPF melter feed to assure nitrite destruction in the SRAT processing cycle. Thus instead of being too reducing, the DWPF feed has been overly oxidizing. This has the potential of promoting foaming in the melter thereby reducing melt and glass production rates [2]. In January 2000, while processing Sludge Batch 1B (SB1B) SRAT Batch 134, the DWPF implemented a more reducing flowsheet in an effort to control REDOX at a target of $Fe^{2+}/\Sigma Fe \sim 0.2$ in order to avoid foaming and improve melt rate. The reduced production rate with oxidized feeds is due, in part, to reduced heat transfer through the foamy layer from excess NO_x produced from nitrate decomposition and excess O_2 from MnO_2 deoxygenation.

1.3 PURPOSE OF THE CURRENT STUDY

The DWPF is currently operating using a sludge-only processing flowsheet, which balances formic acid and nitric acid as reducants and oxidizers, respectively. Since DWPF start-up in 1996, the operating flowsheet has been adjusted for processing of each incoming or existing sludge batch (SB1A, SB1B, and SB2). The next sludge batch, Sludge Batch 3 (SB3), will be primarily Tank 7 sludge mixed with the Sludge Batch 1B (SB1B) heel in Tank 51 and contributions added from Tanks 18 and 19. Sludge Batch 2 (SB2) is currently in Tank 40. The sludge from Tank 7 is expected to contain several components, two of which are carbon containing solid reductants, that are non-typical of DWPF sludge to date.

The possible non-typical components that may be present in SB3 include sand, coal, sodium oxalate, higher levels of noble metals than previously processed, and IE95 zeolite from Tank 19. A maximum of ~81,000 pounds of spent zeolite may be transferred to SB3 [16]. SB3 will also contain Am/Cm feed from F-Area and slurry containing precipitated Pu with Gd from H-Canyon. Scoping studies have been performed by SRTC to assess the effects of sand, coal, the Pu/Gd stream, and the higher levels of noble metals [17,18,19]. A separate study addressed the impacts of zeolite on DWPF waste processing [16]. The current study addresses the interactions of the carbon in the solid reductants, coal and oxalate, with the liquid reductant (formic acid), the liquid oxidizer (nitric acid), and the solid feed oxidizer MnO_2 during DWPF processing. Balancing the solid and liquid reductants and oxidizers ensures that melter feeds are not reduced beyond the REDuction/OXidation (REDOX) equilibrium of 0.33 $Fe^{+2}/\Sigma Fe$. Currently, balancing formic acid (a liquid reductant) and nitric acid (a liquid oxidizer) is the only interaction controlling the REDOX equilibrium in DWPF.

The current study will address the SB3 REDOX issues related to the presence of up to 660,000 pounds (~300 metric tons) of solid sodium oxalate that could be present in Tank 7 [20,21]. In addition, up to ~7,000 pounds of coal may be present in Tank 7, if all of the coal in the K-Area filters had been discharged to this tank [21]. Note that a 1976 analysis of coal in Tank 7 indicated that 72,000 pounds [22] of coal may exist in Tank 7. However, it is believed that the sample analyzed was not representative of the tank contents, e.g. sampling occurred directly under the riser into which the coal filter material had been discharged. In addition, 10,000 pounds of sand from the filters may have been discharged to Tank 7.

2.0 BACKGROUND

2.1 REDOX PROCESS LIMITS

The DWPF melt and glass REDOX equilibria have been well studied. Based on the work of Schreiber[2] and Goldman[3], Jantzen and Plodinec [8] originally defined acceptable REDOX ratios (based on the measured $Fe^{2+}/\Sigma Fe$ ratio) for any DWPF-type melt to be greater than or equal to 0.09 (to prevent foaming via the deoxygenation of MnO_2, Mn_2O_3, and Mn_3O_4 to MnO) and less than or equal to 0.33 (to prevent metallic nickel and nickel sulfide formation). Formate and nitrate concentrations in the melter feed appear to be the major parameters influencing melt REDOX during vitrification. The formate is a reductant while the nitrate is an oxidant. Since the melt REDOX ratio cannot be directly measured during processing,† the melt REDOX ratio has been related to feed reductant (formate) and oxidizer (nitrate) concentrations (which can be measured). Thus the proper balance between reductants and oxidizers ensures production of a high quality glass, free of metal sulfide precipitation, without impacting production rate (e.g., from foaming), melter life (e.g., from metal formation), or glass performance (e.g. from degradation of durability).

2.2 PREVIOUS REDOX MODELING

2.2.1 The {[F]-[N]} Model

To study the effects of feed chemistry on REDOX, previous researchers doped properly* formated batches of simulated DWPF melter feed slurries with varying amounts of formate and nitrate [15, 23, 24, 25, 26]. Triplicate measurements were made of the formate and nitrate concentrations in the melter feed slurries. Many of the slurries were formulated to a target of 45% total solids (by weight) but confirmatory analyses (of the solids or water content) often were not performed.

The melter slurries were vitrified in sealed crucibles, usually in duplicate. Initially melter feed was used to seal the crucibles. This technique did not always adequately seal the crucibles due to crystalline particulates in the sludge fraction of the melter feeds. Later, the crucibles were sealed with a nepheline gel which melted at lower temperatures than the feed to glass conversion so that the crucible sealed before the conversion reactions occurred. Sealed crucibles have been shown to represent the REDOX conditions in scale glass melters whose only source of oxygen is air-inleakage [15]. This will be discussed in more detail in Section 4.8.

---

† Originally the REDOX for a vitrified melter feed sample was to be measured to determine feed acceptability; however, the expense and time necessary for these measurements provided impetus to relate melt REDOX to feed chemistry.

* Properly formated is defined as >66% of the oxidized Mn^{+4} and Mn^{+3} species have been converted to Mn^{+2} species during reflux in the SRAT.

Each sample of vitrified material was prepared and analyzed for reduced (i.e., Fe^{2+}) and total (i.e., ΣFe) iron from which the REDOX ratio was computed [27]. The formate, nitrate, and resulting REDOX information was examined to determine the best possible method of predicting REDOX from feed chemistry as well as the constraints necessary to assure reliable DWPF melter operation.

The early REDOX studies [24,25] suggested that the difference between the normalized molar formate, [F], and nitrate, [N], feed concentrations was an adequate predictor of the REDOX state in a glass:

Equation 1 $Fe^{2+}/\Sigma Fe = -0.8 + 0.87\{[F]-[N]\}$ $R^2 = 0.80$.

During this study, it was shown that at $\{[F]-[N]\}<0.9$ which corresponded to an $Fe^{2+}/\Sigma Fe$ ratio of <0.05, the absolute concentrations of formate and nitrate in the melter feed had no appreciable effect on glass REDOX since the feeds were oxidizer-rich and reductant-poor such that there was no impact on the REDOX ratio. No appreciable impact on glass REDOX causes a plateau to form at $Fe^{2+}/\Sigma Fe$ of ~0 (Figure 1). For overly reduced glasses ($Fe^{2+}/\Sigma Fe \geq 0.6$ and $\{[F]-[N]\}>1.7$) the absolute concentrations of formate and nitrate were shown to have no appreciable effect on glass REDOX. In this overly reduced regime excess reductant had reduced >60% of the ferric iron to ferrous and then began conversion of $NiO \rightarrow Ni°$ and $2SO_4^{=} \rightarrow S_2 + 4O_2$ causing Ni_3S_2 and/or Ni° to form (Figure 1). This causes a second plateau at a $Fe^{2+}/\Sigma Fe$ of ~0.65 (Figure 1). In the range between $Fe^{2+}/\Sigma Fe$~0.05-0.6 or an $\{[F]-[N]\}$ between 0.9 and 1.7, the $Fe^{2+}/\Sigma Fe$ repsonse is linear with respect to $\{[F]-[N]\}$ and Equation 1 was shown to hold (Figure 1).

In 1997, the data used to develop the $\{[F]-[N]\}$ relationship in Equation 1 was revisited because inclusion of any data from the two plateau regions shown in Figure 1 can highly leverage the Ordinary Least Squares (OLS) fit to the data. Hence, glass quality and REDOX measurement criteria were developed to screen the data used for modeling (see discussion in Section 2.2.2). This redefined the population of glasses by excluding those below the $Fe^{+2}/\Sigma Fe$ measurement detection limit of 0.03 and those that precipitated metallic and/or sulfide species. Averaging of formate, nitrate and measured REDOX ratios was used to minimize model error. The OLS fit of the redefined "Model Data" over the $\{[F]-[N]\}$ range between zero and 2.5 (Equation 2) demonstrated that the $\{[F]-[N]\}$ parameter was a less accurate ($R^2 = 0.68$ and an RMSE = 0.109) predictor of waste glass REDOX [15] than had previously been calculated (see Figure 2). The large RMS value indicates that at a given $\{[F]-[N]\}$ there is an associated large scatter in the REDOX response and this can be seen in Figure 1 and Figure 2.

Equation 2 $Fe^{2+}/\Sigma Fe = -0.0257 + 0.31667\{[F]-[N]\}$

In addition, there was no known mechanistic impetus for using the molar difference of the reductants and oxidants for REDOX prediction. This artificially set the relative

oxidation/reduction potentials of nitrate and formate to be equivalent when it was well known that nitric acid is a strong oxidizer and formic acid is a weak reductant.

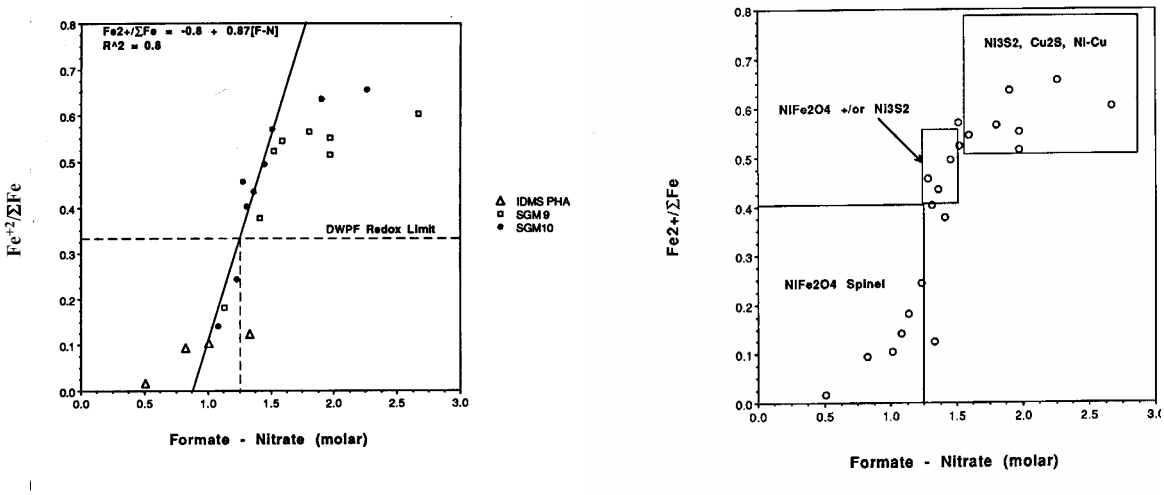

Figure 1. Redox ratio relationship to {[F]-[N]} showing the "S" shaped curvature of the response. Equation 1 holds only for the linear portion of the relationship between $Fe^{2+}/\Sigma Fe \sim 0.05\text{-}0.6$. Note that the $Fe^{2+}/\Sigma Fe$ limits of 0.09 and 0.33 are not derived from this figure but from scale melter experience and Reference 2 as discussed in Section 2.1.

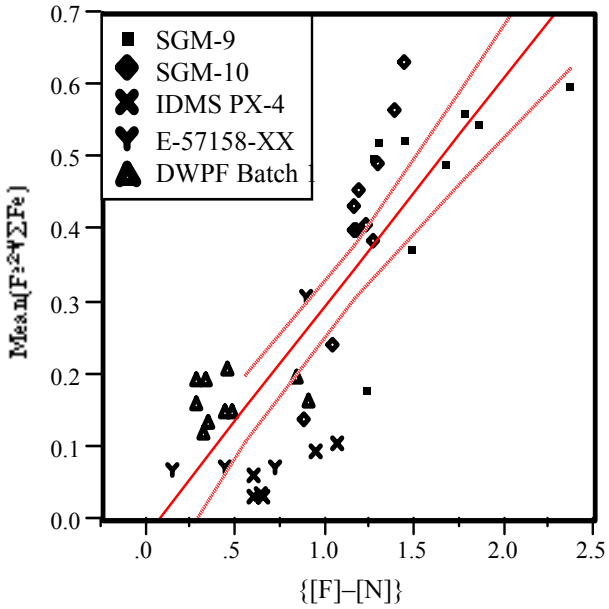

Linear Fit

Fe2+/∑Fe = -0.0257 + 0.31667 {[F]–[N]}

Summary of Fit

RSquare	0.687754
RSquare Adj	0.679537
Root Mean Square Error	0.108973
Mean of Response	0.286587
Observations (or Sum Wgts)	40

Analysis of Variance

Source	DF	Sum of Squares	Mean Square	F Ratio
Model	1	0.9939372	0.993937	83.6988
Error	38	0.4512562	0.011875	**Prob>F**
C Total	39	1.4451934		<.0001

Parameter Estimates

Term	Estimate	Std Error	t Ratio	Prob>|t|
Intercept	-0.025664	0.038233	-0.67	0.5061
{[F]–[N]}	0.3167722	0.034625	9.15	<.0001

Figure 2. Relationship between the iron REDOX ratio (i.e., $Fe^{2+}/\Sigma Fe$) and the difference of mean molar formate [F] and nitrate [N] concentrations as re-determined in the 1997 study [15].

2.2.2 The {[F]-3[N]} Model

In order to generate an improved and mechanistic REDOX model for DWPF the {[F]-[N]} data were screened using the following criteria:

- Glass must be produced from properly formated melter feed material. That is, sufficient formate must be added and the slurry refluxed to ensure that 66-100% of the Mn^{3+} and Mn^{4+} is converted to $Mn(COOH)_2$
- Vitrified material must be visibly black and homogeneous; that is, it must contain no brown discoloration due to metallic copper and/or no crystalline or other metallic material as these species make both reliable REDOX ratio and cation measurements difficult–if not impossible.
- The iron REDOX ratio (i.e., $Fe^{2+}/\Sigma Fe$) is measured using the Baumann colorimetric technique [27] which is identical to the SRTC Mobile Laboratory (ML) Procedure 1.8 [28] and must be greater than or equal to the SRTC measurement detection limit of $Fe^{2+}/\Sigma Fe = 0.03$ [23,24,25,26].
- Both REDOX and feed chemistry measurements (to which the REDOX ratio will be related) must be available for the same sample.
- Measured or as-made total solids information must be available. ("Model Data" samples were either measured for or formulated to be approximately 45% total solids.) Measured total solids is preferred to minimize error.

The redefined data indicated that the relationship between the iron REDOX ratio and molar formate and nitrate concentrations resembled a plane in three-dimensional space (Figure 3). The data given in Appendix A and shown in Figure 3 were regressed using the following model form for describing a plane in three-dimensional space:

Equation 3 $$Fe^{2+}/\Sigma Fe = a[F] + b[N] + c + \varepsilon$$

where ε is the error term resulting from the least-squares regression (since estimated parameters were used for the iron REDOX ratio prediction) and c is the intercept.

The effect of the water content of the slurry feed on REDOX was not assessed in the 1997 study since the bulk of the data used for modeling was constituted to be 45% total solids but not measured. The water content of a melter feed alters the [F] and [N] concentrations and can influence the equilibrium oxygen fugacity (f_{O_2}) in a melter during vitrification [4, 6, 29, 30].[f] Since the effects of water on oxygen fugacity are

[f] Examples are the water gas shift reaction (WGSR) $CO+H_2O \rightarrow CO_2 + H_2$ discussed in Reference 6 and the known $2FeO + H_2O \rightarrow Fe_2O_3 + H_2$ reaction in silicate melts discussed in Reference 30 since H_2O acts as an oxidizer in these and other reactions (see Reference 29).

small relative to the impact of dilution on feed concentrations, the molar formate and nitrate in the {[F]-3[N]} REDOX prediction (i.e., Equation 4 and Equation 5) are transformed to a 45% solids basis. That is, the prediction model for REDOX takes the form:

Equation 4

$$\frac{Fe^{2+}}{\Sigma Fe} = a\left(\frac{45}{\phi}\right)[COOH] + b\left(\frac{45}{\phi}\right)[NO_3] + c = 45a\left(\frac{[COOH]}{\phi}\right) + 45b\left(\frac{[NO_3]}{\phi}\right) + c,$$

where ϕ is the weight percent solids of the slurry being modeled [15].

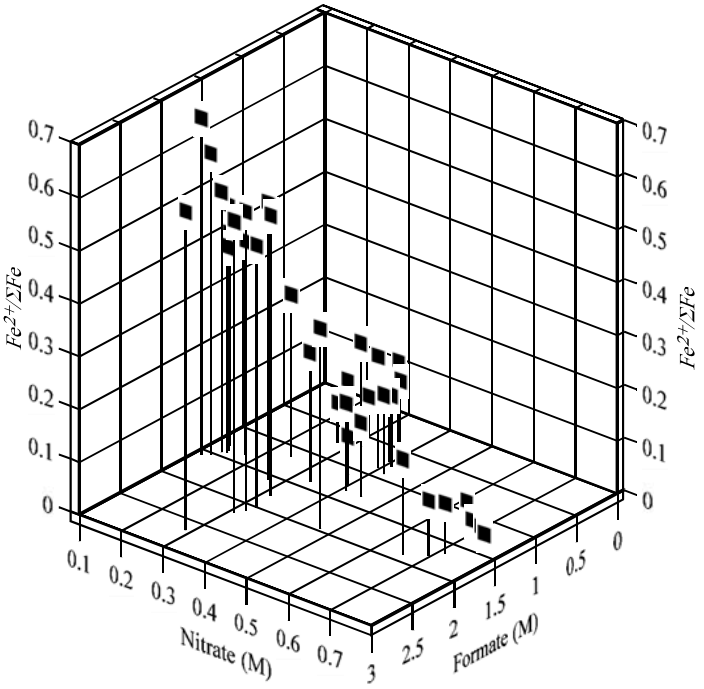

Figure 3. Iron REDOX Ratio (i.e., $Fe^{2+}/\Sigma Fe$) as a Function of Molar Formate, [F], and Nitrate, [N].

The regression of the redefined data showed that there was an {[F]-3[N]} relationship between the feed reductants and oxidants and the REDOX ratio of the glass:

Equation 5

$$\frac{Fe^{2+}}{\Sigma Fe} = 0.217 + 0.253\left(\frac{45}{\phi}\right)[COOH] - 0.739\left(\frac{45}{\phi}\right)[NO_3]$$

The R^2 value of Equation 5 is extremely high ~88% based on 40 data observations with a smaller RMSE (= 0.065) than the {[F]-[N]} correlation. A smaller RMSE means that there is a higher degree of accuracy in the predicted REDOX ratio. Interaction effects (e.g., the cross product of [F] and [N]) and higher order effects (e.g., $[N]^2$ or $[F]^2$) were also examined in the 1997 study but these parameters were shown to not be significant. Thus the {[F]-3[N]} model, based solely on the molar formate and nitrate concentrations in the DWPF feeds, was implemented in DWPF in January 2000 while processing Sludge Batch 1B (SB1B, SRAT Batch 134). The {[F]-3[N]} REDOX model was used to control REDOX at a target $Fe^{2+}/\Sigma Fe \sim 0.2$ in an effort to improve melt rate by reducing the foaming caused by the excess nitric acid being added.

The OLS correlation shown in Equation 5 assumed that melter feeds were properly formated and refluxed to ensure that 66-100% of the Mn^{3+} and Mn^{4+} were converted to Mn^{+2} as $Mn(COOH)_2$. Equation 5 is applicable over molar formate and nitrate concentrations ranging from $0.46 \leq [F] \leq 2.66$ and $0.11 \leq [N] \leq 0.76$, respectively [15].

During the 1997 modeling effort [15] it was shown that an OLS regression was only adequate for REDOX modeling if the error in $Fe^{2+}/\Sigma Fe$ is large relative to the errors in the measurement of the nitrate and formate concentrations. The 1997 analysis was based solely upon the formate and nitrate concentrations and indicated that an OLS approach was appropriate if a 7% bias in the parameter estimates was tolerable. In addition it was assumed that the only feed components having major impacts on REDOX potential in the DWPF glass are the formated and nitrated salts formed in the SRAT that react in the melter cold cap (see Section 2.3).

2.3 MELTER COLD CAP REACTIONS AND REDOX

During the melter feed-to-glass conversion in the DWPF melter, multiple types of reactions occur in the cold cap and in the melt pool. In the cold cap, decomposition, calcination and REDOX reactions occur. In the melt pool, further degassing and homogenization occur primarily by additional REDOX reactions [5, 6, 31]. The gaseous products from the cold cap and the volatile feed components further react with air in the vapor space. In order to represent the gradual nature of the feed-to-glass conversion, a 4-stage cold cap model was developed which approximates the melting of feed solids as a continuous, 4-stage countercurrent process [32]. The temperature of each stage is set progressively higher from the top (solid-gas interface) to the bottom (solid-glass interface) as shown in Figure 4.

Stage 1 represents the initial stage of melting before a melt appears. All oxides remain as solids, and each form an invariant phase [6]. In Stage 1 the formatted salts, NaCOOH, are decomposed to CO, CO_2 and H_2 (see Figure 4). The CO subsequently gets oxidized by the air diffusing into the cold cap from the top and the oxygen being liberated as $NaNO_3$ and HNO_3 denitrate in Stage 2 below (see Figure 4). Thus the overall decomposition and calcination reactions occurring in Stages 1 and 2 can be represented by the combined equation:

Equation 6

$$\underset{MelterFeed1}{2NaCOOH} + \underset{melterFeed}{2\,NaNO_3} \rightarrow \underset{Stage1}{CO\uparrow} + \underset{Stage1}{CO_2\uparrow} + \underset{Stage2}{H_2\uparrow} + \underset{Stage2}{N_2\uparrow} + \underset{Stage2}{2.5O_2\uparrow} + \underset{Stage1+2}{2Na_2O} \rightarrow$$
$$\underset{plenum}{2CO_2\uparrow} + \underset{plenum}{H_2O\uparrow} + \underset{plenum}{N_2O\uparrow} + \underset{glass}{4Na_2O}$$

In Stage 2, all oxides are assumed to be in a liquid state and form a solution [6]. Silica and other non-REDOX species form one melt phase, and all REDOX species such as Fe_2O_3 and MnO form the other. The model assumes that these two melt phases are in equilibrium with each other and with the gas and the invariant condensed phases.

Multiple oxides begin to form during Stage 3 reactions [6]. These oxides are of the spinel type, $NiFe_2O_4$, $MgFe_2O_4$. These oxides are assumed to form a solid solution and coexist with the REDOX species in the same phase. The gas phase at this elevated temperature contains only O_2 and SO_3. Stage 4 represents the final fusion where the oxides formed dissolve in a silica-rich matrix to form silicate groups in the melt (see Figure 4). The dominant forms of Fe^{+2} and Fe^{+3} in the glass, based on thermodynamic calculations, are Fe_2SiO_4 and Fe_2O_3 [6].

In order to represent all four stages of cold cap reaction simultaneously and include terms for reduced and oxidized iron and silica, Equation 6 was modified during the development of the {[F]-3[N]} REDOX correlation (see Equation 7):

Equation 7

$$2Fe(OH)_3 + 6SiO_2 + 6NaCOOH + 2NaNO_3 \rightarrow 2FeSiO_3 + 6CO_2 + N_2 + 4Na_2SiO_3 + 6H_2O$$

A more accurate representation based on the reactions discussed above is:

Equation 8

$$Fe_2O_3 + 5SiO_2 + 6NaCOOH + 2NaNO_3 \rightarrow Fe_2SiO_4 + 6CO_2 + N_2 + 4Na_2SiO_3 + 3H_2O$$

Equation 8 assumes that Fe^{3+} enters the melter as Fe_2O_3 and that $COOH^-$ and NO_3^- both enter as properly formated and nitrated sodium compounds. The formated and nitrated salts react with glass formers such as SiO_2 to form Fe^{+2} and Na_2SiO_3 components in the glass and liberate CO_2, N_2 and H_2O vapors to the melter plenum.

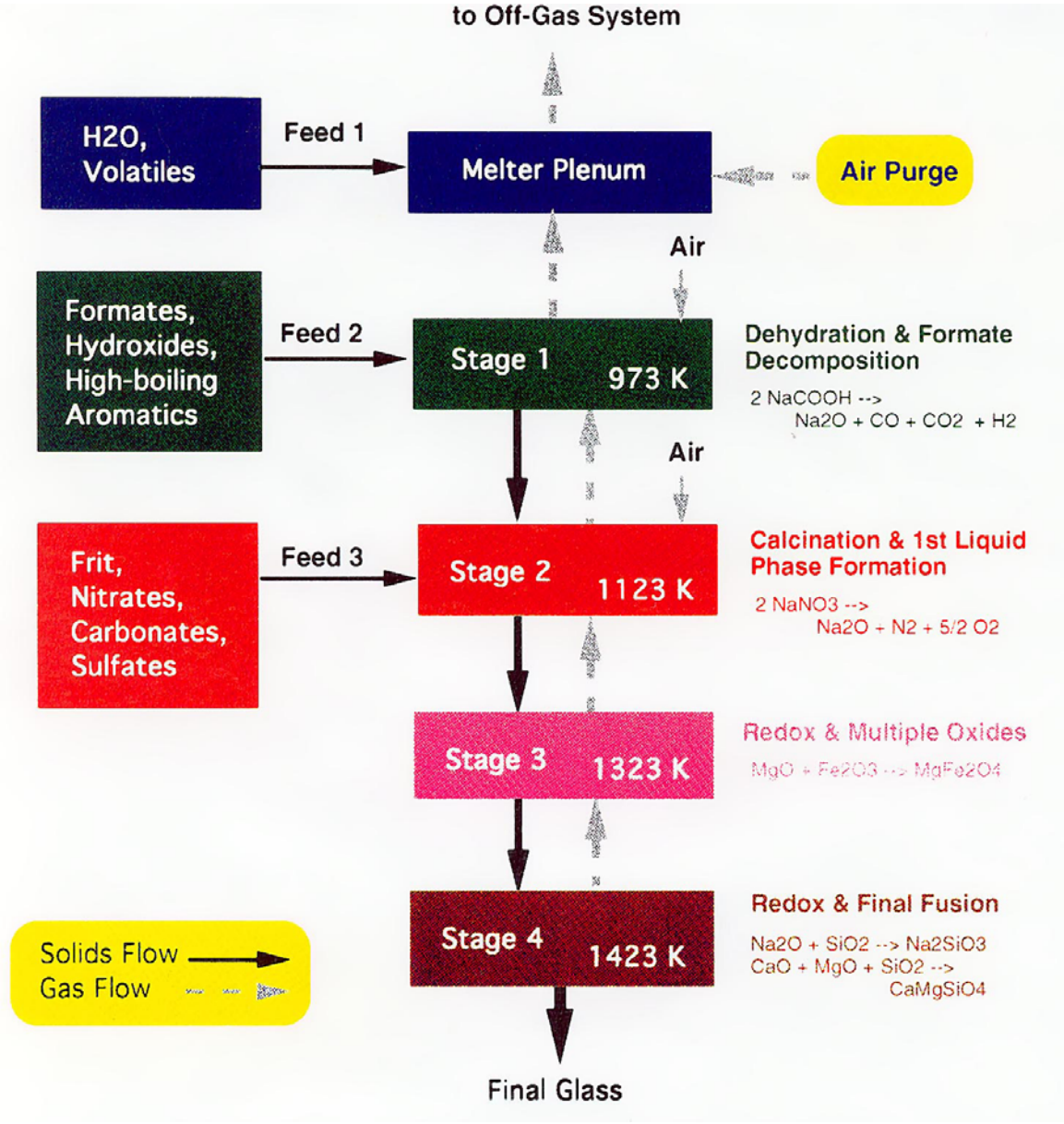

Figure 4. Four stage DWPF cold cap model from Choi [5,31,32].

3.0 EXPERIMENTAL

3.1 Feed Preparation

Twenty-four SB3 SRAT products were tested in this study using Tank 8‡ waste simulants and another 5 SB3 SRAT products were tested using Tank 7 waste simulants (Table I) [33,34,35,36]. Of the twenty-nine SRAT process simulations, three samples were continued through prototypical SME processing (SB3-21, SB3-22, SB3-23) [37].

The SRAT/SME products varied oxalate between 0% to 125% $Na_2C_2O_4$ (Table I) of the projected 660,000 pounds of oxalate, e.g. $\left(\frac{\%oxalate \bullet 660{,}000 lbs}{910{,}000 lbs}\right)$ where $910{,}000 lbs$ represents the total anticipated sludge solids. The wide range of oxalate covered three different scenarios: (1) various sludge washing endpoints between 25-100% and (2) the presence of 25% excess oxalate as a bounding case, and (3) no oxalate.

Coal was varied between 0.07 wt% and 0.7 wt% where the former represented 10% and the latter represented 100% of the coal estimated to be present in Tank 7. The coal additions were on an air-dried sludge basis before sodium oxalate additions were made, i.e. relative to 910,000 lbs. Coal size, type and treatment were varied as shown in Table I. Coal treatment included irradiation and caustic treatment [34] of filter specification size coal (coarse) and fine coal to simulate degradation after years of tank storage. The filter specification size coal was provided by the manufacturer of the K-Area filters and ranged between 0.6 to 0.8mm [19]. The fine coal was ~ 0.21mm in diameter based on documentation by J.R. Fowler.† The coal is ~86% carbon by analysis.[ƒ]

Sand was varied between 0.11 wt% and 1.11 wt% where the former represented 10% and the latter represented 100% of the ~10,000 pounds of sand estimated to be present in Tank 7 from the K-Area filters (Table I). The coarse sand was of the nominal size range of 0.4 to 0.5 mm.† Fine sand was used with fine coal in several simulations. The fine sand was 0.21mm. No attempt was made to simulate the effects of zeolite present in SB3.

The noble metals were varied from 10 wt% to 100 wt% of the amount calculated to be present in Tank 7, e.g. 0.0511 wt% Rh, 0.183 wt% Ru, 0.0275 wt% Pd and 0.0005 wt% Ag [38]. The noble metals weight percents are reported on an air-dried sludge basis before sodium oxalate additions were made. The noble metal additions were made as soluble chloride and nitrate species.

---

‡ The simulated sludge that will be used in this testing is the same sludge that was used in the scoping tests for the effects of Pu and Gd. The sludge was made for processing of Sludge Batch 2 and is representative of Tank 8 material. The sludge simulant was prepared at the University of South Carolina in the FRED cross flow filter facility.

† J.R. Fowler, "Particle Distribution of Coal and Sand in Tank 7," Interoffice Memorandum, September 20, 1979.

ƒ Damon Click, personal communication, March 19, 2003.

The focus of the SRAT runs was multifold, e.g. acid addition strategy, hydrogen generation, component solubility, effects of coal, sand and oxalate on processing, etc. However, during testing, the concentrations of soluble manganese were also quantified. This allowed assessment of the role of soluble manganese during REDOX modeling. Manganese in the air-dried simulated sludges was 2.92 wt% for the Tank 8 simulants and 3.87 wt% in the Tank 7 simulant.

The SRAT runs used for REDOX contained the anticipated levels of noble metals as discussed above and simulants to mimic the contributions from the H-Canyon slurry containing precipitated Pu and Gd that has been added to SB3. Samarium was used as the Pu surrogate for this testing since its behavior is chemically similar to Pu under these conditions, i.e. SRAT runs SB3-5 to SB3-18. The Sm was present at 0.024 wt% while Gd varied from 0.037-0.061 wt%. Mercury was added at a constant 0.076 wt%. All these concentrations are on a wt% air-dried sludge basis. Covering the 10-100% coal and noble metals range while varying oxalate from 0-125% assures that the REDOX modeling covered a wider modeling range than the range over which the model will be implemented for DWPF process control.

Table I Variations in Oxalate, Coal, and Noble Metals in SRAT Batches Tested

Test	Comment	Tank Simulated	Starting Material	Coal %	Type of Coal	Oxalate %	Noble Metals %	Sand %
SB3-1	Baseline	8	SRAT	0	0	0	100	0
SB3-2	Sand/Coal Effect	8	SRAT	100	Act Carbon	0	100	100
SB3-3	Gd Effect	8	SRAT	100	Act Carbon	0	0	100
SB3-4	Gd/noble metals Effect	8	SRAT	100	Act Carbon	0	100	100
SB3-5	50% Oxalate Effect	8	SRAT	0	0	50	100	0
SB3-6	25% Oxalate Effect	8	SRAT	0	0	25	100	0
SB3-7	SB3-5 higher acid	8	SRAT	0	0	50	100	0
SB3-8	SB3-5 coal/sand	8	SRAT	100	Act Carbon	50	100	100
SB3-9	New coal/sand	8	SRAT	100	Spec Size	50	100	100
SB3-10	New coal/sand	8	SRAT	10	Spec Size	50	100	10
SB3-11	Low coal/ sand/noble metals	8	SRAT	10	Spec Size	50	10	10
SB3-12	Irradiated spec coal/sand	8	SRAT	100	Spec Size/Irradiated/ Caustic Treated	50	10	100
SB3-13	Fine coal	8	SRAT	100	Fine	50	10	100
SB3-14	Fine coal	8	SRAT	10	Fine	50	100	10
SB3-15	Irradiated fine coal/sand	8	SRAT	10	Fine/Irradiated/ Caustic Treated	50	10	10
SB3-16	Irradiated fine coal/sand	8	SRAT	100	Fine/Irradiated/ Caustic Treated	50	100	100
SB3-17	SB3-10 with Irradiated coal/sand	8	SRAT	10	Fine/Irradiated/ Caustic Treated	50	100	10
SB3-18	SB3-18 with no oxalate	8	SRAT	100	Fine/Irradiated/ Caustic Treated	0	100	100
SB3-19	Low noble metals, higher acid	8	SRAT	100	Spec Size	56	10	100
SB3-20	Low noble metals, higher acid	8	SRAT	100	Spec Size	75	10	100
SB3-21	High noble metals, higher acid	8	SME/F202	100	Spec Size	75	100	100
SB3-22	Low noble metals, higher acid	8	SME/F320	100	Spec Size	50	10	100
SB3-23	High noble metals, higher acid	8	SME/F320	100	Spec Size	25	100	100
SB3-24	NCSE Evaluation	8	SRAT	100	Spec Size	125	100	100
SB3A-1	Decant 5 oxalate	7	SRAT	100	Spec Size	69	10	100
SB3A-2	Decant 9 oxalate	7	SRAT	100	Spec Size	40	10	100
SB3A-3	Decant 7 oxalate	7	SRAT	100	Spec Size	52	10	100
SB3A-4	No oxalate	7	SRAT	100	Spec Size	0	10	100
SB3-NO	Nitric Acid Only No Formic Acid Decant 5 oxalate	7	SRAT	100	Spec Size	69	10	100

3.2 Feed Analyses

The SRAT feeds were prepared at the Aiken County Technology Laboratory (ACTL) and subsamples were sent to SRTC for sealed crucible vitrification and REDOX measurement. The formate, nitrate, nitrite, and total oxalate concentrations of the SRAT products were measured by Ion Chromatography (IC) as part of the SB3 scoping studies [33,34,35,36,37]. Coal could not be measured since a definitive analysis method was not yet available. The coal values used in this study are calculated from the known batch inputs assuming ideal mixing. Manganese and noble metals (Rh, Ru, Ag, Pd) in the insoluble fraction of the SRAT products were measured by dissolution in Na_2O_2 followed by Inductively Coupled Plasma Emission Spectroscopy (ICP-ES). The soluble manganese was also quantified and the insoluble dried sludges analyzed by x-ray diffraction (XRD). Knowing the form of manganese in the soluble and insoluble solids was needed to evaluate the impact of manganese on REDOX. The measured concentrations of formate, nitrate, nitrite, total oxalate, coal, manganese, and Ru° corresponding to the SRAT/SME runs given in Table I are shown in Table II.

For each subsample, eight different simulated SME compositions were made using two different frits and four different waste loadings (see Section 3.3). Since eight simulated SME products were made from each of the 29 SRAT products listed in Table I there would have been a total of 232 SME products that would have to be analyzed for. When there appeared to be little impact of the different frits on REDOX (see Section 4.3), later simulated SME products were only formulated with Frit 202. In total, 185 simulated SME products were formulated and would have had to have been analyzed for formate, nitrate, nitrite, total oxalate (soluble and insoluble), coal, manganese, Rh, Ru, Ag, Pd. This would have entailed ~1850 analyses for single replicates of each constituent.

A decision was made not to analyze each of the 185 SME products for the above 11 constituents. Instead, the SRAT concentrations in Table II were adjusted for the dilution from the frit added by the following dimensionless factor:

Equation 9

$$\frac{weight_{SRATslurry}(gms)}{\left(weight_{SRATslurry}(gms) + weight_{frit}(gms)\right)}$$

Use of this strategy was dependent on knowing the representative wt% calcine solids in the SRAT product so that the weight of frit required to give a specific waste loading could be calculated. The weight of frit used in each SME product was determined from the calcine solids values by the following equation:

Equation 10

$$weight_{frit}(gms) = \frac{weight_{SRATslurry}(gms) \bullet \left(\frac{calcine_{solids@900^{\circ}C}(wt\%)}{100}\right) \bullet loading_{frit}}{loading_{waste}}$$

where ($loading_{waste} + loading_{frit}$) = 100.

Table II Measured SRAT Concentrations Unadjusted for Frit Additions

Sample ID	C_2O_4, mg/kg	HCO_2, mg/kg	NO_3, mg/kg	NO_2, mg/kg	Coal, mg/kg	Mn, mg/kg	Ru (mg/kg)	Soluble Mn (%)
SB3-1	0	20600	13600	0	0	5112	342	10.7
SB3-2	0	19700	14100	0	1334	4785	343	14.4
SB3-3	0	25600	14300	0	1335	4587	0	68.8
SB3-4	0	19400	14500	0	1353	4976	348	9.85
SB3-5	32200	24200	12300	2900	0	4628	323	28.8
SB3-6	16600	23800	12700	0	0	4891	336	4.85
SB3-7	29000	19000	22200	481	0	3744	251	17.9
SB3-8	26000	18600	22800	0	985	3620	254	17.4
SB3-9	28000	20600	19000	0	986	3946	255	9.7
SB3-10	22750	23100	17500	0	98	3825	254	9.3
SB3-11	22000	25600	14800	1110	98	3934	25	10.6
SB3-12	22800	26600	19100	1050	985	3917	25	9.4
SB3-13	24850	30600	21100	667	997	4079	26	10.3
SB3-14	25300	26000	19200	0	106	4011	274	13.7
SB3-15	22700	33700	18800	936	98	4060	25	10.2
SB3-16	26100	25900	21600	0	981	4025	253	10.9
SB3-17	22000	27500	19400	0	98	3885	252	11.7
SB3-18	0	26600	19600	0	1333	5169	344	47.1
SB3-19	32300	32700	27700	0	1110	3464	29	28.13
SB3-20	41300	30300	27400	0	906	2627	23	73.09
SB3-21	43900	26000	28400	0	914	3332	230	8.22
SB3-22	28900	29300	25100	0	936	3711	26	31.95
SB3-23	18400	20400	19200	0	1043	4522	294	11.26
SB3-24	61000	15400	23300	2240	1034	2502	180	33.17
SB3A-1	43900	30200	26000	457	944	4927	24	13.03
SB3A-2	26100	27600	22100	0	1268	7316	33	9.2
SB3A-3	28800	31300	22400	0	1164	5906	30	5.41
SB3A-4	1000	27500	17800	0	1640	8502	42	64.16
SB3-NO	46350	0	68000	2350	1488	5407	10	5.3

In addition, a calculated SME wt% solids was needed for REDOX modeling since the REDOX models are normalized to a constant wt% solids, e.g. 45 wt% solids, so that feed reactant concentrations are not impacted by feed dilution (see discussion in Section 2.2.2). The SME wt% solids calculation, shown in Equation 11, depends on the SRAT wt% total solids as measured at 110°C:

Equation 11

$$SME_{solids}(wt\%) = \left(\frac{\left(weight_{SRATslurry}(gms) \bullet \frac{solids_{SRAT_{@110^\circ C}}(wt\%)}{100} + weight_{frit}(gms) \right)}{\left(weight_{SRATslurry}(gms) + weight_{frit}(gms) \right)} \right) \bullet 100$$

The waste loading is related to the masses of sludge and frit by:

Equation 12

$$loading_{waste} = \frac{\left(\frac{calcine_{solids@900^\circ C}(wt\%)}{100} \right) \bullet weight_{SRATslurry}(gms)}{\left(\frac{calcine_{solids@900^\circ C}(wt\%)}{100} \right) \bullet weight_{SRATslurry}(gms) + weight_{frit}(gms)}$$

The waste loading in the glass produced can also be calculated from the boron, lithium, or iron concentrations [39]:

Equation 13

$$loading_{waste} = 1 - \frac{X_{measured\ in\ glass}}{X_{frit}} = \frac{Y_{measured\ in\ glass}}{Y_{waste}}$$

where X = concentration of a frit-only species (B or Li) as oxide
Y = concentration of a waste only component (Fe) as oxide

The waste loadings were calculated from the measured boron and lithium concentrations given in Table IV. The calculated waste loadings did not match the target values, which raised the suspicion that some of the sub-samples of the SRAT products received at SRTC from ACTL were not representative and/or the SRAT sludges batched into some of the crucibles were not representative. If these sub-samples were enriched in insoluble solids, a higher than expected waste loading would result. In addition, the amount of insoluble REDOX species (insoluble oxalate, coal, Mn as Mn oxalate) would be increased and the amount of soluble REDOX species (formate, nitrate, soluble oxalate, soluble Mn) would be decreased. The overall effect could be to change the relative amounts of oxidants and reductants in the slurry. The calculated SME wt% solids for use in the REDOX model are also dependent on the SRAT wt% solids, so this quantity would also be affected by the sub-sampling.

To determine if the deviations of the calculated waste loadings were truly significant, the errors in the waste loading expected from the boron measurement were estimated. If the boron measurement is accurate to ±5% with 95% confidence (see Appendix E), then the error in the waste loading calculated from Equation 13 is ±11.7% (see Appendix E). Figure 5 shows the waste loadings calculated from the boron, lithium, and iron analyses versus the target waste loadings. The values found for boron are evenly distributed around the line where measured = targeted (slope = 1.0). The actual slope determined for these data was 1.043. The dashed lines in this figure show the waste loading ± 11.7%. These bounds should approximate the range of calculated waste loadings that could be expected just due to random error in the boron measurement. Therefore, no correction factors were applied to these values.

The waste loadings determined from the Li values were almost uniformly higher than the target values, indicating that a bias in either the Li measurement towards lower than actual values, or a high bias in the Li values used for the frit existed in Equation 13. Figure 6 shows the waste loading calculated from boron plotted versus that calculated from Li. Note that the calculated waste loading based on Li_2O are always biased high from the 1:1 diagonal shown in Figure 6.

Iron had only been analyzed for 36 of the 185 glasses vitrified (see Section 3.5). Whenever iron analyses were available they were used to evaluate whether the B_2O_3 or the Li_2O analyses were biased (see discussion below).

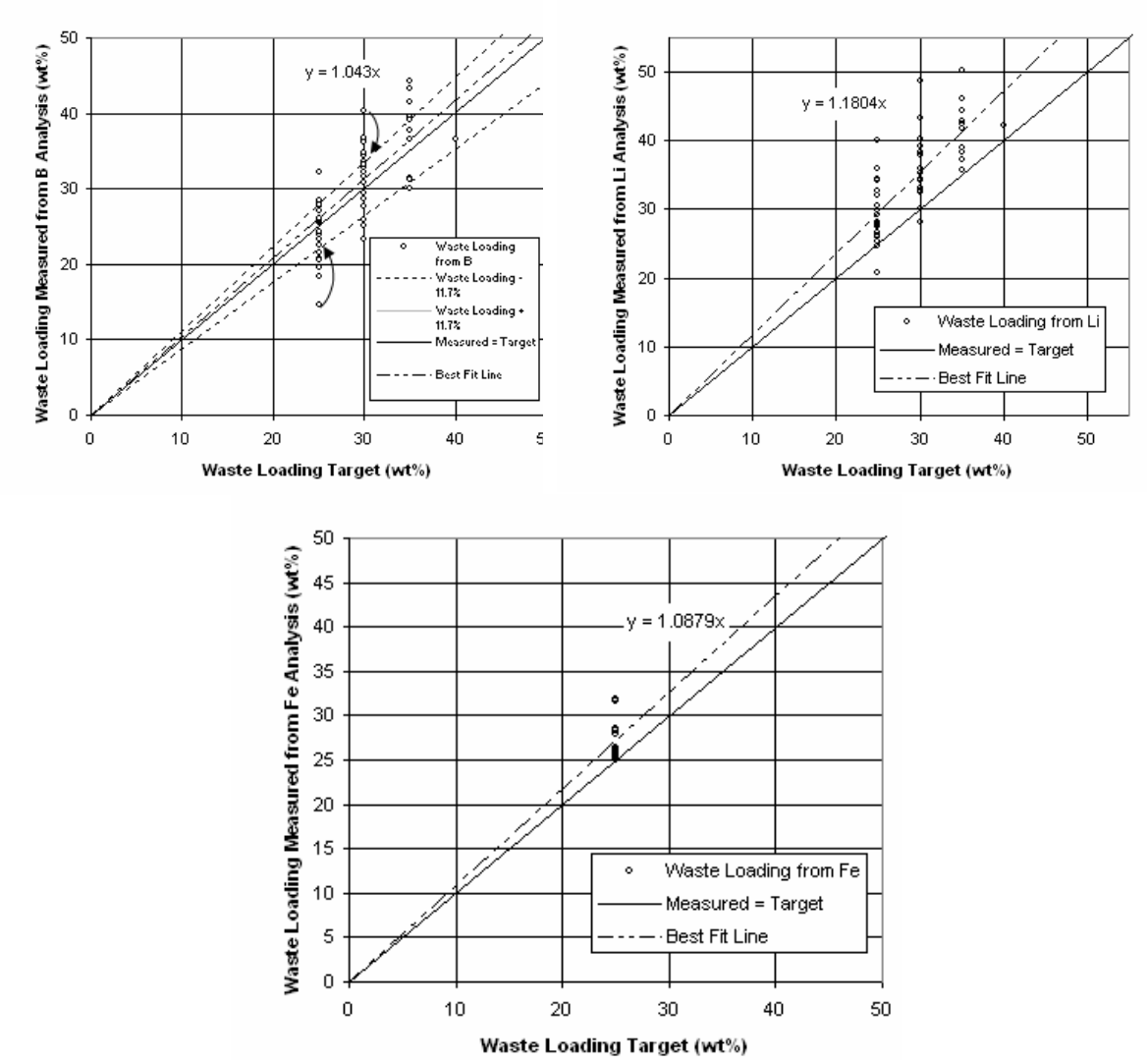

Figure 5. Waste loading measured from elemental analyses vs. target waste loading.

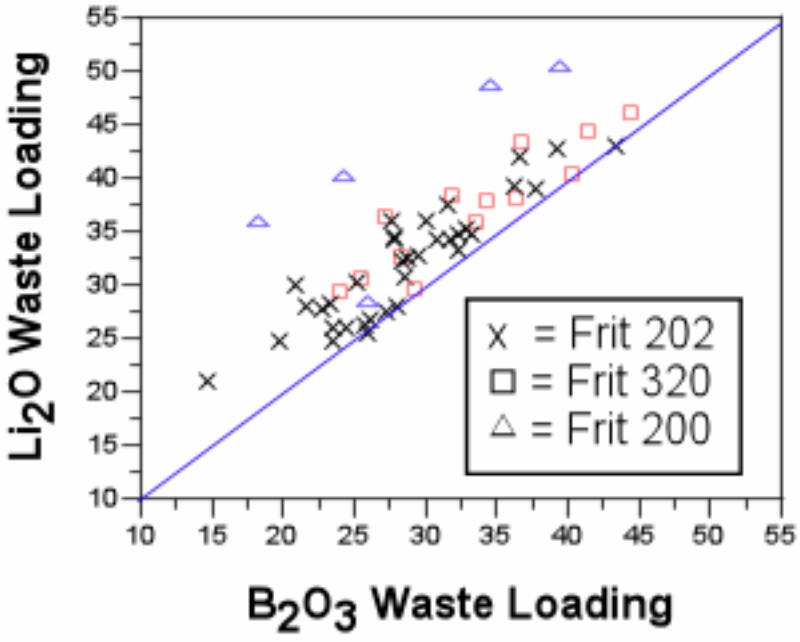

Figure 6. Bias in the calculated waste loading from measured B_2O_3 compared to Li_2O.

All of the calculated waste loadings are shown in Figure 7 as ratios to the target waste loading. The large circles around data points indicate the data that were adjusted using the boron waste loading value. The large squares indicate those data that had boron waste loadings outside the ±11.7% interval, but either had Fe waste loadings closer to the target or Li waste loadings that tended to indicate that the boron waste loading was probably an outlier.

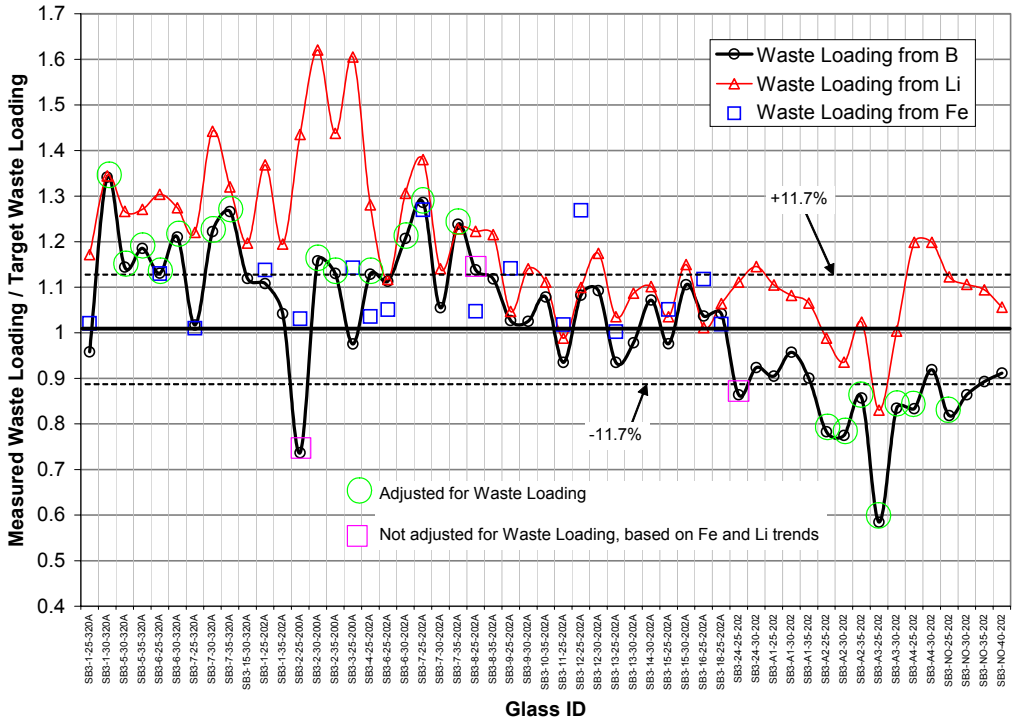

Figure 7. Ratio of measured to target waste loadings for glasses used in REDOX model.

To investigate the representativeness of the SRAT sub-sampling, each sample was analyzed for wt% total solids. A comparison of the original SRAT sample, the sub-sample total solids (re-analyses), and the total solids content calculated from the boron waste loading is shown in Table III. For most of the samples, the re-analysis and the calculated total solids tend to track each other; exceptions to this trend are the SB3A samples, which re-analysis showed were more concentrated, but the waste loading indicated were less concentrated.

The uncertainty of the boron analyses was estimated to be ±5%, which translated to an uncertainty of ±11.7% in the waste loading at a 30 wt% target loading (see Appendix E). For glasses with calculated boron waste loadings greater than ±11.7% from the target, the waste loadings were adjusted as described in Appendix E. Only the adjusted waste loadings are shown in Table III. The target waste loadings that were within the ±11.7% variation are given in Table IV as discussed below.

Table III Total Solids Analyses of SRAT Product

SRAT Run	Original Total Solids (wt%)	Re-analysis Total Solids (wt%)	Total Solids Adjusted Using Waste Loading (wt%)
SB3-1	18.50	20.69 17.00 18.95 19.33	23.7
SB3-2	18.70	19.26	19.59 19.01
SB3-3	19.95	not available	
SB3-4	18.90	insufficient sample	19.15
SB3-5	23.95	24.65	24.65 25.91
SB3-6	21.55	22.35	23.94 24.79
SB3-7	19.40	16.22	22.83 22.32 21.69 23.07
SB3-8	19.35	20.25	19.88
SB3-9	20.11	20.95	NA
SB3-10	19.98	20.5	NA
SB3-11	20.36	25.08	NA
SB3-12	20.52	28.13	NA
SB3-13	20.45	22.22	NA
SB3-14	20.00	20.9	NA
SB3-15	20.35	20.61	NA
SB3-16	19.70	20.42	NA
SB3-17	19.40	19.72	NA
SB3-18	19.05	19.46	NA
SB3-19	21.20	21.09	NA
SB3-20*	20.10	19.96	NA
SB3-24*	20.20	20.96	19.8
SB3A-1	20.20	not available	NA
SB3A-2	21.00	23.57	18.91 18.65 20.38
SB3A-3	20.60	24.18	14.80 19.52
SB3A-4	20.20	20.06	19.03
SB3-NO	23.90	23.79 23.45	NA

*SB3-21, SB3-22 and SB3-23 were SME not SRAT products and were not remeasured because the SME products stayed suspended/homogenized better than the SRAT products.

For the SME products with waste loadings outside the bounds shown in Figure 7, the SRAT sample total solids wt% were adjusted so that the calculated waste loading was within the bounds; this adjustment is shown graphically in Figure 5 for two points by the arrows. The sample analyses were not adjusted all the way to the 'measured equals target' line. The details of the adjustments made and a summary of unadjusted and adjusted values are given in Appendix E. Note that in addition to changing the total solids wt% of the SRAT samples, these adjustments also changed the relative amounts of soluble and insoluble components.

Table IV summarizes the measured REDOX and waste loading data for the glasses made and the SME concentrations adjusted for total solids content, but not adjusted for waste loading. Thus, the SRAT sample analyses given in Table II were adjusted and used to give the adjusted SME values shown in Table V.

Table IV Evaluation of Glass Redox Data and Measured SME Concentrations Used in Redox Modeling

Note: SME concentrations not adjusted for total solids content or waste loading.

Sample ID	Comment*	Measured Li_2O (wt%)	Measured B_2O_3 (wt%)	B_2O_3 waste load (wt%)	Li_2O Waste Load (wt%)	Target Waste Load(wt%)	Measured Fe^{+2}	Measured Total Fe	$Fe^{+2}/\Sigma Fe$	SRAT Total Solids (wt%)	% Calcined SRAT Solids	Frit Used (g)	SRAT Sludge Used (g)	SME Total Solids (wt%)	Formate (mol/kg feed)	Nitrate (mol/kg feed)	Oxalate (mol/kg feed)	Coal (mol/kg feed)	Ru (mol/kg feed)	Mn (mol/kg feed)
SB3-1-25-320		5.77	6.16	23.95	29.29	25	0.049	0.407	0.12	18.5	14.2	17.04	40.10	42.80	0.32120	0.15394	0.00000	0.00000	0.00237	0.06530
SB3-1-30-320		4.87	4.84	40.25	40.32	30	0.029	0.393	0.07	18.5	14.2	13.25	40.08	38.75	0.34397	0.16486	0.00000	0.00000	0.00254	0.06993
SB3-1-35-320	Bad Glass	4.11	3.98	50.86	49.63	35	0.025	0.290	0.08	18.5	14.2	10.55	40.07	35.48	0.36230	0.17364	0.00000	0.00000	0.00268	0.07366
SB3-1-40-320	Bad Glass	3.69	3.65	54.94	54.78	40	0.017	0.302	0.05	18.5	14.2	8.52	40.09	32.79	0.37745	0.18090	0.00000	0.00000	0.00279	0.07674
SB3-2-25-320	ACT-C/F320	5.69	5.99	26.05	30.27	25	0.144	0.338	0.43	18.7	14.2	17.04	40.11	42.94	0.30718	0.15961	0.00000	0.07802	0.00238	0.06113
SB3-2-30-320	Bad Glass	4.85	4.8	40.74	40.56	30	0.312	0.597	0.52	18.7	14.2	13.25	40.02	38.92	0.32881	0.17085	0.00000	0.08352	0.00255	0.06543
SB3-2-35-320	Bad Glass	4.06	3.92	51.60	50.25	35	0.229	0.507	0.45	18.7	14.2	10.55	40.04	35.66	0.34640	0.17999	0.00000	0.08798	0.00269	0.06893
SB3-2-40-320	Bad Glass	3.46	3.45	57.41	57.60	40	0.315	0.702	0.45	18.7	14.2	8.52	40.08	32.95	0.36094	0.18755	0.00000	0.09168	0.00280	0.07182
SB3-3-25-320	ACT-C/F320	5.33	5.69	29.75	34.68	25	0.203	0.419	0.48	19.95	14.2	17.04	40.04	43.85	0.39898	0.16180	0.00000	0.07804	0.00000	0.05857
SB3-3-30-320	ACT-C/F320	4.93	5.15	36.42	39.58	30	0.170	0.405	0.42	19.95	14.2	13.25	40.04	39.86	0.42734	0.17329	0.00000	0.08359	0.00000	0.06273
SB3-3-35-320	Bad Glass	4.57	4.62	42.96	44.00	35	0.076	0.377	0.20	19.95	14.2	10.55	40.09	36.63	0.45028	0.18260	0.00000	0.08807	0.00000	0.06610
SB3-3-40-320	Bad Glass	3.11	3.09	61.85	61.89	40	0.086	0.569	0.15	19.95	14.2	8.52	40.04	34.00	0.46897	0.19018	0.00000	0.09173	0.00000	0.06884
SB3-4-25-320	ACT-C/F320	5.67	6	25.93	30.51	25	0.135	0.432	0.31	18.9	14.3	25.74	60.01	43.24	0.30164	0.16367	0.00000	0.07891	0.00241	0.06339
SB3-4-30-320	Bad Glass	4.93	5.04	37.78	39.58	30	0.239	0.477	0.50	18.9	14.3	20.02	60.01	39.19	0.32320	0.17537	0.00000	0.08455	0.00258	0.06792
SB3-4-35-320	Bad Glass	4.44	4.5	44.44	45.59	35	0.263	0.571	0.46	18.9	14.3	15.93	60.03	35.91	0.34062	0.18482	0.00000	0.08910	0.00272	0.07158
SB3-4-40-320	Bad Glass	3.82	3.93	51.48	53.19	40	0.198	0.509	0.39	18.9	14.3	12.87	60.06	33.21	0.35495	0.19260	0.00000	0.09285	0.00284	0.07459
SB3-5-25-320	Bad Glass	4.67	5.55	31.48	42.77	25	0.172	0.336	0.51	23.95	16.5	29.70	60.02	49.12	0.35968	0.17489	0.24478	0.00000	0.00214	0.05635
SB3-5-30-320		5.06	5.32	34.32	37.99	30	0.176	0.433	0.41	23.95	16.5	23.10	60.01	45.09	0.38821	0.18876	0.26420	0.00000	0.00231	0.06082
SB3-5-35-320		4.53	4.74	41.48	44.49	35	0.223	0.494	0.45	23.95	16.5	18.39	60.04	41.78	0.41159	0.20013	0.28011	0.00000	0.00245	0.06449
SB3-5-40-320	Bad Glass	4.07	4.17	48.52	50.12	40	0.297	0.588	0.50	23.95	16.5	14.85	60.08	39.02	0.43110	0.20962	0.29339	0.00000	0.00256	0.06754
SB3-6-25-320		5.5	5.81	28.27	32.60	25	0.131	0.353	0.37	21.55	15.7	28.27	60.06	46.66	0.35956	0.13929	0.12827	0.00000	0.00226	0.06054
SB3-6-30-320		5.04	5.16	36.30	38.24	30	0.104	0.390	0.27	21.55	15.7	21.98	60.02	42.58	0.38703	0.14993	0.13807	0.00000	0.00243	0.06516
SB3-6-35-320	Bad Glass	4.51	4.72	41.73	44.73	35	0.200	0.565	0.35	21.55	15.7	17.49	60.08	39.24	0.40955	0.15865	0.14610	0.00000	0.00257	0.06895
SB3-6-40-320	Bad Glass	4.14	4.09	49.51	49.26	40	0.160	0.525	0.30	21.55	15.7	14.13	60.05	36.49	0.42804	0.16582	0.15270	0.00000	0.00269	0.07207
SB3-7-25-320		5.67	6.04	25.43	30.51	25	0.042	0.337	0.12	19.4	13	23.40	60.00	42.01	0.30369	0.26512	0.23708	0.00000	0.00179	0.04903
SB3-7-30-320		4.63	5.13	36.67	43.26	30	0.075	0.387	0.19	19.4	13	18.20	60.05	38.15	0.32394	0.28281	0.25290	0.00000	0.00191	0.05230
SB3-7-35-320		4.39	4.51	44.32	46.20	35	0.061	0.427	0.14	19.4	13	14.49	60.03	35.07	0.34004	0.29686	0.26546	0.00000	0.00200	0.05490
SB3-7-40-320	Bad Seal	3.73	3.82	52.84	54.29	40	0.035	0.384	0.09	19.4	13	11.70	60.01	32.55	0.35325	0.30839	0.27577	0.00000	0.00208	0.05703
SB3-8-25-320	ACT-C/F320	5.66	6.02	25.68	30.64	25	0.150	0.398	0.38	19.45	12.7	23.04	60.06	41.78	0.29867	0.26578	0.21354	0.05933	0.00182	0.04762
SB3-8-30-320	ACT-C/F320	5	5.21	35.68	38.73	30	0.138	0.474	0.29	19.45	12.7	17.92	60.03	37.97	0.31824	0.28320	0.22753	0.06321	0.00194	0.05074
SB3-8-35-320	Bad Glass	4.42	4.53	44.07	45.83	35	0.130	0.427	0.30	19.45	12.7	14.26	60.03	34.91	0.33392	0.29715	0.23874	0.06633	0.00203	0.05324
SB3-8-40-320	Bad Glass	3.83	3.91	51.73	53.06	40	0.058	0.409	0.14	19.45	12.7	11.52	60.02	32.42	0.34670	0.30852	0.24788	0.06887	0.00211	0.05528
SB3-9-25-320	Bad Glass	5.56	5.93	26.79	31.86	25	0.254	0.302	0.84	20.1	13.33	23.94	60.08	42.87	0.32726	0.21913	0.22752	0.05875	0.00180	0.05136
SB3-9-30-320	Bad Glass	5.19	5.46	32.59	36.40	30	0.290	0.520	0.56	20.1	13.33	18.62	60.06	39.01	0.34935	0.23392	0.24287	0.06272	0.00193	0.05482

Sample ID	Comment*	Measured Li_2O (wt%)	Measured B_2O_3 (wt%)	B_2O_3 waste load (wt%)	Li_2O Waste Load (wt%)	Target Waste Load(wt%)	Measured Fe^{+2}	Measured Total Fe	$Fe^{+2}/\Sigma Fe$	SRAT Total Solids (wt%)	% Calcined SRAT Solids	Frit Used (g)	SRAT Sludge Used (g)	SME Total Solids (wt%)	Formate (mol/kg feed)	Nitrate (mol/kg feed)	Oxalate (mol/kg feed)	Coal (mol/kg feed)	Ru (mol/kg feed)	Mn (mol/kg feed)
SB3-9-35-320	Bad Glass	4.78	4.98	38.52	41.42	35	0.161	0.527	0.31	20.1	13.33	14.82	60.04	35.92	0.36707	0.24578	0.25519	0.06590	0.00202	0.05760
SB3-9-40-320	Bad Glass	4.36	4.56	43.70	46.57	40	0.112	0.447	0.25	20.1	13.33	11.97	60.10	33.37	0.38165	0.25555	0.26533	0.06852	0.00210	0.05989
SB3-10-25-320	Bad Glass	5.09	5.98	26.17	37.62	25	0.164	0.330	0.50	19.95	13.19	23.76	60.01	42.65	0.36766	0.20220	0.18520	0.00585	0.00180	0.04988
SB3-10-30-320	CC/F320	5.1	5.36	33.83	37.50	30	0.173	0.446	0.39	19.95	13.19	18.48	60.02	38.79	0.39240	0.21581	0.19766	0.00624	0.00192	0.05323
SB3-10-35-320	CC/F320	4.59	4.85	40.12	43.75	35	0.121	0.493	0.24	19.95	13.19	14.71	60.02	35.71	0.41220	0.22670	0.20764	0.00656	0.00202	0.05592
SB3-10-40-320	Bad Glass	4.23	4.35	46.30	48.16	40	0.200	0.564	0.35	19.95	13.19	11.88	60.01	33.18	0.42840	0.23561	0.21580	0.00682	0.00210	0.05812
SB3-11-25-320	CC/F320	6.16	6.58	18.77	24.51	25	0.089	0.225	0.39	20.4	13.09	23.49	60.06	42.78	0.40884	0.18894	0.17971	0.00587	0.00018	0.05147
SB3-11-30-320	CC/F320	5.83	6.6	18.52	28.55	30	0.088	0.209	0.42	20.4	13.09	18.27	60.04	38.97	0.43607	0.20152	0.19168	0.00626	0.00019	0.05490
SB3-11-35-320	CC/F320	5.54	6.19	23.58	32.11	35	0.099	0.244	0.40	20.4	13.09	14.54	60.01	35.93	0.45782	0.21157	0.20123	0.00657	0.00020	0.05764
SB3-11-40-320	CC/F320	5.35	5.89	27.28	34.44	40	0.124	0.355	0.35	20.4	13.09	11.88	60.06	33.55	0.47483	0.21943	0.20871	0.00682	0.00021	0.05978
SB3-12-25-320	CC/F320	6.11	6.45	20.37	25.12	25	0.077	0.256	0.30	20.5	13.21	23.76	60.06	43.04	0.42344	0.23709	0.18564	0.05881	0.00018	0.05108
SB3-12-30-320	CC/F320	5.34	5.6	30.86	34.56	30	0.090	0.318	0.28	20.5	13.21	18.48	60.04	39.21	0.45189	0.25302	0.19811	0.06277	0.00019	0.05452
SB3-12-35-320	CC/F320	4.9	5.17	36.17	39.95	35	0.143	0.400	0.36	20.5	13.21	14.71	60.03	36.15	0.47465	0.26576	0.20809	0.06593	0.00020	0.05726
SB3-12-40-320	Bad Glass	4.45	4.69	42.10	45.47	40	0.168	0.419	0.40	20.5	13.21	11.88	60.04	33.63	0.49335	0.27623	0.21629	0.06852	0.00021	0.05952
SB3-13-25-320	CC/F320	5.76	6.21	23.33	29.41	25	0.146	0.359	0.41	20.45	13.33	23.99	60.03	43.16	0.48573	0.25351	0.20175	0.05936	0.00018	0.05305
SB3-13-30-320	CC/F320	5.1	5.31	34.44	37.50	30	0.157	0.409	0.38	20.45	13.33	18.66	60.08	39.30	0.51874	0.27074	0.21547	0.06339	0.00020	0.05665
SB3-13-35-320	Bad Glass	4.63	4.86	40.00	43.26	35	0.135	0.407	0.33	20.45	13.33	14.85	60.03	36.23	0.54500	0.28444	0.22637	0.06660	0.00021	0.05952
SB3-13-40-320	Bad Glass	4.27	4.49	44.57	47.67	40	0.143	0.506	0.28	20.45	13.33	12.00	60.04	33.70	0.56658	0.29570	0.23534	0.06924	0.00021	0.06187
SB3-14-25-320	Bad Glass	5.76	6.12	24.44	29.41	25	0.139	0.302	0.46	20	13.37	24.07	60.04	42.90	0.41233	0.22105	0.20522	0.00631	0.00194	0.05211
SB3-14-30-320	Bad Glass	5.13	5.38	33.58	37.13	30	0.147	0.375	0.39	20	13.37	18.72	60.05	39.01	0.44036	0.23608	0.21917	0.00673	0.00207	0.05566
SB3-14-35-320	Bad Glass	4.79	5.05	37.65	41.30	35	0.162	0.477	0.34	20	13.37	14.90	60.07	35.90	0.46283	0.24812	0.23036	0.00708	0.00217	0.05850
SB3-14-40-320	Bad Glass	4.41	4.65	42.59	45.96	40	0.197	0.540	0.36	20	13.37	12.03	60.01	33.36	0.48117	0.25796	0.23948	0.00736	0.00226	0.06081
SB3-15-25-320	Bad Glass	5.5	5.91	27.04	32.60	25	0.146	0.395	0.37	20.35	13.14	23.65	60.07	42.85	0.53722	0.23217	0.18509	0.00586	0.00018	0.05302
SB3-15-30-320		5.23	5.38	33.58	35.91	30	0.129	0.390	0.33	20.35	13.14	18.40	60.01	39.04	0.57302	0.24764	0.19742	0.00625	0.00019	0.05656
SB3-15-35-320	Bad Seal	3.75	3.8	53.09	54.04	35	0.123	0.766	0.16	20.35	13.14	14.64	60.06	35.96	0.60198	0.26016	0.20740	0.00657	0.00020	0.05942
SB3-15-40-320	Bad Glass	4.18	4.13	49.01	48.77	40	0.153	0.405	0.38	20.35	13.14	11.83	60.02	33.46	0.62544	0.27029	0.21548	0.00682	0.00021	0.06173
SB3-16-25-320	Bad Glass	6.03	6.31	22.10	26.10	25	0.178	0.317	0.56	19.7	13.24	23.83	60.01	42.53	0.41185	0.24935	0.21228	0.05851	0.00179	0.05243
SB3-16-30-320	Bad Glass	5.01	5.08	37.28	38.60	30	0.207	0.481	0.43	19.7	13.24	18.54	60.07	38.64	0.43969	0.26621	0.22663	0.06247	0.00191	0.05598
SB3-16-35-320	Bad Glass	4.46	4.48	44.69	45.34	35	0.285	0.578	0.49	19.7	13.24	14.76	60.05	35.54	0.46190	0.27965	0.23808	0.06562	0.00201	0.05881
SB3-16-40-320	Bad Glass	3.9	3.89	51.98	52.21	40	0.344	0.565	0.61	19.7	13.24	11.92	60.03	33.00	0.48009	0.29066	0.24745	0.06820	0.00209	0.06112
SB3-17-25-320	CC/F320	5.75	6	25.93	29.53	25	0.121	0.359	0.34	19.4	12.95	23.32	60.02	41.95	0.44005	0.22536	0.18006	0.00588	0.00180	0.05093
SB3-17-30-320	Bad Glass	4.89	5.04	37.78	40.07	30	0.139	0.483	0.29	19.4	12.95	18.13	60.05	38.09	0.46927	0.24033	0.19202	0.00627	0.00192	0.05431
SB3-17-35-320	Bad Glass	4.39	4.61	43.09	46.20	35	0.187	0.509	0.37	19.4	12.95	14.44	60.05	35.02	0.49256	0.25226	0.20155	0.00658	0.00201	0.05701
SB3-17-40-320	Bad Glass	3.83	3.93	51.48	53.06	40	0.103	0.450	0.23	19.4	12.95	11.66	60.03	32.51	0.51159	0.26200	0.20933	0.00684	0.00209	0.05921
SB3-18-25-320	Bad Glass	5.68	5.94	26.67	30.39	25	0.011	0.443	0.02	19.05	14.28	25.71	60.02	43.32	0.41376	0.22133	0.00000	0.07777	0.00238	0.06587
SB3-18-30-320	Bad Glass	5	5.23	35.43	38.73	30	0.094	0.446	0.21	19.05	14.28	19.99	60.03	39.27	0.44334	0.23716	0.00000	0.08333	0.00255	0.07058
SB3-18-35-320	Bad Glass	4.62	4.78	40.99	43.38	35	0.089	0.469	0.19	19.05	14.28	15.91	60.04	36.01	0.46716	0.24989	0.00000	0.08781	0.00269	0.07437
SB3-18-40-320	Bad Glass	3.9	4.08	49.63	52.21	40	0.036	0.445	0.08	19.05	14.28	12.85	60.01	33.33	0.48673	0.26036	0.00000	0.09149	0.00280	0.07749

Sample ID	Comment*	Measured Li_2O (wt%)	Measured B_2O_3 (wt%)	B_2O_3 waste load (wt%)	Li_2O Waste Load (wt%)	Target Waste Load(wt%)	Measured Fe^{+2}	Measured Total Fe	$Fe^{+2}/\Sigma Fe$	SRAT Total Solids (wt%)	% Calcined SRAT Solids	Frit Used (g)	SRAT Sludge Used (g)	SME Total Solids (wt%)	Formate (mol/kg feed)	Nitrate (mol/kg feed)	Oxalate (mol/kg feed)	Coal (mol/kg feed)	Ru (mol/kg feed)	Mn (mol/kg feed)
SB3-1-25-202		4.5	5.69	27.70	34.21	25	0.028	0.263	0.10	18.5	14.2	17.04	40.02	42.84	0.32101	0.15385	0.00000	0.00000	0.00237	0.06526
SB3-1-30-202	Bad Glass	2.99	3.54	55.02	56.29	30	0.050	0.355	0.14	18.5	14.2	13.25	40.04	38.77	0.34387	0.16481	0.00000	0.00000	0.00254	0.06991
SB3-1-35-202		3.98	5	36.47	41.81	35	0.032	0.267	0.12	18.5	14.2	10.55	40.02	35.50	0.36219	0.17359	0.00000	0.00000	0.00268	0.07363
SB3-1-40-202	Bad Glass	2.95	3.26	58.58	56.87	40	0.016	0.361	0.04	18.5	14.2	8.52	40.03	32.80	0.37736	0.18086	0.00000	0.00000	0.00279	0.07672
SB3-2-25-200		3.02	9.3	18.42	35.88	25	0.101	0.415	0.24	18.7	14.2	17.04	40.00	42.99	0.30693	0.15948	0.00000	0.07796	0.00238	0.06108
SB3-2-30-200		2.42	7.44	34.74	48.62	30	0.083	0.389	0.21	18.7	14.2	13.25	40.05	38.91	0.32887	0.17088	0.00000	0.08353	0.00255	0.06544
SB3-2-35-200		2.34	6.89	39.56	50.32	35	0.053	0.391	0.14	18.7	14.2	10.55	40.05	35.65	0.34642	0.18000	0.00000	0.08799	0.00269	0.06894
SB3-2-40-200	Bad Glass	2.17	6.42	43.68	53.93	40	0.054	0.399	0.14	18.7	14.2	8.52	40.05	32.96	0.36091	0.18753	0.00000	0.09167	0.00280	0.07182
SB3-3-25-200		2.82	8.62	24.39	40.13	25	0.128	0.463	0.28	19.95	14.2	17.04	40.03	43.85	0.39895	0.16178	0.00000	0.07804	0.00000	0.05856
SB3-3-30-200	Bad Glass	2.58	7.81	31.49	45.22	30	0.197	0.536	0.37	19.95	14.2	13.25	40.07	39.84	0.42743	0.17333	0.00000	0.08361	0.00000	0.06274
SB3-3-35-200	Bad Glass	2.07	6.14	46.14	56.05	35	0.036	0.436	0.08	19.95	14.2	10.55	40.01	36.65	0.45008	0.18252	0.00000	0.08804	0.00000	0.06607
SB3-3-40-200	Bad Glass	1.96	5.85	48.68	58.39	40	0.060	0.489	0.12	19.95	14.2	8.52	40.01	34.00	0.46891	0.19015	0.00000	0.09172	0.00000	0.06883
SB3-4-25-202		4.65	5.65	28.21	32.02	25	0.048	0.349	0.14	18.9	14.3	25.74	60.04	43.24	0.30168	0.16369	0.00000	0.07892	0.00241	0.06339
SB3-4-30-202	Bad Glass	4.12	4.85	38.37	39.77	30	0.071	0.348	0.20	18.9	14.3	20.02	60.01	39.19	0.32319	0.17537	0.00000	0.08454	0.00258	0.06791
SB3-4-35-202	Bad Glass	3.97	4.62	41.30	41.96	35	0.106	0.458	0.23	18.9	14.3	15.93	60.05	35.90	0.34065	0.18484	0.00000	0.08911	0.00272	0.07158
SB3-4-40-202	Bad Glass	3.05	3.32	57.81	55.41	40	0.107	0.473	0.23	18.9	14.3	12.87	60.03	33.22	0.35493	0.19258	0.00000	0.09285	0.00284	0.07458
SB3-5-25-202	Bad Glass	5.59	5.78	26.56	18.27	25	0.210	0.415	0.50	23.95	16.5	29.70	60.03	49.12	0.35969	0.17490	0.24479	0.00000	0.00214	0.05635
SB3-5-30-202	Bad Glass	4.41	5.21	33.80	35.53	30	0.233	0.407	0.57	23.95	16.5	23.10	60.01	45.09	0.38822	0.18877	0.26421	0.00000	0.00231	0.06082
SB3-5-35-202	Bad Glass	4.16	4.81	38.88	39.18	35	0.229	0.448	0.51	23.95	16.5	18.39	60.02	41.79	0.41155	0.20011	0.28008	0.00000	0.00245	0.06448
SB3-5-40-202	Bad Glass	3.71	4.31	45.24	45.76	40	0.266	0.522	0.51	23.95	16.5	14.85	60.03	39.03	0.43103	0.20958	0.29334	0.00000	0.00256	0.06753
SB3-6-25-202		4.93	5.68	27.83	27.92	25	0.102	0.304	0.34	21.55	15.7	28.26	60.00	46.67	0.35946	0.13925	0.12824	0.00000	0.00226	0.06052
SB3-6-30-202		4.16	5.02	36.21	39.18	30	0.112	0.388	0.29	21.55	15.7	21.98	60.03	42.58	0.38705	0.14994	0.13808	0.00000	0.00243	0.06516
SB3-6-35-202	Bad Glass	4.17	4.9	37.74	39.04	35	0.111	0.378	0.29	21.55	15.7	17.49	60.00	39.26	0.40943	0.15861	0.14606	0.00000	0.00257	0.06893
SB3-6-40-202	Bad Glass	3.31	3.58	54.51	51.61	40	0.104	0.362	0.29	21.55	15.7	14.13	60.04	36.50	0.42803	0.16581	0.15270	0.00000	0.00269	0.07206
SB3-7-25-202		4.48	5.34	32.15	34.50	25	0.093	0.483	0.19	19.4	13	23.40	60.03	42.01	0.30373	0.26516	0.23712	0.00000	0.00179	0.04903
SB3-7-30-202		4.5	5.38	31.64	34.21	30	0.062	0.439	0.14	19.4	13	18.20	60.02	38.15	0.32391	0.28278	0.25287	0.00000	0.00191	0.05229
SB3-7-35-202		3.9	4.46	43.33	42.98	35	0.058	0.370	0.16	19.4	13	14.49	60.05	35.07	0.34007	0.29688	0.26548	0.00000	0.00200	0.05490
SB3-7-40-202	Bad Glass	3.4	3.86	50.95	50.29	40	0.052	0.400	0.13	19.4	13	11.70	60.03	32.55	0.35328	0.30841	0.27580	0.00000	0.00208	0.05703
SB3-8-25-202		4.75	5.63	28.46	30.56	25	0.097	0.357	0.27	19.45	12.7	23.04	60.03	41.79	0.29862	0.26574	0.21350	0.05932	0.00182	0.04761
SB3-8-30-202	Bad Seal	4.49	5.33	32.27	34.36	30	0.055	0.388	0.14	19.45	12.7	17.92	60.02	37.97	0.31823	0.28319	0.22752	0.06321	0.00194	0.05074
SB3-8-35-202		3.93	4.79	39.14	42.54	35	0.087	0.493	0.18	19.45	12.7	14.26	60.02	34.91	0.33391	0.29715	0.23874	0.06633	0.00203	0.05324
SB3-8-40-202	Bad Glass	3.45	3.88	50.70	49.56	40	0.048	0.360	0.13	19.45	12.7	11.52	60.02	32.42	0.34670	0.30852	0.24788	0.06887	0.00211	0.05528
SB3-9-25-202		5.05	5.85	25.67	26.17	25	0.096	0.395	0.24	20.1	13.33	23.94	60.00	42.89	0.32714	0.21905	0.22743	0.05873	0.00180	0.05134
SB3-9-30-202		4.5	5.45	30.75	34.21	30	0.089	0.396	0.22	20.1	13.33	18.62	60.01	39.02	0.34930	0.23388	0.24284	0.06271	0.00193	0.05482
SB3-9-35-202	Bad Glass	4.11	4.82	38.75	39.91	35	0.085	0.390	0.22	20.1	13.33	14.82	60.01	35.92	0.36703	0.24576	0.25516	0.06589	0.00202	0.05760
SB3-9-40-202	Bad Glass	3.81	4.49	42.95	44.30	40	0.172	0.450	0.38	20.1	13.33	11.97	60.02	33.39	0.38158	0.25550	0.26528	0.06850	0.00210	0.05988
SB3-10-25-202	Bad Glass	5.63	5.96	24.27	17.69	25	0.193	0.391	0.49	19.95	13.19	23.76	60.02	42.65	0.36767	0.20221	0.18520	0.00585	0.00180	0.04988
SB3-10-30-202	Bad Glass	4.26	5.03	36.09	37.72	30	0.156	0.416	0.37	19.95	13.19	18.48	60.04	38.79	0.39243	0.21583	0.19768	0.00624	0.00192	0.05324

Sample ID	Comment*	Measured Li_2O (wt%)	Measured B_2O_3 (wt%)	B_2O_3 waste load (wt%)	Li_2O Waste Load (wt%)	Target Waste Load(wt%)	Measured Fe^{+2}	Measured Total Fe	$Fe^{+2}/\Sigma Fe$	SRAT Total Solids (wt%)	% Calcined SRAT Solids	Frit Used (g)	SRAT Sludge Used (g)	SME Total Solids (wt%)	Formate (mol/kg feed)	Nitrate (mol/kg feed)	Oxalate (mol/kg feed)	Coal (mol/kg feed)	Ru (mol/kg feed)	Mn (mol/kg feed)
SB3-10-35-202		4.18	4.9	37.74	38.89	35	0.139	0.407	0.34	19.95	13.19	14.71	60.01	35.71	0.41217	0.22669	0.20762	0.00656	0.00202	0.05591
SB3-10-40-202	Bad Glass	3.7	4.33	44.98	45.91	40	0.202	0.534	0.38	19.95	13.19	11.88	60.03	33.17	0.42844	0.23563	0.21581	0.00682	0.00210	0.05812
SB3-11-25-202		5.15	6.03	23.38	24.71	25	0.122	0.315	0.39	20.4	13.09	23.49	60.03	42.79	0.40878	0.18891	0.17968	0.00587	0.00018	0.05146
SB3-11-30-202	Bad Glass					30				20.4	13.09	18.27	60.01	38.98	0.43602	0.20150	0.19165	0.00626	0.00019	0.05489
SB3-11-35-202	Bad Glass					35	0.363	1.210	0.30	20.4	13.09	14.54	60.06	35.91	0.45791	0.21161	0.20128	0.00658	0.00020	0.05765
SB3-11-40-202	Bad Glass					40	0.345	1.260	0.27	20.4	13.09	11.75	60.04	33.43	0.47568	0.21982	0.20909	0.06956	0.00021	0.05989
SB3-12-25-202		4.96	5.74	27.06	27.49	25	0.116	0.346	0.33	20.5	13.21	23.76	60.08	43.03	0.42350	0.23712	0.18567	0.05882	0.00018	0.05109
SB3-12-30-202		4.43	5.29	32.78	35.23	30	0.144	0.415	0.35	20.5	13.21	18.48	60.03	39.21	0.45186	0.25300	0.19810	0.06276	0.00019	0.05451
SB3-12-35-202	Bad Glass	4.06	4.84	38.50	40.64	35	0.145	0.387	0.37	20.5	13.21	14.71	60.03	36.15	0.47465	0.26576	0.20809	0.06593	0.00020	0.05726
SB3-12-40-202	Bad Glass	3.62	4.31	45.24	47.08	40	0.140	0.345	0.40	20.5	13.21	11.88	60.03	33.64	0.49334	0.27622	0.21628	0.06852	0.00021	0.05952
SB3-13-25-202		5.07	6.03	23.38	25.88	25	0.108	0.316	0.34	20.45	13.33	23.99	60.09	43.15	0.48585	0.25357	0.20181	0.05938	0.00018	0.05306
SB3-13-30-202		4.61	5.56	29.35	32.60	30	0.129	0.366	0.35	20.45	13.33	18.66	60.03	39.31	0.51863	0.27068	0.21542	0.06338	0.00020	0.05664
SB3-13-35-202	Bad Glass	3.94	4.8	39.01	42.40	35	0.167	0.460	0.36	20.45	13.33	14.85	60.03	36.23	0.54502	0.28445	0.22638	0.06661	0.00021	0.05952
SB3-13-40-202	Bad Glass	3.83	4.57	41.93	44.01	40	0.142	0.343	0.41	20.45	13.33	12.00	60.06	33.70	0.56661	0.29572	0.23535	0.06924	0.00021	0.06188
SB3-14-25-202	Bad Glass	5.02	5.88	25.29	26.61	25	0.152	0.324	0.47	20	13.37	24.07	60.09	42.88	0.41244	0.22111	0.20528	0.00631	0.00194	0.05213
SB3-14-30-202		4.58	5.34	32.15	33.04	30	0.142	0.383	0.37	20	13.37	18.72	60.07	39.01	0.44040	0.23610	0.21919	0.00673	0.00207	0.05566
SB3-14-35-202	Bad Glass	4.2	4.95	37.10	38.60	35	0.151	0.443	0.34	20	13.37	14.90	60.08	35.90	0.46285	0.24814	0.23037	0.00708	0.00217	0.05850
SB3-14-40-202	Bad Glass	3.97	4.66	40.79	41.96	40	0.156	0.445	0.35	20	13.37	12.03	60.10	33.34	0.48131	0.25803	0.23955	0.00736	0.00226	0.06083
SB3-15-25-202		5.07	5.95	24.40	25.88	25	0.125	0.326	0.38	20.35	13.14	23.65	60.01	42.87	0.53706	0.23210	0.18503	0.00586	0.00018	0.05301
SB3-15-30-202		4.48	5.26	33.16	34.50	30	0.169	0.469	0.36	20.35	13.14	18.40	60.03	39.04	0.57306	0.24766	0.19744	0.00625	0.00019	0.05656
SB3-15-35-202	Bad Glass	4.05	4.72	40.03	40.79	35	0.204	0.529	0.39	20.35	13.14	14.64	60.03	35.97	0.60192	0.26013	0.20738	0.00657	0.00020	0.05941
SB3-15-40-202	Bad Glass	4.01	4.55	42.19	41.37	40	0.143	0.467	0.31	20.35	13.14	11.83	60.02	33.46	0.62544	0.27030	0.21548	0.00682	0.00021	0.06173
SB3-16-25-202		5.11	5.83	25.92	25.29	25	0.119	0.371	0.32	19.7	13.24	23.84	60.05	42.52	0.41191	0.24939	0.21231	0.05852	0.00179	0.05244
SB3-16-30-202	Bad Glass	4.5	5.14	34.69	34.21	30	0.249	0.502	0.50	19.7	13.24	18.55	60.02	38.65	0.43961	0.26616	0.22659	0.06245	0.00191	0.05597
SB3-16-35-202	Bad Glass	3.93	4.56	42.06	42.54	35	0.241	0.458	0.53	19.7	13.24	14.76	60.04	35.54	0.46190	0.27965	0.23807	0.06562	0.00201	0.05881
SB3-16-40-202	Bad Glass	3.22	3.62	54.00	52.92	40	0.309	0.525	0.59	19.7	13.24	11.92	60.01	33.01	0.48006	0.29065	0.24744	0.06820	0.00209	0.06112
SB3-17-25-202	Bad Seal	4.68	5.36	31.89	31.58	25	0.018	0.386	0.05	19.4	12.95	23.31	60.04	41.94	0.44010	0.22539	0.18008	0.00588	0.00180	0.05094
SB3-17-30-202	Bad Glass	4.38	5.2	33.93	35.96	30	0.142	0.476	0.30	19.4	12.95	18.13	60.03	38.10	0.46924	0.24031	0.19200	0.00627	0.00191	0.05431
SB3-17-35-202	Bad Glass	3.81	4.49	42.95	44.30	35	0.153	0.471	0.32	19.4	12.95	14.43	60.08	35.01	0.49264	0.25230	0.20158	0.00658	0.00201	0.05702
SB3-17-40-202	Bad Glass + Bad Seal	3.23	3.61	54.13	52.78	40	0.096	0.528	0.18	19.4	12.95	11.66	60.02	32.51	0.51157	0.26199	0.20932	0.00684	0.00209	0.05921
SB3-18-25-202		5.02	5.82	26.05	26.61	25	0.017	0.384	0.04	19.05	14.28	25.70	60.04	43.32	0.41382	0.22136	0.00000	0.07778	0.00238	0.06588
SB3-18-30-202	Bad Glass	4.33	5.16	34.43	36.70	30	0.023	0.410	0.06	19.05	14.28	19.99	60.06	39.27	0.44340	0.23718	0.00000	0.08334	0.00255	0.07059
SB3-18-35-202	Bad Glass	3.94	4.66	40.79	42.40	35	0.014	0.374	0.04	19.05	14.28	15.99	60.04	36.07	0.46669	0.24964	0.00000	0.08772	0.00269	0.07430
SB3-18-40-202	Bad Glass	3.35	3.87	50.83	51.02	40	0.017	0.313	0.05	19.05	14.28	12.85	60.07	33.32	0.48682	0.26041	0.00000	0.09150	0.00280	0.07750
SB3-19-25-202	Bad Glass	4.34	5.14	34.69	36.55	25	0.166	0.402	0.41	21.7	13.3	22.23	60.00	42.87	0.53010	0.32599	0.26782	0.06749	0.00021	0.04601
SB3-19-30-202	Bad Glass	4.16	4.79	39.14	39.18	30	0.222	0.421	0.53	21.7	13.3	17.29	60.03	39.21	0.56402	0.34685	0.28496	0.07181	0.00022	0.04895
SB3-19-35-202	Bad Glass	3.75	4.33	44.98	45.18	35	0.210	0.455	0.46	21.7	13.3	13.76	60.01	36.31	0.59096	0.36342	0.29856	0.07524	0.00023	0.05129

Sample ID	Comment*	Measured Li_2O (wt%)	Measured B_2O_3 (wt%)	B_2O_3 waste load (wt%)	Li_2O Waste Load (wt%)	Target Waste Load(wt%)	Measured Fe^{+2}	Measured Total Fe	$Fe^{+2}/\Sigma Fe$	SRAT Total Solids (wt%)	% Calcined SRAT Solids	Frit Used (g)	SRAT Sludge Used (g)	SME Total Solids (wt%)	Formate (mol/kg feed)	Nitrate (mol/kg feed)	Oxalate (mol/kg feed)	Coal (mol/kg feed)	Ru (mol/kg feed)	Mn (mol/kg feed)
SB3-19-40-202	Bad Glass	3.28	3.7	52.99	52.05	40	0.077	0.468	0.16	21.7	13.3	11.12	60.00	33.94	0.61291	0.37691	0.30965	0.07804	0.00024	0.05319
SB3-20-25-202	Bad Glass	4.48	5.1	35.20	34.50	25	0.184	0.362	0.51	21.5	13.4	20.97	60.02	41.83	0.49886	0.32749	0.34778	0.05595	0.00017	0.03543
SB3-20-30-202	Bad Glass	4	4.7	40.28	41.52	30	0.078	0.410	0.19	21.5	13.4	16.31	60.00	38.28	0.52930	0.34748	0.36901	0.05936	0.00018	0.03760
SB3-20-35-202	Bad Glass	3.64	4.26	45.87	46.78	35	0.078	0.420	0.19	21.5	13.4	12.98	60.02	35.46	0.55347	0.36334	0.38586	0.06207	0.00019	0.03931
SB3-20-40-202	Bad Glass	3.26	3.64	53.75	52.34	40	0.063	0.425	0.15	21.5	13.4	10.49	60.00	33.18	0.57299	0.37616	0.39946	0.06426	0.00019	0.04070
SB3-21-30-202	Bad Glass/SME	4.75	5.99	23.89	30.56	30	0.226	0.324	0.70	21.7	13.3	17.00	60.00	38.99	0.45012	0.35693	0.38872	0.05935	0.00177	0.04726
SB3-22-30-320	SME	5.19	5.9	27.16	36.40	30	0.176	0.430	0.41	21.5	13.4	17.10	60.00	38.91	0.50659	0.31505	0.25557	0.06070	0.00020	0.05257
SB3-23-30-320	SME	5.03	5.52	31.85	38.36	30	0.110	0.502	0.22	19.9	13.9	18.30	60.00	38.62	0.34730	0.23730	0.16022	0.06660	0.00223	0.06307
SB3-24-25-202		4.94	6.17	21.60	27.78	25	0.113	0.275	0.41	20.2	12.8	23.04	60.09	51.80	0.24732	0.30685	0.50107	0.06229	0.00129	0.03292
SB3-24-30-202		4.49	5.69	27.70	34.36	30	0.127	0.281	0.45	20.2	12.8	17.92	60.06	49.00	0.26353	0.32697	0.53391	0.06637	0.00137	0.03508
SB3-24-35-202	Bad Glass	4.25	5.36	31.89	37.87	35	0.159	0.497	0.32	20.2	12.8	14.26	60.01	47.40	0.27645	0.34300	0.56009	0.06962	0.00144	0.03680
SB3-24-40-202	Bad Glass	3.69	4.67	40.66	46.05	40	0.274	0.531	0.52	20.2	12.8	11.52	60.01	51.80	0.28705	0.35615	0.58157	0.07229	0.00149	0.03821
SB3A-1-25-202		4.95	6.09	22.62	27.63	25	0.126	0.339	0.37	20.2	11.9	21.43	60.03	49.00	0.49448	0.31638	0.36765	0.05798	0.00018	0.06609
SB3A-1-30-202		4.62	5.61	28.72	32.46	30	0.110	0.327	0.34	20.2	11.9	16.67	60.09	47.40	0.52526	0.33606	0.39053	0.06158	0.00019	0.07020
SB3A-1-35-202		4.29	5.39	31.51	37.28	35	0.177	0.477	0.37	20.2	11.9	13.26	60.07	42.32	0.54963	0.35166	0.40865	0.06444	0.00019	0.07346
SB3A-1-40-202	Bad Glass	3.73	4.66	40.79	45.47	40	0.178	0.611	0.29	20.2	11.9	10.71	60.08	38.54	0.56947	0.36435	0.42340	0.06677	0.00020	0.07611
SB3A-2-25-202		5.15	6.33	19.57	24.71	25	0.132	0.346	0.38	21	13.4	24.12	50.05	35.52	0.41379	0.24054	0.20014	0.07130	0.00022	0.08986
SB3A-2-30-202		4.92	6.04	23.25	28.07	30	0.083	0.399	0.21	21	13.4	18.76	60.10	33.05	0.46733	0.27166	0.22604	0.08053	0.00025	0.10149
SB3A-2-35-202		4.39	5.51	29.99	35.82	35	0.125	0.404	0.31	21	13.4	14.93	60.05	41.19	0.49110	0.28548	0.23753	0.08463	0.00026	0.10665
SB3A-2-40-202	Bad Glass	4.07	5.12	34.94	40.50	40	0.137	0.451	0.30	21	13.4	12.07	60.04	37.53	0.51059	0.29681	0.24696	0.08799	0.00027	0.11088
SB3A-3-25-202		5.42	6.72	14.61	20.76	25	0.056	0.192	0.29	20.6	12.5	22.50	60.06	34.63	0.50588	0.26283	0.23808	0.07056	0.00022	0.07820
SB3A-3-30-202		4.78	5.9	25.03	30.12	30	0.124	0.335	0.37	20.6	12.5	17.50	60.06	32.27	0.53850	0.27977	0.25343	0.07511	0.00023	0.08324
SB3A-3-35-202	Bad Glass	4.24	5.36	31.89	38.01	35	0.203	0.616	0.33	20.6	12.5	13.93	60.04	46.69	0.56444	0.29325	0.26564	0.07873	0.00024	0.08725
SB3A-3-40-202	Bad Glass	3.78	4.74	39.77	44.74	40	0.152	0.675	0.23	20.6	12.5	11.25	60.10	39.79	0.58574	0.30431	0.27566	0.08170	0.00025	0.09055
SB3A-4-25-202		4.79	6.23	20.84	29.97	25	0.102	0.509	0.20	20.2	14.1	25.39	60.02	36.73	0.42937	0.20176	0.00799	0.09604	0.00029	0.10875
SB3A-4-30-202		4.38	5.7	27.57	35.96	30	0.099	0.608	0.16	20.2	14.1	19.74	60.05	34.22	0.45981	0.21607	0.00855	0.10285	0.00031	0.11646
SB3A-4-35-202	Bad Glass	4.05	5.36	31.89	40.79	35	0.209	0.598	0.35	20.2	14.1	15.71	60.05	42.24	0.48431	0.22758	0.00901	0.10833	0.00033	0.12267
SB3A-4-40-202	Bad Glass	3.82	4.95	37.10	44.15	40	0.086	0.403	0.21	20.2	14.1	12.00	60.05	38.52	0.50921	0.23928	0.00947	0.11390	0.00035	0.12898
SB3-NO-25-202	No Formic	4.92	6.26	20.46	28.07	25	0.011	0.355	0.03	23.9	13.45	24.16	60.01	35.55	0.00000	0.81841	0.37553	0.08841	0.00000	0.07017
SB3-NO-30-202	No Formic	4.57	5.83	25.92	33.19	30	0.014	0.411	0.03	23.9	13.45	18.79	60.07	33.12	0.00000	0.87441	0.40123	0.09446	0.00000	0.07497
SB3-NO-35-202	No Formic	4.22	5.41	31.26	38.30	35	0.011	0.385	0.03	23.9	13.45	14.95	60.08	43.92	0.00000	0.91911	0.42174	0.09929	0.00000	0.07880
SB3-NO-40-202	No Formic	3.95	5	36.47	42.25	40	0.015	0.505	0.03	23.9	13.45	12.07	60.00	39.94	0.00000	0.95557	0.43847	0.10323	0.00000	0.08193
MM Feed 200	SME	3.37	8.43	26.05	28.45	25.5	0.068	0.394	0.17	18.1	13.9	24.00	60.00	47.00	0.34913	0.22120	0.00000	0.00000	0.00000	0.09633
MM Feed 320	SME	5.555	5.59	30.99	31.92	25.5	0.064	0.360	0.18	17.95	13.7	24.00	60.00	47.00	0.36182	0.19816	0.00000	0.00000	0.00000	0.12143

* Discussion of shading and designation of "Bad Glass" and effects of coal can be found in Section 3.4 and Section 4.1.

Table V Adjusted SME Concentrations, REDOX, and Electron Equivalents Used for Model

Sample ID	B_2O_3 Waste Loading (wt%)	Li_2O Waste Loading (wt%)	Fe_2O_3 Waste Loading (wt%)	Target Waste Loading (wt%)	REDOX $Fe^{+2}/\Sigma Fe$	Adjusted SME Total Solids (wt%)	Adjusted Oxalate (mol/kg)	Adjusted Formate (mol/kg)	Adjusted Nitrate (mol/kg)	Adjusted Coal (mol/kg)	Adjusted Mn (mol/kg)	Electron Equivalents (mol/kg feed @ 45 wt% solids)
SB3-1-25-320	23.95	29.29	25.52	25	0.119	42.80	0.000	0.321	0.154	0.000	0.065	-0.271
SB3-1-30-320	40.25	40.32	Not measured	30	0.074	40.47	0.000	0.322	0.154	0.000	0.098	-0.360
SB3-5-30-320	34.32	37.99	Not measured	30	0.407	43.24	0.270	0.385	0.187	0.000	0.064	0.820
SB3-5-35-320	41.48	44.49	Not measured	35	0.451	41.06	0.298	0.401	0.195	0.000	0.074	0.956
SB3-6-25-320	28.27	32.6	28.25	25	0.370	46.66	0.128	0.360	0.139	0.000	0.061	0.400
SB3-6-30-320	36.3	38.24	Not measured	30	0.267	42.01	0.155	0.375	0.145	0.000	0.076	0.527
SB3-7-25-320	25.43	30.51	25.25	25	0.125	42.01	0.237	0.304	0.265	0.000	0.049	0.141
SB3-7-30-320	36.67	43.26	Not measured	30	0.193	37.75	0.284	0.315	0.275	0.000	0.063	0.317
SB3-7-35-320	44.32	46.2	Not measured	35	0.142	36.02	0.318	0.325	0.283	0.000	0.073	0.446
SB3-15-30-320	33.58	35.91	Not measured	30	0.331	39.04	0.197	0.573	0.248	0.006	0.057	0.702
SB3-1-25-202	27.7	34.21	28.45	25	0.105	42.84	0.000	0.321	0.154	0.000	0.065	-0.271
SB3-1-35-202	36.47	41.81	Not measured	35	0.118	35.50	0.000	0.362	0.174	0.000	0.074	-0.369
SB3-2-25-200	18.42	35.88	25.77	25	0.242	42.99	0.000	0.307	0.159	0.078	0.061	0.006
SB3-2-30-200	34.74	48.62	Not measured	30	0.212	37.27	0.000	0.325	0.169	0.089	0.070	0.027
SB3-2-35-200	39.56	50.32	Not measured	35	0.136	33.67	0.000	0.345	0.179	0.090	0.071	0.017
SB3-3-25-200	24.39	40.13	28.57	25	0.275	43.85	0.000	0.399	0.162	0.078	0.059	0.189
SB3-4-25-202	28.21	32.02	25.89	25	0.138	43.24	0.000	0.302	0.164	0.079	0.063	-0.027
SB3-6-25-202	27.83	27.92	26.27	25	0.336	46.67	0.128	0.359	0.139	0.000	0.061	0.400
SB3-6-30-202	36.21	39.18	Not measured	30	0.288	42.66	0.161	0.371	0.144	0.000	0.080	0.536
SB3-7-25-202	32.15	34.5	31.75	25	0.193	42.24	0.281	0.291	0.254	0.000	0.065	0.327
SB3-7-30-202	31.64	34.21	Not measured	30	0.141	38.15	0.253	0.324	0.283	0.000	0.052	0.166
SB3-7-35-202	43.33	42.98	Not measured	35	0.155	35.40	0.307	0.328	0.286	0.000	0.070	0.400

Sample ID	B_2O_3 Waste Loading (wt%)	Li_2O Waste Loading (wt%)	Fe_2O_3 Waste Loading (wt%)	Target Waste Loading (wt%)	REDOX $Fe^{+2}/\Sigma Fe$	Adjusted SME Total Solids (wt%)	Adjusted Oxalate (mol/kg)	Adjusted Formate (mol/kg)	Adjusted Nitrate (mol/kg)	Adjusted Coal (mol/kg)	Adjusted Mn (mol/kg)	Electron Equivalents (mol/kg feed @ 45 wt% solids)
SB3-8-25-202	28.46	30.56	26.18	25	0.272	41.79	0.234	0.299	0.266	0.059	0.048	0.373
SB3-8-35-202	39.14	42.54	Not measured	35	0.175	34.91	0.262	0.334	0.297	0.066	0.053	0.500
SB3-9-25-202	25.67	26.17	28.53	25	0.243	42.89	0.227	0.327	0.219	0.059	0.051	0.631
SB3-9-30-202	30.75	34.21	Not measured	30	0.225	39.02	0.243	0.349	0.234	0.063	0.055	0.740
SB3-10-35-202	37.74	38.89	Not measured	35	0.342	35.71	0.208	0.412	0.227	0.007	0.056	0.549
SB3-11-25-202	23.38	24.71	25.45	25	0.387	42.79	0.180	0.409	0.189	0.006	0.051	0.539
SB3-12-25-202	27.06	27.49	31.72	25	0.334	43.03	0.186	0.424	0.237	0.059	0.051	0.562
SB3-12-30-202	32.78	35.23	Not measured	30	0.346	39.21	0.198	0.452	0.253	0.063	0.055	0.658
SB3-13-25-202	23.38	25.88	25.06	25	0.342	43.15	0.202	0.486	0.254	0.059	0.053	0.670
SB3-13-30-202	29.35	32.6	Not measured	30	0.352	39.31	0.215	0.519	0.271	0.063	0.057	0.785
SB3-14-30-202	32.15	33.04	Not measured	30	0.371	39.01	0.219	0.440	0.236	0.007	0.056	0.568
SB3-15-25-202	24.4	25.88	26.28	25	0.382	42.87	0.185	0.537	0.232	0.006	0.053	0.600
SB3-15-30-202	33.16	34.5	Not measured	30	0.360	39.04	0.197	0.573	0.248	0.006	0.057	0.703
SB3-16-25-202	25.92	25.29	27.95	25	0.321	42.52	0.212	0.412	0.249	0.059	0.052	0.588
SB3-18-25-202	26.05	26.61	25.47	25	0.044	43.32	0.000	0.414	0.221	0.078	0.066	-0.104
SB3-22-30-320	27.16	36.40	Not measured	30	0.41	38.91	0.256	0.507	0.315	0.061	0.053	0.960
SB3-23-30-320	31.85	38.36	Not measured	30	0.22	38.62	0.160	0.347	0.327	0.067	0.063	0.648
SB3-24-25-202	21.6	27.78	Not measured	25	0.411	42.32	0.501	0.247	0.307	0.062	0.033	1.221
SB3-24-30-202	27.7	34.36	Not measured	30	0.453	38.54	0.534	0.264	0.327	0.066	0.035	1.428
SB3A-1-25-202	22.62	27.63	Not measured	25	0.371	41.19	0.368	0.494	0.316	0.058	0.066	1.068
SB3A-1-30-202	28.72	32.46	Not measured	30	0.335	37.53	0.391	0.525	0.336	0.062	0.070	1.245
SB3A-1-35-202	31.51	37.28	Not measured	35	0.370	34.63	0.409	0.550	0.352	0.064	0.073	1.412

Sample ID	B_2O_3 Waste Loading (wt%)	Li_2O Waste Loading (wt%)	Fe_2O_3 Waste Loading (wt%)	Target Waste Loading (wt%)	REDOX $Fe^{+2}/\Sigma Fe$	Adjusted SME Total Solids (wt%)	Adjusted Oxalate (mol/kg)	Adjusted Formate (mol/kg)	Adjusted Nitrate (mol/kg)	Adjusted Coal (mol/kg)	Adjusted Mn (mol/kg)	Electron Equivalents (mol/kg feed @ 45 wt% solids)
SB3A-2-25-202	19.57	24.71	Not measured	25	0.380	44.92	0.177	0.425	0.247	0.058	0.073	0.409
SB3A-2-30-202	23.25	28.07	Not measured	30	0.207	40.70	0.196	0.481	0.280	0.064	0.080	0.491
SB3A-2-35-202	29.99	35.82	Not measured	35	0.309	36.73	0.229	0.495	0.288	0.080	0.101	0.719
SB3A-3-25-202	14.61	20.76	Not measured	25	0.292	40.86	0.156	0.543	0.282	0.032	0.035	0.392
SB3A-3-30-202	25.03	30.12	Not measured	30	0.371	40.24	0.237	0.546	0.284	0.067	0.075	0.830
SB3A-4-25-202	20.84	29.97	Not measured	25	0.200	45.92	0.005	0.436	0.205	0.087	0.099	0.019
SB3A-4-30-202	27.57	35.96	Not measured	30	0.163	39.94	0.005	0.460	0.216	0.103	0.116	0.043
MM Feed 200 SME	26.05	28.45	Not measured	25.5	0.173	47.00	0.000	0.511	0.210	0.000	0.096	-0.210
MM Feed 320 SME	29.24	29.68	Not measured	25.5	0.178	47.00	0.000	0.467	0.202	0.000	0.121	-0.304

3.3 Crucible Vitrification

Portions of the 500g SRAT products‡ were shaken and immediately 40-60 grams of slurry was pipetted with a slurry pipette. This amount of slurry was put into a crucible and mixed with Frit 320 (higher alkali) or Frit 202 (lower alkali). The {[F]-3[N]} REDOX correlation [15] was developed for both sludge-only and coupled DWPF operations and covers a wide range of frit compositions. During previous modeling efforts there did not appear to be any effect of frit composition on REDOX although higher alkali is known to stabilize oxidized alkali-ferric iron ($NaFeO_2$) [40] and alkali-manganic ($NaMnO_2$) [41] complexes in glass over their reduced counterparts. In addition, Schrieber, et. al. found small differences in the REDOX of Frit 165 (lower alkali) and Frit 131 (higher alkali) [42]. Since Frit 320 (currently being used in DWPF for the remainder of SB2 processing) and Frit 202 (used in DWPF during non-radioactive startup and a candidate for SB3 processing) differ widely in Na^+ content these were viewed as two frit extremes necessary for testing. Waste loadings of 25, 30, 35, and 40 wt% were targeted with each frit in order to vary the total Fe content of the glass.

Mixing SRAT product and frit provided a "simulated Slurry Mix Evaporator (SME)" product for REDOX evaluation although the simulated SME products were not subjected to a SME process cycle to account for additional losses or gains in reductants or oxidants. The exceptions are SB3-21, SB3-22 and SB3-23, which were subjected to a SME cycle. Therefore, the model developed from these data is applicable to (1) SME concentrations measured after the SME process cycle is complete or (2) SRAT product concentrations adjusted for SME process cycle losses.

Between 40-60 grams of SRAT product were added to each SME batch at the targeted waste loadings (see Table IV). This was the maximum amount of SRAT sample that could be vitrified since eight combinations of frit and waste loadings were being prepared from the 500g of SRAT product. The melting of the SME product was performed in sealed alumina crucibles as described in ITS-00052, Rev. 0 (Vitrification of Melter Slurries for Glass Redox ($Fe^{+2}/\Sigma Fe$) and Chemical Composition Measurement). This procedure supercedes, but is identical to, GTOP-3-046 used to develop the {[F]-[N]} and the {[F]-3[N]} DWPF REDOX algorithms [15]. In these previous studies, it was shown that crucible data could be combined with data from pilot scale melters and that the sealed crucible data REDOX was representative of the REDOX in an unbubbled melt. This will also be demonstrated in this study (see Section 4.9).

One change was made to ITS-00052, Rev. 0 at the beginning of the current study and that was to homogenize (stir) the semi-dry (peanut butter consistency) SME product to eliminate any effects of sludge settling during the drying step. During vitrification of SB3-1, the baseline SB3 SRAT sample, this stirring step was not performed. These eight

‡ If the melter feed contains formic acid or nitric acid, the feed must be refluxed before performing the crucible studies so that redox controlling formate and/or nitrate compounds (such as NaCOOH and $NaNO_3$) form prior to the melter feed being tested.

SME samples formed a refractory layer on the glass-air surface that trapped bubbles from gases that were trying to escape during the feed-to-glass conversion (Figure 8-left) and an "orange-peel" texture on the glass surface (Figure 8-right). Once the stirring step was implemented, the gasesous bubbles, refractory layer and orange-peel texture were no longer observed. The stirring step is currently being incorporated into ITS-00052.

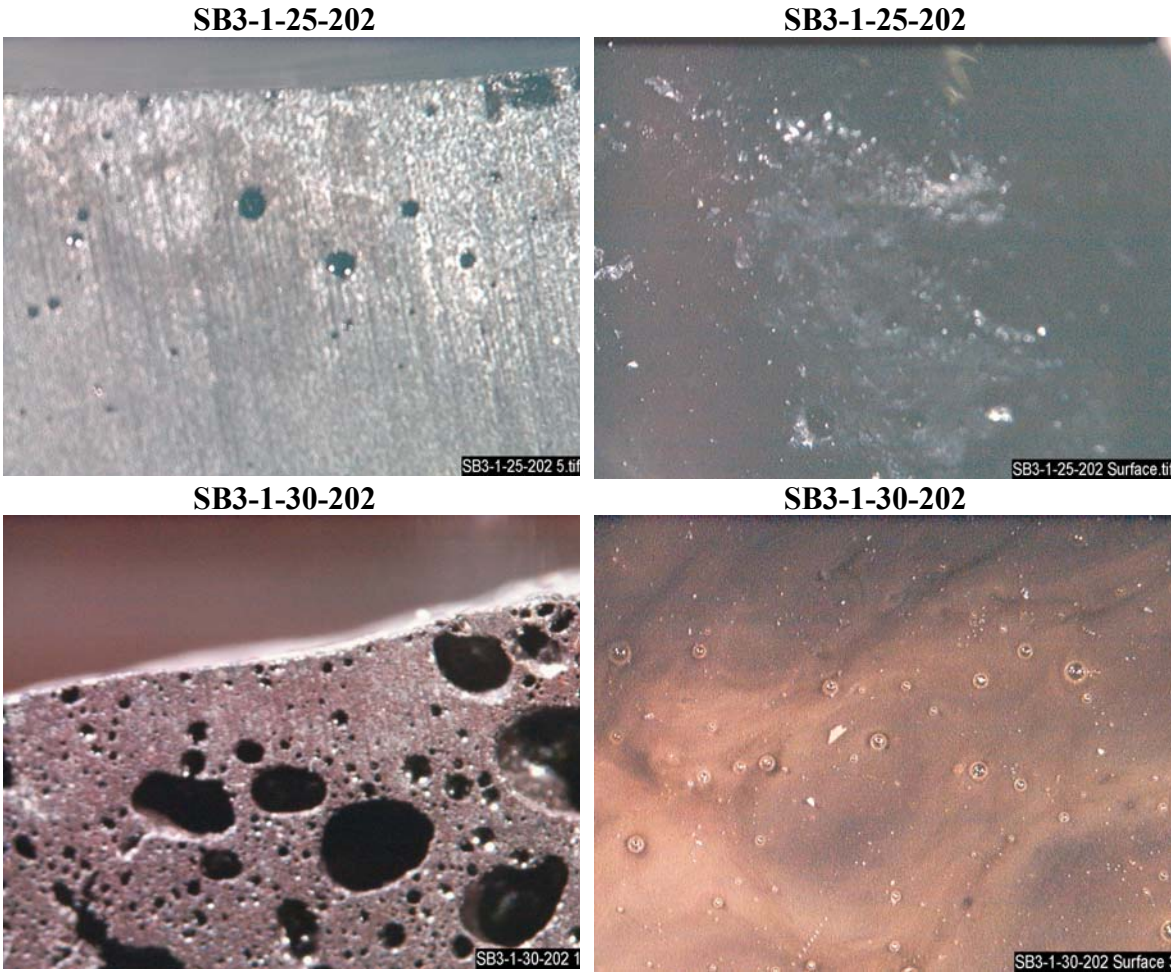

Figure 8. Optical microscope observation of a thin (a few mm) refractory layer on the top of SB3-1 after vitrification which caused bubbles to be trapped near the upper surface under the refractory layer (left) and created an "orange-peel" texture on the vitrified glass product (right).

Sealed crucible vitrification is achieved by sealing Al_2O_3 crucibles with nepheline ($NaAlSiO_4$) gel that melts at a temperature lower than that at which the slurry vitrifies. This causes the crucible to seal before the slurry vitrifies so that air inleakage does not occur during vitrification. This is extremely important as air inleakage will alter the glass REDOX ratio, $Fe^{2+}/\Sigma Fe$, and allow oxidizers and reductants to escape rather than reacting with the transition elements in the glass. During the 185 SME vitrifications in sealed crucibles, only a few lids became unsealed when the sample was properly dried to peanut

butter consistency. Most, but not all, of these samples were rerun. One set of tests was performed leaving the crucibles in the oven for 3 hours instead of the required 1 hour test. This was done to see if the oxalate and coal took longer to react than other reductants previously tested. No change in REDOX was observed in the longer tests than in the one hour tests and so no change was made to ITS-00052.

Vitrification of 40-60 grams of SRAT product with the appropriate amount of frit created only about ¼" of glass in each 100mL crucible. The crucibles were sectioned in half, visual inspections were performed and documented. Half of the samples were sent for analysis and half were archived for future analyses if needed.

3.4 REDOX Measurement

All samples of the vitrified SME product were sent to the SRTC Mobile Laboratory (ML) for $Fe^{+2}/\Sigma Fe$ analysis. All samples were also examined visually at 10X magnification. Good glass (see Table IV) was "black and shiny." Bad glass (see Table IV) contained crystals and/or metallic globules. Visual examination at 10X magnification is consistent with the manner in which previous determinations of good and bad glass have been performed [15,23]. The crystalline species were identified for only a few samples which was considered representative. One sample exhibiting REDOX values of $Fe^{+2}/\Sigma Fe>0.33$ was sent for X-ray Diffraction (XRD) analysis and three samples for Scanning Electron Microscopy (SEM) to identify the crystalline species that were seen visually.

Only one sample replicate from each SME batch was sent to the SRTC-ML for $Fe^{+2}/\Sigma Fe$ analysis by the Baumann method [27, 28]. This is the methodology used to develop the {[F]-[N]} and the {[F]-3[N]} DWPF REDOX models [15, 23]. In this method, a dissolution is performed and two absorbances representing the REDOX state in a given glass are measured: (1) one for Fe^{2+} and (2) one for the total Fe (or ΣFe) after all Fe^{3+} was forcibly reduced to Fe^{2+}. The iron REDOX ratio appropriate for control–the fraction of iron present in the reduced state or $Fe^{2+}/\Sigma Fe$–is computed from these two measured absorbances. The best estimate of the REDOX ratio for a glass from n measurements is the average of the n computed ratios (from the n pairs of measured absorbances):

Equation 14

$$\frac{Fe^{2+}}{\Sigma Fe} = \frac{1}{n}\sum_{i=1}^{n}\left(\frac{Fe_i^{2+}}{\Sigma Fe_i}\right) = \overline{\left(\frac{Fe^{2+}}{\Sigma Fe}\right)}$$

Samples in this study were dissolved once and two sets of absorbances read for the single dissolution. The n pairs of measured absorbances from each sample were averaged and then the REDOX ratio was calculated. These averages are tabulated in Table IV. The DWPF Environmental Assessment (EA) glass [43], with a known REDOX, was always analyzed in tandem as a standard.

The error structure in the REDOX measurement was examined during the development of the {[F]-3[N]} REDOX model [15]. Moments (e.g., means, standard deviations, and

correlations) were estimated for the computed EA glass REDOX ratios and for data obtained from the Oak Ridge Consolidated Neutralization Facility (CNF) measured by the Baumann [27] REDOX method. From these data, there was no indication that the errors in the computed iron REDOX ratio were relative to the magnitudes of the ratios. The pertinent variance components for the computed $Fe^{2+}/\Sigma Fe$ REDOX ratio are given in Reference 15 as a residual variance of 0.002163 and a sample-to-sample variance of 0.000697.

3.5 Glass Analyses

The glass sample ID values used throughout this study include the SRAT batch ID, the frit ID, and the target waste loading. Thus glass SB3-1-25-202 was made from SRAT batch SB3-1 at a target waste loading of 25 wt% with frit 202.

All of the glasses were dissolved by Na_2O_2 fusion and analyzed for B and Li by ICP-ES. The B and Li oxide values were used to calculate the actual waste loadings achieved in each SRAT-frit mixture against the target REDOX, as previously described in Section 3.2.

Whole element chemistry of one glass from each set of SRAT batches (for batches SB3-1 through SB3-18 only) was analyzed to verify the waste loadings and total oxide sums, e.g. only 36 of the 185 glasses made were analyzed. These comparisons are shown in Table VI. Note that Gd_2O_3 and Sm_2O_3 were not analyzed. Since the contribution from these elements, when present, was small, the oxide sums given in Table VI are almost all (one exception) within 100±5% indicating quality analyses.

The whole element chemistry also demonstrates that for pairs of glasses made at the same target waste loading, the waste sludge constituents (solids) often vary widely from each other at different frit compositions. For example, the Al_2O_3 and Fe_2O_3 content of SB3-1-25-202 are 7.76 and 13.65 while the companion SB3-1-25-320 values are 6.67 and 12.24. These types of differences are seen in other pairs of values given in Table VI and demonstrate the difficulties with accurately batching target waste loading despite repetitive mixing and shaking of the SRAT solids.

3.6 Quality Assurance

All the data reported in this study were developed under the quality assurance given in technical task plan WSRC-RP-2002-00341 [44]. The research program and task plan were developed to address TTR - HLW/DWPF/TTR-02-0017. The data are recorded in notebooks WSRC-NB-2002-00156, WSRC-NB-2002-00199, WSRC-NB-2003-00034.

Table VI Glass Analyses For Simulated SME Samples at Target Waste Loading of 25%

oxide wt%	Al_2O_3	B_2O_3	Fe_2O_3	Li_2O	SiO_2	Na_2O	BaO	CaO	Cr_2O_3	CuO	K_2O	MgO	MnO	NiO	PbO	PdO	RhO_2	RuO_2	ZnO	ZrO_2	Total
Batch1/Standard	4.83	8.29	12.84	4.47	50.51	9.40	0.14	1.26	0.10	0.38	3.54	1.42	1.73	0.72	0.00	0.00	0.00	0.03	0.00	0.07	99.73
SB3-1-25-202	7.76	5.69	13.65	4.50	50.93	7.45	0.11	1.38	0.13	0.06	0.26	1.43	1.39	1.28	0.05	0.00	0.02	0.05	0.13	0.23	96.50
SB3-1-25-320	6.67	6.16	12.24	5.77	53.38	11.47	0.10	0.96	0.11	0.06	0.04	0.05	1.22	1.10	0.04	0.00	0.02	0.04	0.11	0.19	99.72
SB3-2-25-202	6.59	9.30	11.73	3.02	51.85	10.47	0.09	0.97	0.12	0.06	0.10	1.46	1.23	1.15	0.05	0.00	0.02	0.04	0.12	0.20	98.56
SB3-2-25-320	6.32	5.99	11.81	5.69	53.98	10.96	0.10	0.79	0.12	0.07	0.05	0.05	1.18	1.32	0.05	0.01	0.02	0.04	0.12	0.19	98.86
SB3-3-25-202	7.25	8.62	13.35	2.82	49.89	10.60	0.09	1.21	0.13	0.07	0.08	1.41	1.35	1.30	0.06	0.00	0.00	0.03	0.12	0.21	98.59
SB3-3-25-320	6.98	5.69	11.98	5.33	51.89	11.17	0.10	0.89	0.12	0.05	0.05	0.06	1.11	1.13	0.04	0.00	0.00	0.03	0.11	0.19	96.92
SB3-4-25-202	6.64	5.65	12.26	4.65	54.41	6.80	0.09	1.09	0.12	0.05	0.06	1.51	1.24	1.18	0.04	0.00	0.02	0.04	0.10	0.20	96.17
SB3-4-25-320	6.58	6.00	12.02	5.67	53.25	11.08	0.09	0.97	0.12	0.05	0.00	0.06	1.17	1.11	0.04	0.00	0.02	0.04	0.10	0.19	98.58
SB3-5-25-202	6.01	5.78	10.52	5.59	53.50	15.93	0.09	0.92	0.10	0.09	0.00	0.08	1.04	1.05	0.05	0.00	0.03	0.03	0.10	0.17	101.07
SB3-5-25-320	6.71	5.55	10.37	4.67	56.71	11.26	0.07	0.95	0.10	0.05	0.03	1.45	1.01	1.05	0.05	0.00	0.00	0.03	0.10	0.17	100.34
SB3-6-25-202	6.23	5.68	10.57	4.93	55.69	8.89	0.08	1.08	0.21	0.06	0.10	1.53	1.10	1.04	0.04	0.00	0.03	0.04	0.09	0.19	97.56
SB3-6-25-320	6.18	5.81	11.38	5.50	52.74	13.68	0.10	1.03	0.11	0.06	0.00	0.06	1.19	1.08	0.04	0.00	0.00	0.03	0.11	0.18	99.28
SB3-7-25-202	7.12	5.34	12.67	4.48	51.92	12.54	0.09	1.18	0.14	0.19	0.05	1.42	1.26	1.21	0.04	0.00	0.02	0.04	0.13	0.20	100.08
SB3-7-25-320	5.69	6.04	10.08	5.67	51.57	14.61	0.08	0.89	0.10	0.26	0.05	0.05	1.03	0.98	0.04	0.00	0.01	0.04	0.13	0.16	97.49
SB3-8-25-202	6.04	5.63	10.53	4.75	53.67	11.42	0.08	1.00	0.30	0.07	0.03	1.49	1.06	1.02	0.04	0.01	0.04	0.03	0.10	0.16	97.47
SB3-8-25-320	6.59	6.02	10.63	5.66	53.65	15.11	0.09	0.92	0.11	0.05	0.01	0.05	1.06	0.99	0.04	0.00	0.01	0.03	0.10	0.17	101.28
SB3-9-25-202	6.04	5.85	10.74	5.05	54.21	10.85	0.07	0.98	0.10	0.07	0.08	1.53	1.06	0.99	0.04	0.00	0.01	0.03	0.09	0.16	97.98
SB3-9-25-320	8.48	5.93	9.32	5.56	52.94	14.78	0.08	0.82	0.09	0.07	0.13	0.05	0.96	0.92	0.03	0.00	0.00	0.03	0.09	0.14	100.42
SB3-10-25-202	6.16	5.96	9.61	5.63	53.50	15.80	0.08	0.84	0.09	0.09	0.06	0.07	0.94	0.89	0.04	0.00	0.00	0.04	0.11	0.15	100.05
SB3-10-25-320	5.14	5.98	9.71	5.09	53.93	16.07	0.08	0.93	0.09	0.05	0.07	0.08	0.94	0.88	0.03	0.00	0.00	0.03	0.09	0.16	99.36
SB3-11-25-202	5.96	6.03	9.77	5.15	57.68	10.91	0.07	0.95	0.10	0.05	0.05	1.58	0.98	0.93	0.04	0.00	0.00	0.02	0.09	0.16	100.52
SB3-11-25-320	3.75	6.58	6.44	6.16	57.61	16.99	0.05	0.55	0.07	0.04	0.01	0.03	0.69	0.61	0.02	0.00	0.00	0.01	0.05	0.09	99.74
SB3-12-25-202	6.80	5.74	12.15	4.96	55.23	11.04	0.08	1.07	0.13	0.05	0.00	1.48	1.12	1.10	0.04	0.00	0.00	0.03	0.10	0.19	101.30
SB3-12-25-320	4.33	6.45	7.58	6.11	57.09	16.05	0.06	0.63	0.07	0.04	0.00	0.03	0.77	0.72	0.02	0.00	0.00	0.01	0.06	0.11	100.14
SB3-13-25-202	5.68	6.03	9.77	5.07	58.74	11.45	0.06	0.92	0.09	0.05	0.03	1.55	0.97	0.93	0.03	0.00	0.00	0.02	0.07	0.14	101.61
SB3-13-25-320	6.38	6.21	10.10	5.76	54.51	14.92	0.08	0.86	0.09	0.05	0.00	0.05	0.99	0.94	0.03	0.00	0.00	0.02	0.09	0.15	101.25
SB3-14-25-202	6.02	5.88	9.98	5.02	57.69	11.22	0.07	0.97	0.09	0.05	0.03	1.53	0.97	0.91	0.03	0.00	0.00	0.03	0.08	0.15	100.72
SB3-14-25-320	7.56	6.12	9.18	5.76	51.89	14.02	0.07	0.79	0.09	0.04	0.07	0.04	0.89	0.87	0.04	0.00	0.00	0.03	0.08	0.14	97.67
SB3-15-25-202	5.94	5.95	10.28	5.07	58.25	11.55	0.07	1.00	0.10	0.05	0.05	1.55	1.04	0.98	0.03	0.00	0.00	0.02	0.08	0.16	102.19
SB3-15-25-320	6.28	5.91	11.58	5.50	52.91	14.20	0.09	1.05	0.11	0.06	0.02	0.06	1.12	1.07	0.04	0.00	0.00	0.03	0.12	0.19	100.33
SB3-16-25-202	7.03	5.83	10.86	5.11	57.30	11.50	0.07	1.03	0.10	0.05	0.03	1.53	1.10	1.04	0.03	0.00	0.00	0.03	0.09	0.17	102.90
SB3-16-25-320	5.47	6.31	8.23	6.03	57.60	16.07	0.07	0.77	0.08	0.03	0.04	0.04	0.83	0.73	0.03	0.00	0.00	0.03	0.09	0.14	102.59
SB3-17-25-202	9.74	5.36	10.24	4.68	55.35	11.58	0.07	0.99	0.10	0.05	0.00	1.43	1.07	0.99	0.03	0.00	0.00	0.04	0.09	0.17	101.98
SB3-17-25-320	5.74	6.00	9.98	5.75	55.52	15.12	0.08	0.92	0.09	0.05	0.06	0.05	0.98	0.94	0.03	0.00	0.00	0.03	0.10	0.16	101.59
SB3-18-25-202	7.04	5.82	12.11	5.02	58.95	7.43	0.08	1.05	0.12	0.06	0.02	1.49	1.15	1.12	0.04	0.00	0.02	0.03	0.11	0.19	101.86
SB3-18-25-320	7.36	5.94	12.50	5.68	56.99	12.36	0.10	1.11	0.12	0.07	0.05	0.06	1.22	1.15	0.05	0.00	0.01	0.04	0.13	0.24	105.19

4.0 REGRESSION ANALYSIS OF MODEL CRUCIBLE DATA

In this study, REDOX measurement, prediction, and control information pertinent to DWPF (i.e., feed or glass produced from simulated waste sludge) is examined. The REDOX data developed in this study are designated as "Model Data" while REDOX data available from previous studies at SRS, Pacific Northwest National Laboratory (PNNL), and West Valley Nuclear Services (WVNS) are designated as "Validation Data." In Section 4.0 the "Model Data" developed in this study will be discussed and assessed against recent SME analyses available from DWPF, SRTC minimelter studies, and SRTC Slurry-fed Melt Rate Furnace (SMRF) studies. In Section 5.0 the "Model Data" developed in this study will be assessed against historical data from SRS and the open literature.

The SRTC historical REDOX data that were previously used to develop the {[F]-3[N]} correlation given in the 1997 report are also used in the development of the REDOX model in this study. These data were utilized in 1997 with the concentration units of mol/L (molar) normalized to 45 wt% solids. In this study, the concentration units were chosen to be mol/kg of feed normalized to 45 wt% solids. The conversion factor between these units is the density of the feed. The use of mol/kg in this study eliminated the need to estimate the SME melter feed density.

In order to use the data from the 1997 study that are expressed as mol/L, the data needed to be converted to mol/kg at the given wt% solids using the density, then adjusted to 45 wt% solids using the ratio of wt% solids, as shown below.

$$C_1\,(mol/kg\ \ slurry) = \frac{C_1\,(mol/L)}{\rho_1\,(kg/L)}$$
$$where\ \rho_1 = density\ at\ initial\ total\ solids\ content\ T_1$$

For example, at 35 wt% solids (T_1), the density is about 1.256 kg/L. This density value is from a correlation of density versus total solids that was derived from SRTC and DWPF data. This correlation is shown in Figure 9. The supporting data for this correlation is given in Appendix F. When the concentration in mol/kg is adjusted to 45% solids, the following results:

$$C_1^{norm}\,(mol/kg\ \ slurry) = \frac{C_1\,(mol/L)}{\rho_1\,(kg/L)} \times \frac{45\,wt\%\ \ solids}{T_1\,wt\%\ \ solids}$$

This method normalizes the concentration on a 'per mass of slurry' basis using the total solids in wt%, which makes intuitive sense; when mol/kg slurry is divided by the actual total solids content, the result is a concentration expressed as mol/kg solids:

$$C_1^{'}\,(mol/kg\ \ solids) = \frac{C_1\,(mol/L)}{\rho_1\,(kg/L)} \times \frac{1}{T_1\,wt\%\ \ solids}$$

The previously used normalization multiplied the mol/L concentration by the total solids ratio, where the intermediate result would be:

$$M_1^{'}\left(\frac{mol/L}{kg\ solids/kg\ slurry}\right) = M_1\,(mol/L) \times \frac{100}{T_1\ wt\%\ solids}\left(or\ \frac{kg\ slurry}{kg\ \ solids}\right)$$

where in the volumetric based mol/L has been adjusted by a mass term. The previous normalization would have made more physical sense if the concentrations had first been converted to mol/kg, then normalized, then converted back to mol/L.

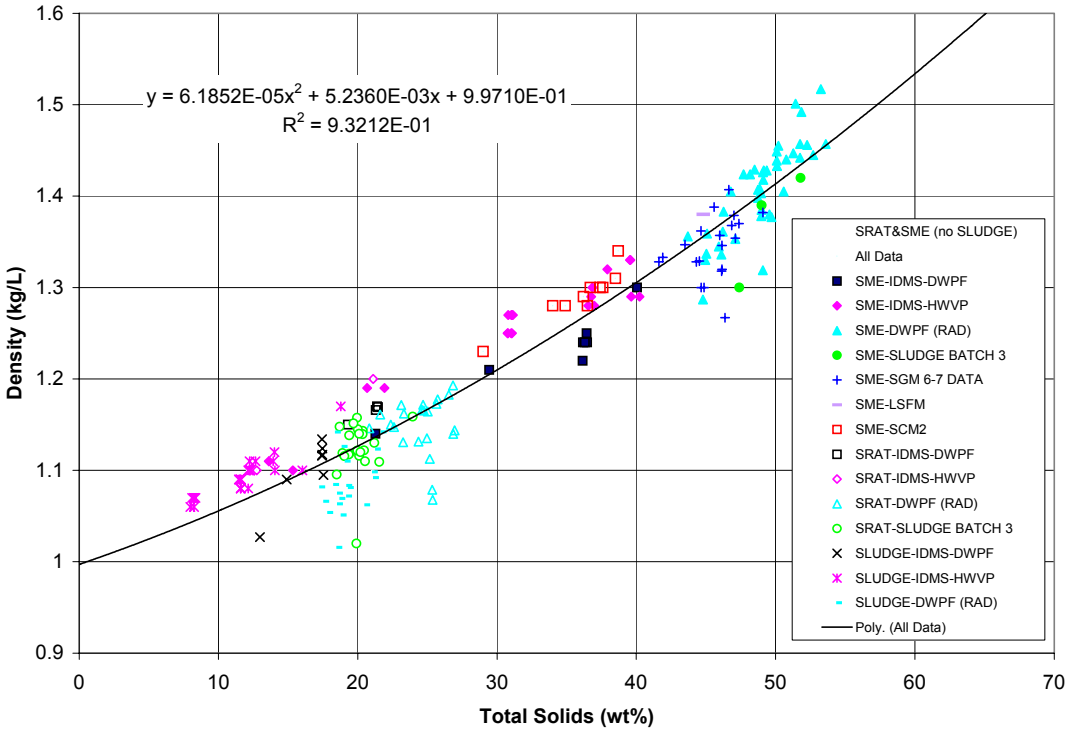

Figure 9. Density correlated to total solids.

4.1 Glass Modeling Criteria

The crucible REDOX data and SME feed analyses used in this study are provided in Table IV. Those glasses with measured REDOX ratios less than 0.03 are below the detection limit (BDL) [23,24,25,26] for the REDOX analysis technique and are omitted from modeling. Those glasses whose measured REDOX values are proximate to the detection limit (i.e., $Fe^{2+}/\Sigma Fe \leq 0.05$ but ≥ 0.03) are used recognizing that analyte data can be inaccurate to ±100% in this region. Glasses included in model data had to adhere to the following criteria:

- Glass must be produced from refluxed melter feed material to ensure conversion to nitrate and formate species.

- Vitrified material must be visibly black and homogeneous; that is, it must contain no brown discoloration due to metallic copper and/or no crystalline or other metallic material as these species make both reliable REDOX ratio and cation measurements difficult–if not impossible.

- The iron REDOX ratio (i.e., $Fe^{2+}/\Sigma Fe$) is measured using the Baumann colorimetric technique [27,28] and must be greater than or equal to the SRTC detection limit of $Fe^{2+}/\Sigma Fe \leq 0.03$ [23,24,25,26].

- Both REDOX and feed chemistry measurements (to which the REDOX ratio will be related) must be available for the same sample.

- Measured or as-made total solids information must be available. ("Model Data" samples were either measured or formulated to be approximately 45% total solids.)

These are the same criteria that were applied during development of the {[F]-3[N]} REDOX modeling in 1997. Most of the glasses at high waste loadings crystallized significant amounts of spinel and other phases and were designated as "bad glass" in Table IV. Since the crucibles had been air-quenched from the melt temperature of 1150°C and each crucible only contained about ½" of glass, the samples were cooled rapidly enough to avoid crystallization. Crystallization must, therefore, be due to high waste loadings and/or surface reaction of the feed with coal. X-ray diffraction analysis was only performed on one glass and SEM analyses on three glasses (see discussion in Section 3.4) because the spinels, metallic phases, and sulfides formed are typical of the phases seen in previous REDOX studies. Therefore, the type of crystallization was not defined for each and every glass studied.

During visual inspection at 10X magnification, waste loadings between 22.5% and 62.5% had some type of crystallization, surface reaction with coal, or brown swirls that were deemed to be "bad glass" in Table IV. This is the same magnification and criteria used during the development of the 1997 REDOX model. These glasses are excluded from "Model Data" and shown as shaded in Table IV. During the visual observations it became apparent that the coarse coal and the activated charcoal floated on the glass sample surface (see comment column in Table IV) and caused a surface reaction that was not characteristic of the entire sample (see Figure 11-SB3-19-30-202). In addition, there appeared to be a reaction layer that penetrated the glass from the upper surface (see Figure 12) which was different from the reaction layers observed in SB3-1 before a stirring step was added to the sealed crucible vitrification procedure, e.g. note the absence of bubbles. Therefore, the effects of waste loading on crystallization cannot be separated from the effects of REDOX on crystallization.

As seen in Figure 11 (SB3-19-30-202), crystallization and metallic deposits were often found floating on the glass surface and not characteristic of the bulk. This appeared to have been a local reaction with coal that had floated on the glass pool during vitrification. The thin amount of glass in the bottom of each crucible (due to the limited amount of SRAT product available and the necessity of making 8 SME batches from each SRAT batch) made it difficult to get a glass REDOX sample that was free of these local surface interactions. This was especially true of the samples made with Frit 320 and coarse coal. This may be an effect of the glass viscosity and should be examined further. Samples that had highly variable REDOX measurements that were made from Frit 320 and coarse coal (CC) and/or activated charcoal (ACT) were also deleted from "Model Data". They are shown as shaded in Table IV. Lastly, any samples that the seal integrity was compromised were not used in "Model Data" and are shaded in Table IV.

X-ray diffraction analyses indicated that sample SB-19-25-202 with a $Fe^{+2}/\Sigma Fe$ of 0.41 had precipitated Ni_3S_2 (Heazlewoodite) and a metallic species consisting of Ni°, Cr°, and Fe° resembling steel (Figure 10). Note that the samples were ground in an agate mortar and pestle so the metallic steel precipitates are not considered contamination from grinding.

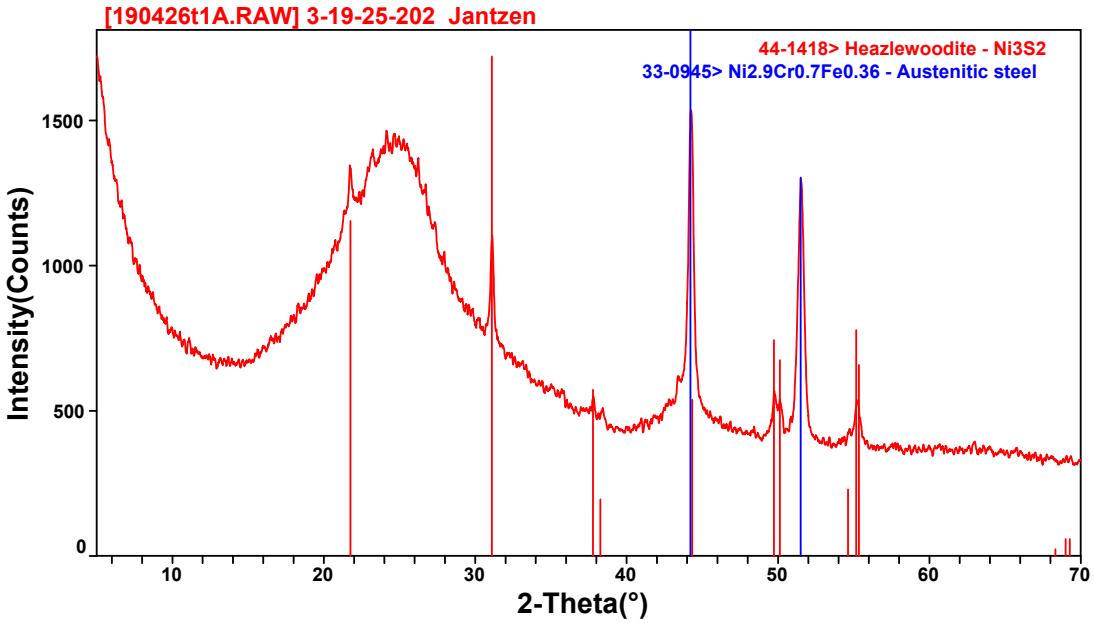

Figure 10. X-Ray Diffraction Spectra of Reduced Sample SB3-19-25-202.

Scanning Electron Microscopy (SEM) of the surface layer of SB3-19-30-202 is shown in Figure 11. Energy dispersive analysis by X-ray (EDAX) of the surface features indicated that the dark round metallic looking globules were enriched in Fe, Ni, Ti and carbon, confirming the identification of a metallic phase in the companion sample SB3-19-25-202. The dark spongy looking phase was mostly carbon with Si, Al, and Na from the glass matrix and a trace of Ni.

The SEM's shown in Figure 11– SB3-19-35-202 represent the 35wt% waste loaded samples which had formed numerous small triangular crystals whose morphology is consistent with spinel. EDAX analysis of the triangular crystals showed that they were enriched in Fe, Ni and Cr, also typical of spinel. The areas identified as Spot 1 in Figure 11- SB3-19-35-202 appears to be phase separated and EDAX analysis indicated that the second phase was enriched in Si compared to the matrix.

The SEM's shown in Figure 11– SB3-19-40-202 represent the 40 wt% samples which had formed numerous triangular and hexagonal spinel crystals. EDAX analysis of the spinel crystals showed that they were enriched in Fe, Ni and Cr as in sample SB3-19-35-202. The areas identified as Spot 4 in Figure 11-lower left are spinels imbedded in some unreacted material. EDAX analysis of Spot 3 (the matrix) indicates that it is glass that is somewhat enriched in Fe while the spinels (Spot 4) are Ni-Fe spinels devoid of Cr. None of the samples shown in the SEM's in Figure 11 were used in "Model Data" but are shown as examples of "bad glass" and/or glass reacted locally with carbon containing species.

SB3-19-30-202

SB3-19-30-202

SB3-19-35-202

SB3-19-35-202

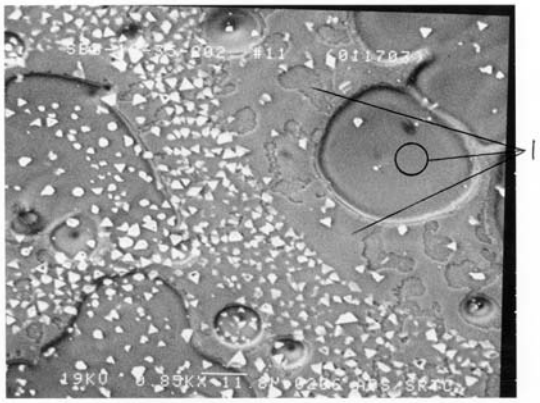

SB3-19-40-202

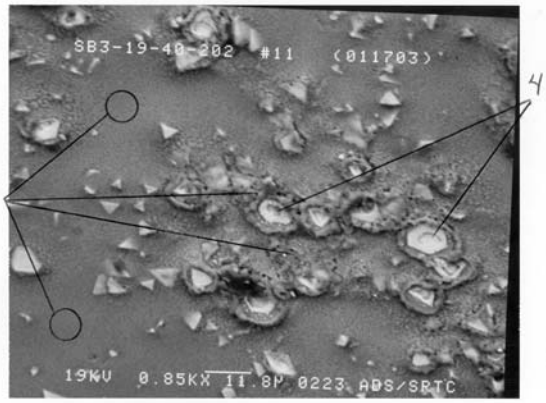

SB3-19-40-202

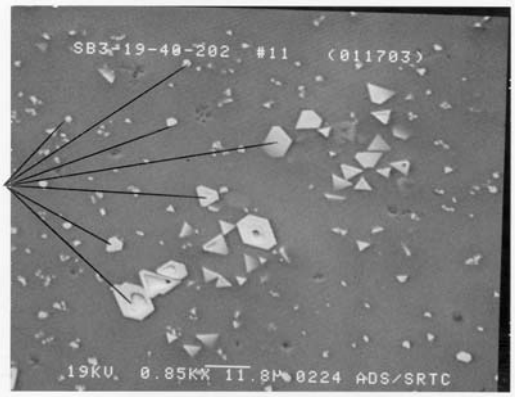

Figure 11. Scanning Electron Micrographs (SEM) of the metallic and crystalline species formed on glasses in this study as a surface reaction with coal.

Figure 12. Reaction front in REDOX glasses observed when sectioned. White area in lower left is bottom of Al_2O_3 crucible. Thickness from bottom of crucible to top of glass is ~1/2 inch.

4.2 Model Parameter Ranges

The "Model Data" used in this study are presented in Table V. While previous studies have shown that the REDOX of a glass vitrified in a sealed crucible can be reasonably predicted from measured molar formate and nitrate concentrations in the feed, it must be shown that this can be expanded to include the role of other reductants and oxidants. Any resulting prediction will be validated against other information so as to be useful for process control.

The REDOX ratios in the current study overlap those used in the 1997 REDOX modeling study. The REDOX ratios in the 1997 study spanned the following ranges: $0.03 \leq Fe^{2+}/\Sigma Fe \leq 0.635$. For comparison, the current model spans $0.04 \leq Fe^{2+}/\Sigma Fe \leq 0.45$. The distribution of the current REDOX ratio is shown by the darker shaded regions in Figure 13 compared to the lighter shaded regions, e.g. the 1997 REDOX ratios.

The independent variable (X) in the REDOX correlations was previously either {[F]-[N]} or {[F]-3[N]}, whereas the Molar Electron Equivalents (ξ) is a much more complicated combination of concentrations (see Section 4.7 for the development of this model):

Equation 15

$$\xi \text{ (mol/kg feed)} = 2[F] + 4[C] + 4[O_T] - 5[N] - 2[Mn]$$

where [F] = formate (mol/kg feed)
[C] = coal (carbon) (mol/kg feed)
[O_T] = total oxalate, soluble and insoluble (mol/kg feed)
[N] = nitrate + nitrite (mol/kg feed)
[Mn] = manganese (mol/kg feed)

The range of ξ for the 53 data points analyzed in this study is $-0.37 \leq \xi \leq 1.43$ (Δ=1.80), while the range for the 1997 data was $-1.06 \leq \xi \leq 2.51$ (Δ=3.57). The 1997 data covered about twice the range of ξ as the data developed in this study. A decision was made to merge the 53 data values in this study (from Table IV) with 67[f] data values from 1997 after the pertinent Mn values for the historic data were located (see Appendix A). The 120 pooled REDOX values define the "Model Data" used in this study.

The distributions of the mean measured REDOX ratios from Table IV can be directly compared to the mean measured REDOX ratios from the 1997 study. However, the formate and nitrate concentrations from the 1997 study were divided by the slurry density to enable the comparison to be made on a consistent basis (see Section 5.1), e.g. mol/kg feed at 45% solids. The independent variables used in the 1997 regression analyses possess the following ranges: $0.23 \leq$ formate (mol/kg) ≤ 1.87; and $0.06 \leq$ nitrate (mol/kg) ≤ 0.59. The independent variables used in the current study (53 data points) cover narrower ranges: $0.24 \leq$ formate (M) ≤ 0.68; and $0.14 \leq$ nitrate (M) ≤ 0.38. This can be seen in Figure 13 as the darker shading, which corresponds, to the moments and quantiles for the "Model Data" used in this study.

The current study examines the effects of additional solid reductants such as sodium oxalate and coal and an additional feed oxidizer, manganese. A plot of the total feed reductants (formate, oxalate, and coal) and total oxidants (nitrate and manganese) are shown in Figure 14. The concentration data for the total reductants and total oxidizers are developed in mol/kg feed at 45% solids. Figure 14 indicates that the total reductant concentration (dark shading) examined in this study covers a narrower range (lighter shading) than the formate ranges covered in the 1997 REDOX modeling effort (compare Figure 14 to Figure 13). The current oxidizer concentrations (darker shading) examined in this study also cover a narrower range than the nitrate concentrations covered in the 1997 REDOX modeling effort. This is because target REDOX values were concentrated around a $Fe^{2+}/\Sigma Fe$ ratio of ~0.2 which is more oxidizing than the REDOX values studied in 1997.

---

[f] The formate, nitrate and REDOX values in Appendix A were comprised of 123 individual analyses that were averaged for the 1997 modeling. During the current REDOX modeling the 1997 individual values given in Appendices B, C, and D were used since the newly gathered data was comprised of individual analyses. Of the 123 values from 1997, only 72 measurements had $Fe^{+2}/\Sigma Fe$ ratios greater than the detection limit. Of the 72 values, two were missing formate concentrations, one was missing a nitrate concentration, and two were missing Mn values. This left a 1997 data pool of 67 samples.

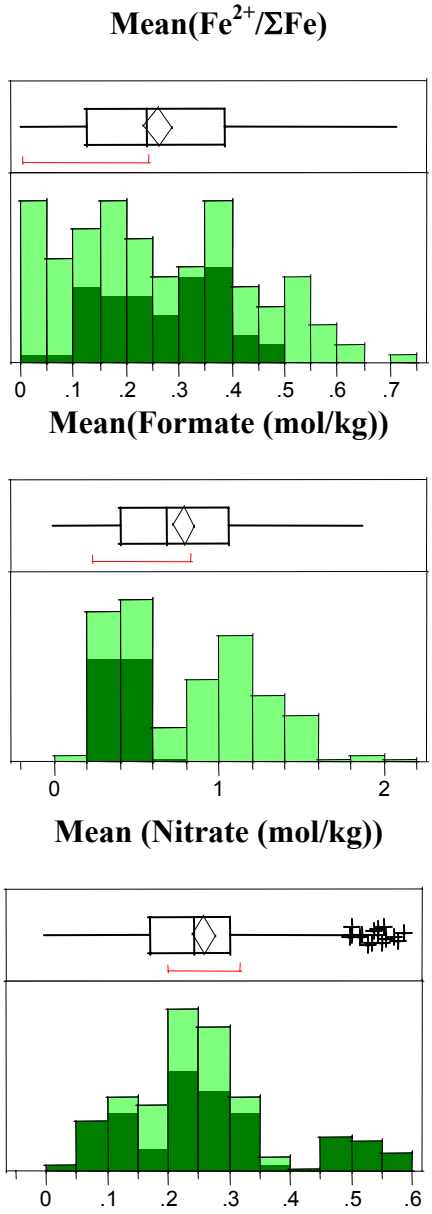

Quantiles

maximum	100.0%	0.45276
median	50.0%	0.27538
minimum	0.0%	0.04433

Moments

Mean	0.26702
Std Dev	0.10731
Upper 95% Mean	0.29660
Lower 95% Mean	0.23744
N	53

Quantiles

maximum	100.0%	0.68430
median	50.0%	0.40878
minimum	0.0%	0.24732

Moments

Mean	0.40968
Std Dev	0.09242
Upper 95% Mean	0.43515
Lower 95% Mean	0.38421
N	53

Quantiles

maximum	100.0%	0.37742
median	50.0%	0.23712
minimum	0.0%	0.13925

Moments

Mean	0.23540
Std Dev	0.05899
Upper 95% Mean	0.25166
Lower 95% Mean	0.21914
N	53

Figure 13. Distribution Summary for Parameters Used in REDOX Prediction (i.e., "Model Data")

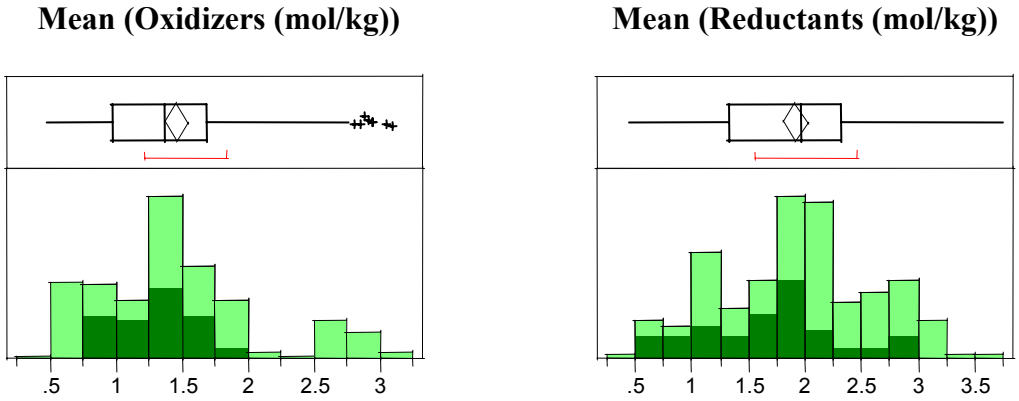

Figure 14. Distribution Summary for Grouped Feed Parameters Used in REDOX Prediction (i.e., "Model Data"). Moments for "Model Data" used in this study correspond to the darker shaded data only.

4.3 The Effect of Alkali on REDOX

Whole element chemical analyses of the SRAT calcine solids were available from References [33,34,35,36]. Frit analyses were available from the vendor. Combining the frit with the calcine SRAT solids analyses at the waste loadings determined in Table IV from the B_2O_3 analyses, allowed a final glass composition to be calculated for each of the SME vitrifications. While these glass analyses are estimates, they were used to determine if there was an alkali-REDOX effect as predicted in the literature (References 40,41).

For all of the glasses in Table IV, the measured REDOX ratio was plotted against the calculated redox (see Section 4.8) as shown in Figure 15. The data was regressed by frit type. Frit 202 (lower in alkali) is shown in red and Frit 320 (higher in alkali) is shown in green. The 95% confidence intervals are shown for the Frit 202 data in red. It can easily be seen that the OLS fit of the Frit 320 glasses falls well within the 95% confidence bands of the Frit 202 data. Since these two frits, and the glasses derived from them, differ widely in Σalkali oxides, e.g. $Li_2O + Na_2O + K_2O$ (see Table VI), it can readily be seen that there is no statistically significant difference in the redox response as a function of alkali. Therefore, the alkali-iron and alkali-manganese effects on glass REDOX discussed in the open literature were not considered during modeling.

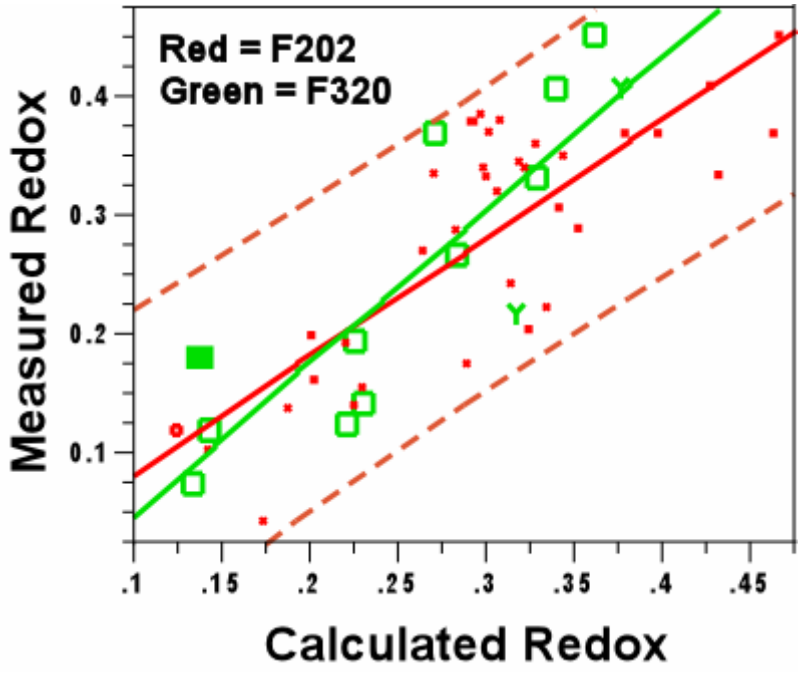

Figure 15. Comparison of the measured REDOX for frits of different alkali content.

4.4 The Role of Manganese

The distribution of the soluble manganese values given in Table II showed no relation to any combination of feed oxidizers or reductants. This is because manganese can complex with formate as soluble $Mn(COOH)_2$ in the SRAT supernate, as insoluble MnO_2 in the SRAT insoluble solids, or as insoluble manganous oxalate in the SRAT insoluble solids. The role as $Mn(COOH)_2$ is pH dependent, e.g. $Mn(COOH)_2$ is stable at near neutral pH while aqueous Mn^{+2} is soluble at lower SRAT pH values. Therefore, a measurement of the soluble Mn in the SRAT supernate is insufficient to determine if 66% of the Mn^{+4} has been reduced to Mn^{+2} when the SRAT/SME pH values fluctuate and oxalate is present.

In addition, manganese oxalate has recently been found during the Differential Scanning Calorimetry (DSC) analysis of Tank 7 sludge.‡ X-ray diffraction (XRD) analysis of the dried SRAT solids also showed the presence of manganous oxalate $C_2MnO_4 \bullet 2H_2O$ and ferrous oxalate which is isostructural ($C_2FeO_4 \bullet 2H_2O$) and indistinguishable from manganous oxalate during XRD analysis. REDOX measurements on the dried sludge did not substantiate the presence of reduced Fe^{+2} as ferrous oxalate, which led to the conclusion that the oxalate in the SRAT product must be manganous oxalate and not ferrous oxalate. Subsequent Scanning Electron Microscopy (SEM) analyses of the dried SRAT product by C.C. Herman also indicated the presence of $MnSO_4$, manganous sulfate.

‡ Fernando Fondeur, personal communication February 28, 2003

X-ray diffraction analysis of two different pairs of SME solids generated in the current study was performed. The frit had been added to the SRAT products to prepare the simulated SME products about a month before the XRD analysis. These SME products were then dried at 90°C overnight. The pairs of SME feeds examined were SB3-7-35-320 and SB3-7-35-202 and SB3-8-35-320 and SB3-8-35-202. The SME feeds made with Frit 320 and Frit 202 contained both the manganous $C_2MnO_4 \bullet 2H_2O$ and sodium oxalate ($Na_2C_2O_4$). In addition, calcium oxalate, whewellite, $C_2CaO_4 \bullet H_2O$ was found along with $NaNO_3$. A difference spectra between the pairs was run overnight and is shown in Figure 16 as the bottom spectra. It demonstrates that there is less whewellite in the sample made with Frit 202 than in the sample made with Frit 320 indicating that there may be some reaction of the oxalate in the SME with the frit components. Since this had no apparent effect on REDOX it was not investigated any further.

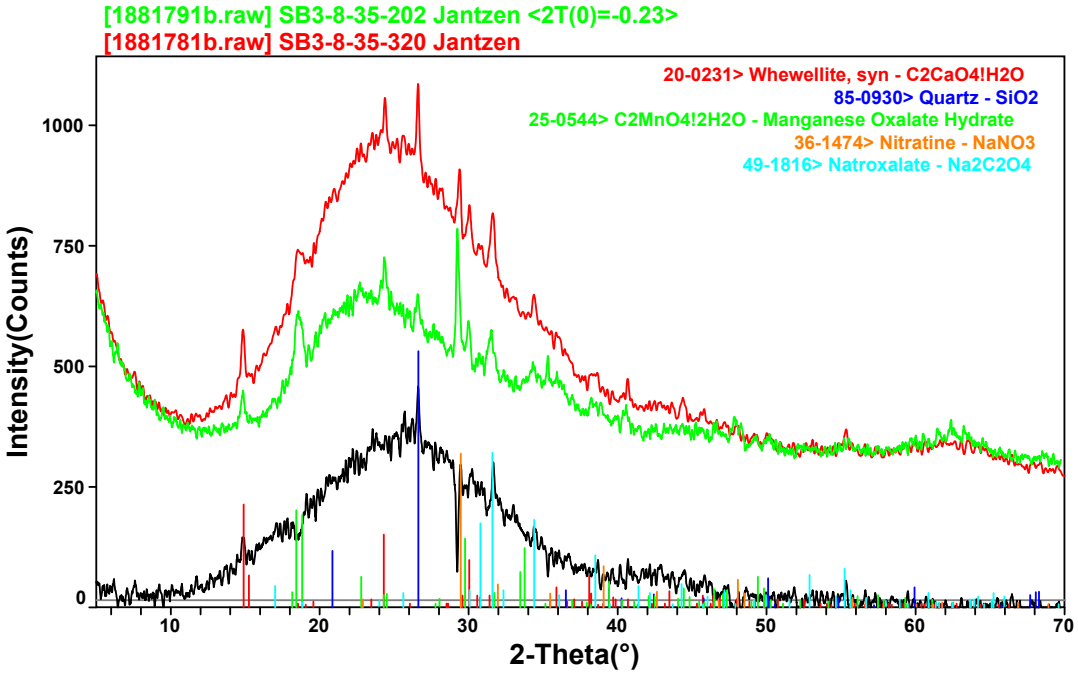

Figure 16. Comparison of SB3-8-35 SME products made with Frit 202 and Frit 320.

In addition, there appears to be a strong correlation of the measured REDOX values in this study with the molar MnO in the glass (Figure 17). The molar MnO of the glass was calculated from the SRAT solids MnO and the frit compositions used at the measured waste loadings based on B_2O_3 analyses. Due to (1) the relationship between the MnO content and the REDOX and the (2) complex role of manganese in the presence and absence of oxalate, a decision was made to include the effects of manganese as an oxidizer in the current REDOX evaluation. This meant that in order to include the Scale Glass Melter (SGM) and Integrated DWPF Melter System (IDMS) glasses used in the development of the {[F]-3[N]} correlation, that the archival manganese values had to be determined and added to the data in Appendix A.

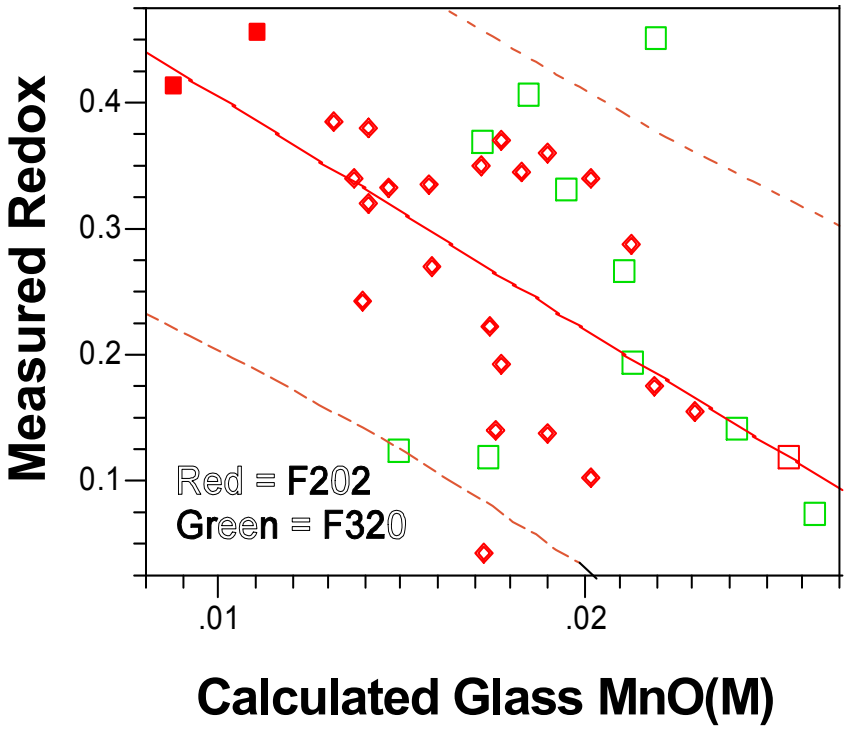

Figure 17. Relationship between molar MnO in the glasses studied and the measured REDOX value, $Fe^{+2}/\Sigma Fe$.

4.5 Significance of REDOX Measurements on Melter Plenum Oxygen Fugacity

The ElectroMotive Force (EMF) REDOX series for DWPF glasses, as illustrated in Figure 18, was experimentally determined by Schreiber, et al.[2]. This ordering of REDOX couples in oxygen fugacity-REDOX ratio space defines an electrochemical series in terms of the ease of reduction of particular multivalent ions [2]. Note further that the oxygen fugacity is a function of the total iron in the glass (as indicated by the broken lines representing differing iron concentrations). Using Figure 18, the measured iron REDOX and total iron in the glass can be used to indicate both the oxygen fugacity (availability of oxygen) in the plenum to combust organics (assuming no incoming air from bubblers) and the relative fraction of other ions in the reduced or oxidized state in a DWPF glass.

The ratio of the Fe^{+2} to the total iron is indicated across the top of Schreiber's REDOX series (Figure 18). The relation between the $Fe^{+2}/\Sigma Fe$ and the log f_{O_2} can then be quantified from this graphical description at ~ 10 wt% total iron by the following relationship:

Equation 16

$$-\log f_{O_2}(EMF) = -3.42 - 9.08 * \left(\frac{Fe^{+2}}{\Sigma Fe} \right)$$

By substituting the measured $\left(\frac{Fe^{+2}}{\Sigma Fe} \right)$ ratio for all the glasses in "Model Data" into Equation 16, one can then determine if there will be enough oxygen present in the DWPF plenum to combust all the organics present. This relationship holds because, as shown in Section 4.9, the sealed crucible tests correspond to the REDOX and f_{O_2} conditions in the DWPF melter.

The REDOX ratios in "Model Data" span between 0.04 to 0.45 which corresponds to a logarithmic oxygen fugacity range of –3.8 to –7.5 at the melt temperature of 1150°C. If the REDOX ratio is constrained between the REDOX ratio detection limit of 0.03 and the upper REDOX limit of 0.33, then the corresponding logarithm of the oxygen fugacity values are –3.8 to –6.33 at the melt temperature of 1150°C.

The published correlation [45] between log oxygen fugacity and temperature for the equilibrium between graphite(C)-CO-CO_2 demonstrates that at any logarithm of the oxygen fugacity more positive than –15, graphite (C) can be oxidized to CO and CO_2. Therefore, as long as the DWPF glass REDOX is controlled at a REDOX ratio of <0.33 $Fe^{+2}/\Sigma Fe$, then there will be sufficient oxygen available in the melter plenum to combust carbon (coal) and any other organics to CO_2.

The measured CO_2 and CO values of Choi, et. al. [46], determined during the carbon balance combustion runs performed during the SGM-9 campaign when the total carbon content in the feed was 2.19 wt%, confirm the above calculations. The measured CO_2 and CO ratios [46] in the off-gas were converted to moles and the logarithm of the ratio of CO_2/CO calculated. This ratio can then be converted to log oxygen fugacity using the published relationship between log CO_2/CO, temperature, and oxygen fugacity [47]. The calculation of the published CO_2 and CO values indicated a logarithm of the oxygen Sfugacity in the off-gas of -9, a more positive value than the –15 needed to combust coal.

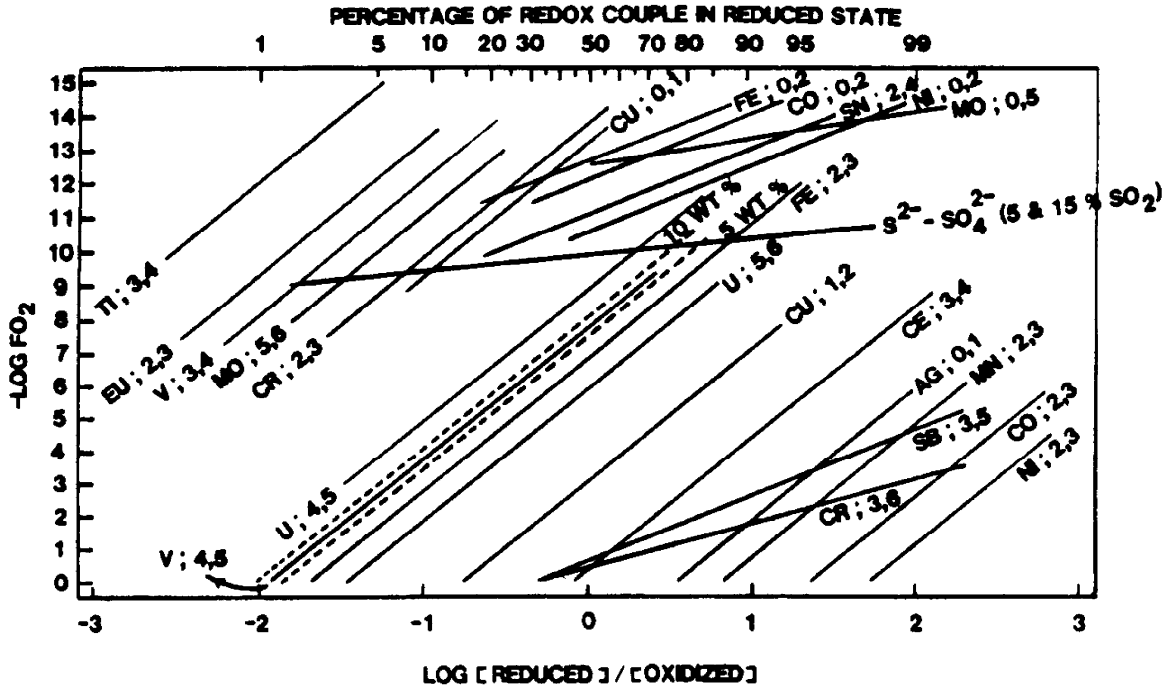

Figure 18. Schreiber's relationship between imposed oxygen fugacity (–log $f(O_2)$) and the REDOX ratio (log([reduced ion]/[oxidized ion])) for multivalent elements doped into SRL-131 melt at 1150°C. The broken lines represent 5 and 10 wt% Fe in SRL-131. Such an ordering of the REDOX couples in fugacity-REDOX space defines an ElectroMotive Force (EMF) series describing the ease of reduction of the ions represented.

4.6 Development of Basis for the Electron Equivalents REDOX Model

The thermodynamic modeling by Choi [5,6] indicates that N_2 and CO_2 gases are thermodynamically the most stable species in the DWPF melter cold cap at the depth at which the REDOX equilibrium reactions occur. Iron enters the DWPF melter mainly as Fe^{3+} and reacts with NaCOOH and $NaNO_3$ in the melter cold cap to form reduced species such as Fe^{2+} and N_2 as well as oxidized CO_2. Subsequently, a portion of the N_2 gas is oxidized to NO_x (i.e., NO and NO_2) gases in the cold cap as the N_2 diffuses upward through the cold cap. Tests conducted in the Integrated DWPF Melter System (IDMS) indicated that at 300°C the ratio of NO_2 to total NO_x in the melter off-gas was approximately 88%; at 800°C, NO gas predominates, with greater than 99% NO at plenum temperatures [48].

While a cold cap probably does not exist in the sealed crucible tests, the feed-to-glass conversion reactions will be the same whether they occur in a surface layer or in the glass bulk. There is evidence of a reaction front in the sealed crucible glasses when they are sectioned (see Figure 12) indicating that there may be a surface reaction like a cold cap reaction that occurs during the sealed crucible tests.

In Section 2.3 it was shown that the combined reactions from all four stages of cold cap reaction could be represented simultaneously (assuming these reactions occur in the bulk glass) by Equation 8 shown below for reference:

$$Fe_2O_3 + 5SiO_2 + 6NaCOOH + 2NaNO_3 \rightarrow Fe_2SiO_4 + 6CO_2 + N_2 + 4Na_2SiO_3 + 3H_2O$$

Equation 8 assumes that Fe^{3+} enters the melter as Fe_2O_3 and that $COOH^-$ and NO_3^- both enter as properly formated and nitrated sodium compounds. The formated and nitrated salts react with glass formers such as SiO_2 to form Fe^{+2} and Na_2SiO_3 components in the glass and liberate CO_2, N_2 and H_2O vapors to the melter plenum.

Reduction of a species such as Fe^{+3} or N^{+5} can be defined as making an atom or molecule less positive (or more negative) in the electrical sense.[f] Oxidation of reduced carbon in organic species such as formates, oxalates, and carbon (coal, graphite) to CO_2, can be defined as making an atom or molecule more positive (or less negative). Both processes involve the transfer of electrons. The pertinent REDOX half reactions that express the combined equilibrium for the individual reactions occurring in the melter cold cap (Equation 8) can be expressed as given in Table VII where the contributions from the individual molar electron transfers involved in the oxidation/reduction reactions can easily be seen.

[f] The Chemistry of the Iron-Based Processes, Mike Ware, World Wide Web

Table VII Reduction/Oxidation Half Reactions Considered During REDOX Modeling

Reduction/Oxidation Half Reactions		
$NO_3^- + 6H^+ + 5e^-$	$\longrightarrow$	$½N_2 + 3H_2O$
$Fe^{3+} + e^-$	$\longrightarrow$	Fe^{2+}
$Mn^{4+} + 2e^-$	$\longrightarrow$	Mn^{2+}
$COOH^-$	$\longrightarrow$	$CO_2 + H^+ + 2e^-$
$C_2O_4^=$	$\longrightarrow$	$2CO_2 + 2e^-$
$C + 2O^{-2}$	$\longrightarrow$	$CO_2 + 4e^-$

Rewriting Equation 8, the glass-forming cold cap reaction, in terms of Fe^{2+} and Fe^{3+} and omitting the SiO_2 provides the following reaction between the reduced formate salt and the oxidized nitrated salt (the reactive species in the cold cap):

Equation 17

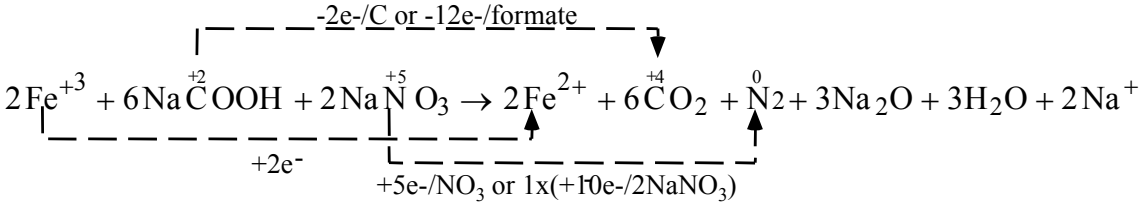

The oxidation/reduction equilibrium shown in Equation 17 between nitrate and formate indicates that one mole of nitrate gains 5 electrons when it is reduced to N_2 while one mole of carbon in formate loses 2 electrons during oxidation to CO_2. This is an oxidant/reductant ratio of 5:2 which indicates that nitrate is approximately 2½ times as effective an oxidizing agent as formate is a reducing agent (when nitrogen gas is the reaction product). Equation 17 indicates that the molar ratio of formate to nitrate is 3:1 to reduce Fe^{3+} to Fe^{2+}. That is, sufficient formate must be present to reduce the nitrate, and also reduce the Fe^{3+} to Fe^{2+}.

The oxidation/reduction equilibrium shown in Equation 18 between coal and the oxidized nitrated salt indicates that one mole of nitrate gains 5 electrons when it is reduced to N_2 while one mole of carbon in coal loses 4 electrons during oxidation to CO_2. This is an oxidant/reductant ratio of 5:4 which indicates that nitrate is only 1¼ times as effective an oxidizing agent as coal is a reducing agent (when nitrogen gas is the reaction product).

Equation 18

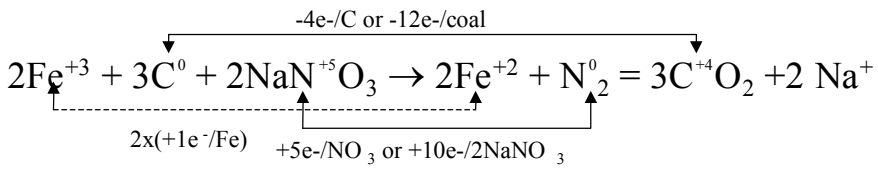

The oxidation/reduction equilibrium between the reduced alkali oxalate and the oxidized sodium nitrate salt is given in Equation 19. This theoretical reaction, written in the format of the preceding cold cap reactions, indicates that one mole of nitrate should gain 5 electrons when it is reduced to N_2 while one mole of carbon in oxalate should lose 1 electron during oxidation to CO_2. This is an oxidant/reductant ratio of 5:1 which indicates that nitrate is 5 times as effective an oxidizing agent as the carbon in oxalate is a reducing agent (when nitrogen gas is the reaction product).

Equation 19

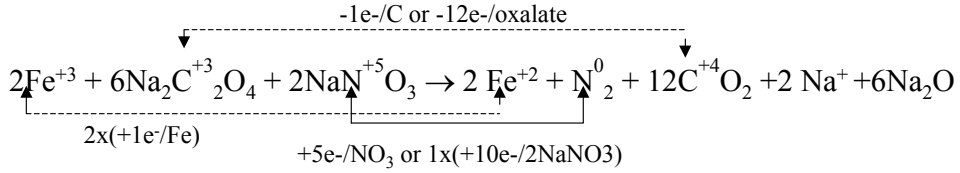

However, during REDOX modeling the data indicated that oxalate appeared to be twice as strong a reductant as indicated by Equation 19. During further investigation of the apparent increase in the reducing power of oxalate, data became available that demonstrated that oxalate salts convert to oxalic acid and then disproportionate to formic acid and CO_2 during SRAT processing [49] via Equation 20.

Equation 20 $HC_2^{+3}O_4^- \rightarrow HC^{+2}O_2^- + CO_2 \uparrow$

Experimentally, it was found that between 8-37% of the oxalate present in the SRAT was determined to disproportionate during processing into HCOOH and CO_2 gas [49].

Therefore, it was assumed that disproportionation also occurs in the cold cap when the liquid slurry impacts the melt pool surface. The pertinent oxidation/reduction equilibrium for oxalate, including the disproportionation, would then be as expressed in Equation 21. This equation includes the decomposition of the oxalate into formic acid and CO_2. Since only half of the oxalate is acting as a reductant, the reduction potential of oxalate is doubled.

Equation 21

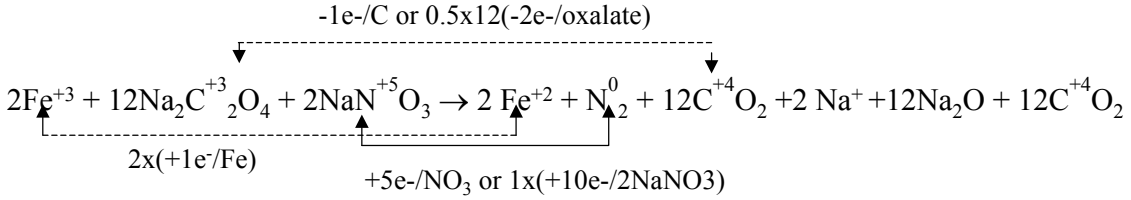

When the nitrate and reductant equations are combined the form of the overall oxidation/reduction equations take on the form below:

Equation 22

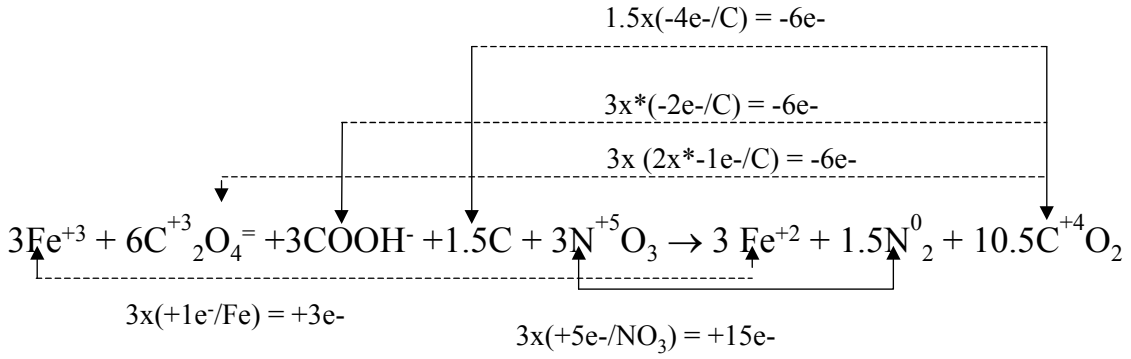

This demonstrates that the relative factors for the electrons exchanged upon oxidation and reduction are 4 for the number of moles of coal, 2 for the number of moles of formate, 4 for the number of moles of oxalate (2 carbons/mole of oxalate at $2e^-$/carbon plus disproportionation), and 5 for the number of moles of nitrate. Therefore, the basis for the relation of REDOX to electron equivalent transfers for Equation 22 is:

Equation 23

$$\frac{Fe^{2+}}{\Sigma Fe} = f\left(2[F] + 4[C] + 4[O_T] - 5[N]\right) = f(\xi)$$

where f = indicates a function
[F] = formate (mol/kg feed)
[C] = coal (carbon) (mol/kg feed)
$[O_T]$ = $oxalate_{total}$ (soluble and insoluble) (mol/kg feed)
[N] = nitrate + nitrite (mol/kg feed)
ξ = sum molar Electron Equivalents transferred

If an oxidation/reduction reaction is added to Equation 23 to include the reduction of Mn^{+4} species to Mn^{+2} species then ξ becomes $\left(2[F] + 4[C] + 4[O_T] - 5[N] - 2[Mn]\right)$. In addition, the effectiveness of the oxidants and reductants depends on their concentrations relative to the other slurry components. The molar Electron Equivalents term must, therefore, be multiplied by the factor 45/T, where T is the total solids (wt%) content of the slurry. This factor puts all concentrations on a consistent basis of 45 wt% total solids. The normalized molar Electron Equivalents, ξ, are then:

$$\xi\left(\begin{array}{c} mol/kg\ feed \\ @45\,wt\%\,solids \end{array}\right) = \left(2[F] + 4[C] + 4[O_T] - 5[N] - 2[Mn]\right)\frac{45}{T}$$

which gives a final REDOX dependency given in Equation 24 below:

Equation 24

$$\frac{Fe^{2+}}{\Sigma Fe} = f\left[\left(2[F]+4[C]+4[\mathrm{O_T}]-5[N]-2[Mn]\right)\frac{45}{T}\right] = f[\xi]$$

where f = indicates a function
[F] = formate (mol/kg feed)
[C] = coal (carbon) (mol/kg feed)
$[\mathrm{O_T}]$ = $\mathrm{oxalate_{Total}}$ (soluble and insoluble) (mol/kg feed)
[N] = nitrate + nitrite (mol/kg feed)
[Mn] = manganese (mol/kg feed)
T = total solids (wt%)

$$\xi = \left(2[F]+4[C]+4[\mathrm{O_T}]-5[N]-2[Mn]\right)\frac{45}{T}$$

The REDOX data is then fit as a linear function of ξ:

$$\frac{Fe^{2+}}{\Sigma Fe} = b + m\xi$$

where b and m are constants that are fit from experimental data.

4.7 Fitting the Electron Equivalents REDOX Model to "Model Data"

Two potential methods of fitting Equation 24 to the REDOX data are described below. These include using Equation 24 as it is with data that have been normalized to 45 wt% solids, and fitting an additional adjustment for measured waste loadings. For all of the regressions discussed below only "Model Data" from the crucible melts generated in this study and the data used to generate the {[F]-3[N]} model (Appendix) were used to fit the model. Additional data from DWPF, Minimelter, and Slurry-Fed Melt Rate Furnace (SMRF) glasses were used as "Full and Pilot Scale Validation Data." Note that data points for glasses made without any formic acid are not shown in any of the models discussed above; these data points lie at very negative ξ values with low (<0.015) REDOX values below the analytical detection limit of 0.03. These data do not fit the model since the model predicts the REDOX will be zero at ξ= -1.02. For all ξ less than about -0.86, the REDOX should be considered to be below the detection limit.

The data presented in Table V (normalized to 45 wt% total solids) and the data from Appendix A from the development of the {[F]-3[N]} model were fit to the Electron Equivalents parameters as shown in Equation 24. This plot is shown in Figure 19. The

same data (normalized to 45 wt% total solids and adjusted for measured waste loading) were fit to Equation 24 and shown for comparison in Figure 20. Note that the data from Appendix A indicated by the plus values in Figure 20 span a wider range in terms of both the x and the y parameters than the data generated in this study. However, the fit of the Electron Equivalents model to a data set including oxalate, coal and manganese is important in that it shows the robust nature of this approach to REDOX modeling. It also indicates that inclusion of a manganese term should have been investigated during the development of the previous {[F]-3[N]} and {[F]-[N]} REDOX models.

A comparison of Figure 19 and Figure 20 demonstrates that the fit of the data with or without adjustment for waste loading is excellent, with R^2 values between 0.81 and 0.80. There is virtually no difference in the slopes or intercepts with the additional adjustment for the measured waste loadings. This is because an adjustment had been made in converting the data in Table III to the values shown in Table IV for frit dilution at the target waste loading. The additional adjustment for measured waste loading discussed below appears to have little value and the REDOX model given in Figure 19, $\frac{Fe^{2+}}{\Sigma Fe} = 0.1942 + 0.1910\xi$, is the DWPF Electron Equivalents model that will be assessed against the Validation Data in Sections 4.8 and 5.0.

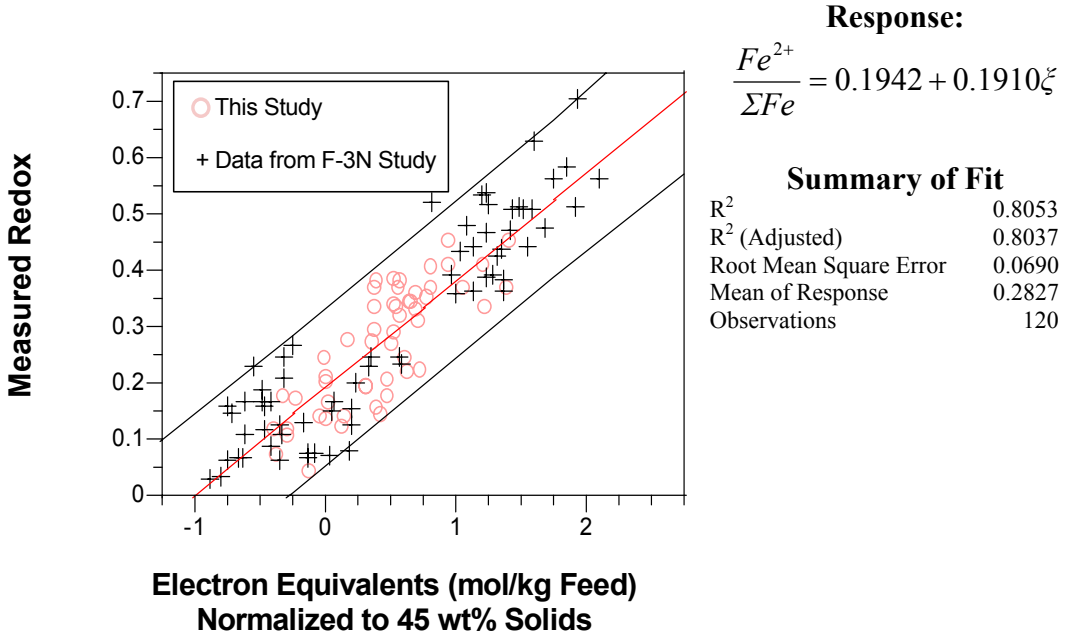

Figure 19. REDOX model with formate, oxalate, coal, nitrate, and manganese normalized for 45 wt% solids.

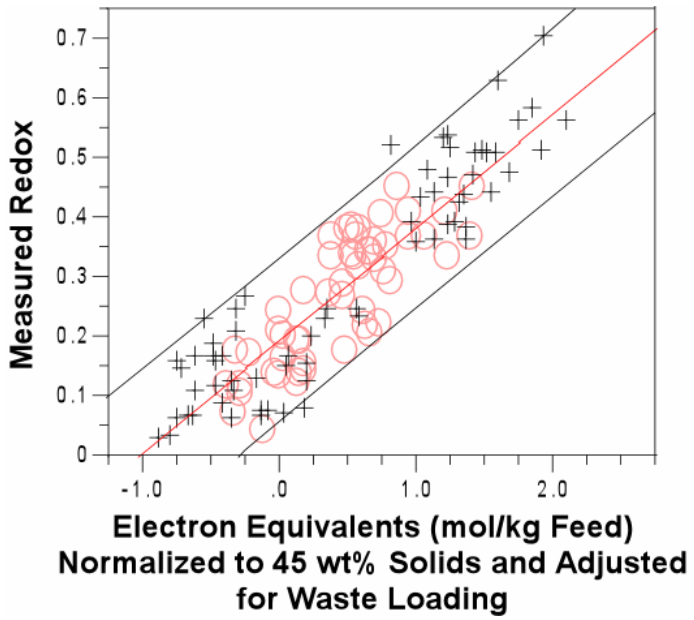

Response:

$$\frac{Fe^{2+}}{\Sigma Fe} = 0.1939 + 0.1911\xi'$$

Summary of Fit

R^2	0.8004
R^2 (Adjusted)	0.7987
Root Mean Square Error	0.0699
Mean of Response	0.2827
Observations	120

Figure 20.REDOX model regression with formate, oxalate, coal, nitrate, and manganese normalized for 45 wt% solids and adjusted for waste loading.

The regression analysis shown in Figure 20 was performed on the SME concentration data that were corrected to 45 wt% total solids. Selected data points also were adjusted by the measured waste loading to correct for feed batching errors due to sludge sub-sampling for the data developed in this study. The data were also regressed without the latter adjustment. The results of these regressions are compared to the results of Figure 20 in Table VIII. The regression of the waste loaded adjusted data gives essentially the same parameters as the unadjusted data, but the R^2 is slightly smaller.

Table VIII Summary of "Model Data" Regressions

Summary of Regressions $\frac{Fe^{2+}}{\Sigma Fe} = b + mX$	X = ξ' mol/kg feed normalized to 45 wt% solids, adjusted by waste loading	X = ξ mol/kg feed normalized to 45 wt% solids
Intercept, b	0.1939	0.1942
Slope, m	0.1911	0.1910
R^2 (Adjusted)	0.7987	0.8037
Root Mean Square Error	0.0699	0.0690
Mean of Response	0.2827	0.2827
Observations	120	120

4.8 Validation of the Electron Equivalents Redox Model With DWPF, Minimelter, and Slurry-Fed Melt Rate Furnace (SMRF)

Data for three glasses produced in melters were analyzed for REDOX and are shown in Table IX. The DWPF sample REDOX was from a sample pulled from the pour spout and analyzed at SRTC in the Shielded Cell Facility (SCF). The feed to the melter was comprised mostly of melter feed from SME Batch 224. The target REDOX was ~0.2 based on the {[F]-3[N]} model. Samples of minimelter feeds were vitrified in closed crucibles (see Table IV) and preliminary analysis of the redox indicated that the target REDOX of 0.2 using the {[F]-3[N]} model was achieved in the closed crucible tests while a REDOX of 0.12 was achieved after continuous feeding in the minimelter (see Table IX). SRTC experience has shown that the minimelter air-inleakage is higher than in the DWPF type melters which may contribute to the lower REDOX measured for the minimelter samples. In addition, the minimelter sampling allows the sample to flow onto a steel paddle during which time it may partially oxidize. The SRTC ML reanalyzed the REDOX of the minimelter sample in duplicate and a REDOX value of 0.14 was measured. Both values are shown in Table IX. Lastly, Slurry-fed Melt Rate Furnace (SMRF) tests were performed at a target REDOX of 0.22 using an interim version of the Electron Equivalents model. The resulting measured REDOX values shown in Table IX indicate a measured REDOX of 0.239 which is an average of 10 REDOX values measured after the SMRF had achieved steady state conditions (a total of 16 samples were measured).

These data from these validation melter tests are plotted in Figure 21 along with the "Model Data" and the fitted model. The Electron Equivalents term is fitted using the SME analyses. All three data points fit will within the 95% confidence interval.

Table IX Data for Glasses Produced in Melters

Sample ID	B_2O_3 Waste Loading (wt%)	Li_2O Waste Loading (wt%)	Target Waste Loading (wt%)	MEASURED REDOX $Fe^{+2}/\Sigma Fe$	SME Total Solids (wt%)	Electron Equivalents (mol/kg feed @ 45 wt% solids)
DWPF SME 224 Frit 200	35.35	32.06	NA	0.21	47.7	-0.0746
Minimelter MMG025 Frit 320	25.31	29.41	25.5	0.12 0.14	47.0	-0.304
SMRF SB3 Frit 202	30.56	30.76	NA	0.239*	47.1	0.634
	Oxalate (mol/kg)	**Formate (mol/kg)**	**Nitrate (mol/kg)**	**Coal (mol/kg)**	**Mn (mol/kg)**	
DWPF SME 224 Frit 200	0	0.795	0.312	0	0.0551	
Minimelter MMG025 Frit 320	0	0.467	0.202	0	0.121	
SMRF SB3 Frit 202	0.367	0.530	0.432	0.0736	0.0915	

* Average of 10 REDOX measurements on 5 samples taken after the SMRF reached steady state melt conditions

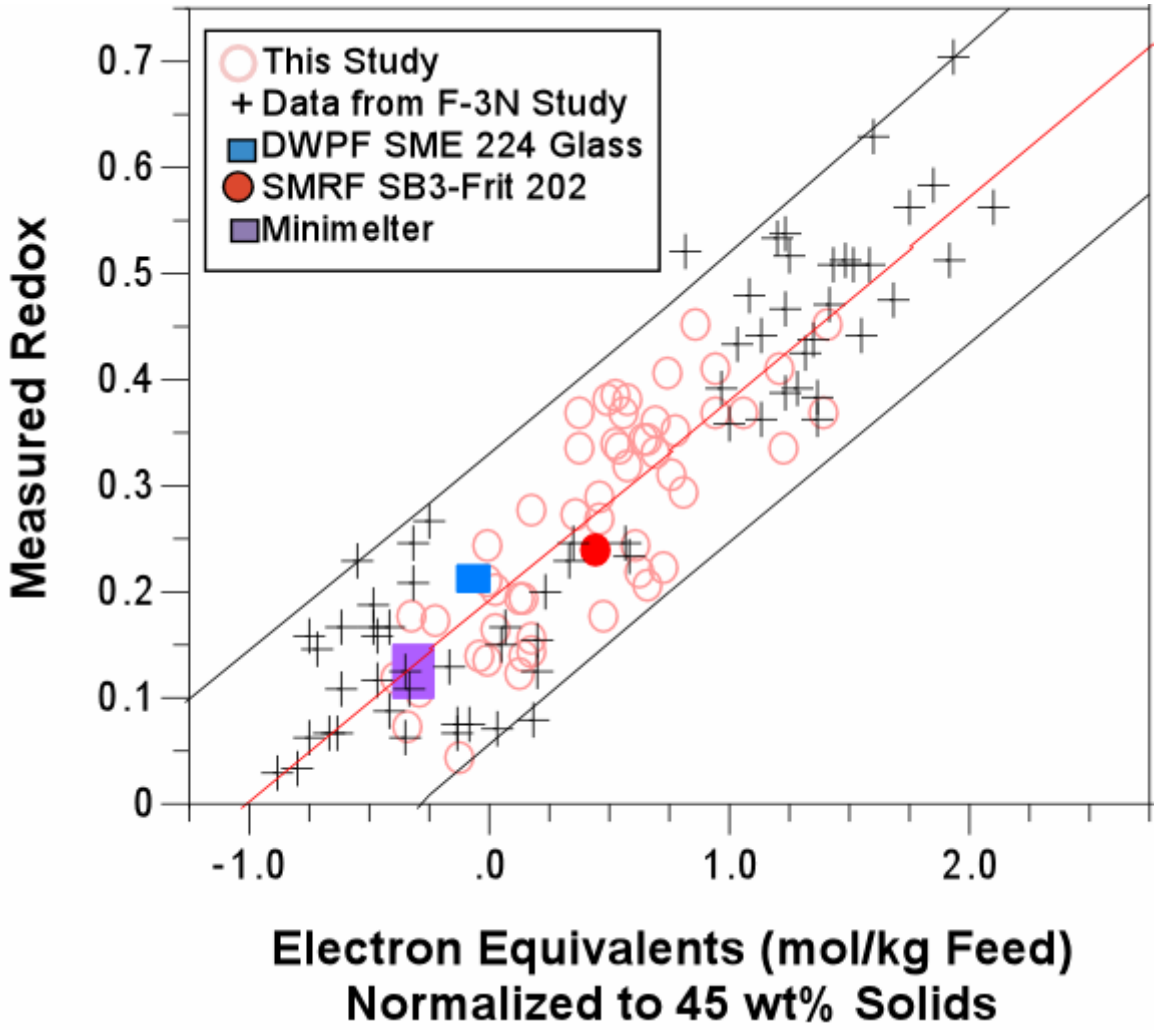

Figure 21. Melter glass REDOX data compared to "Model Data" where the Electron Equivalents is based on SME compositions

The data from Figure 21 are re-plotted in Figure 22 along with the same REDOX values plotted versus the Electron Equivalents calculated from the SRAT measurements that do not account for any SME losses. All values are shifted to the left and would predict more oxidizing glasses than predicted from the SME analyses. However, the three melter data points all fit well within the 95% confidence interval. A correction factor for the SME losses is needed if the SRAT values were to be used.

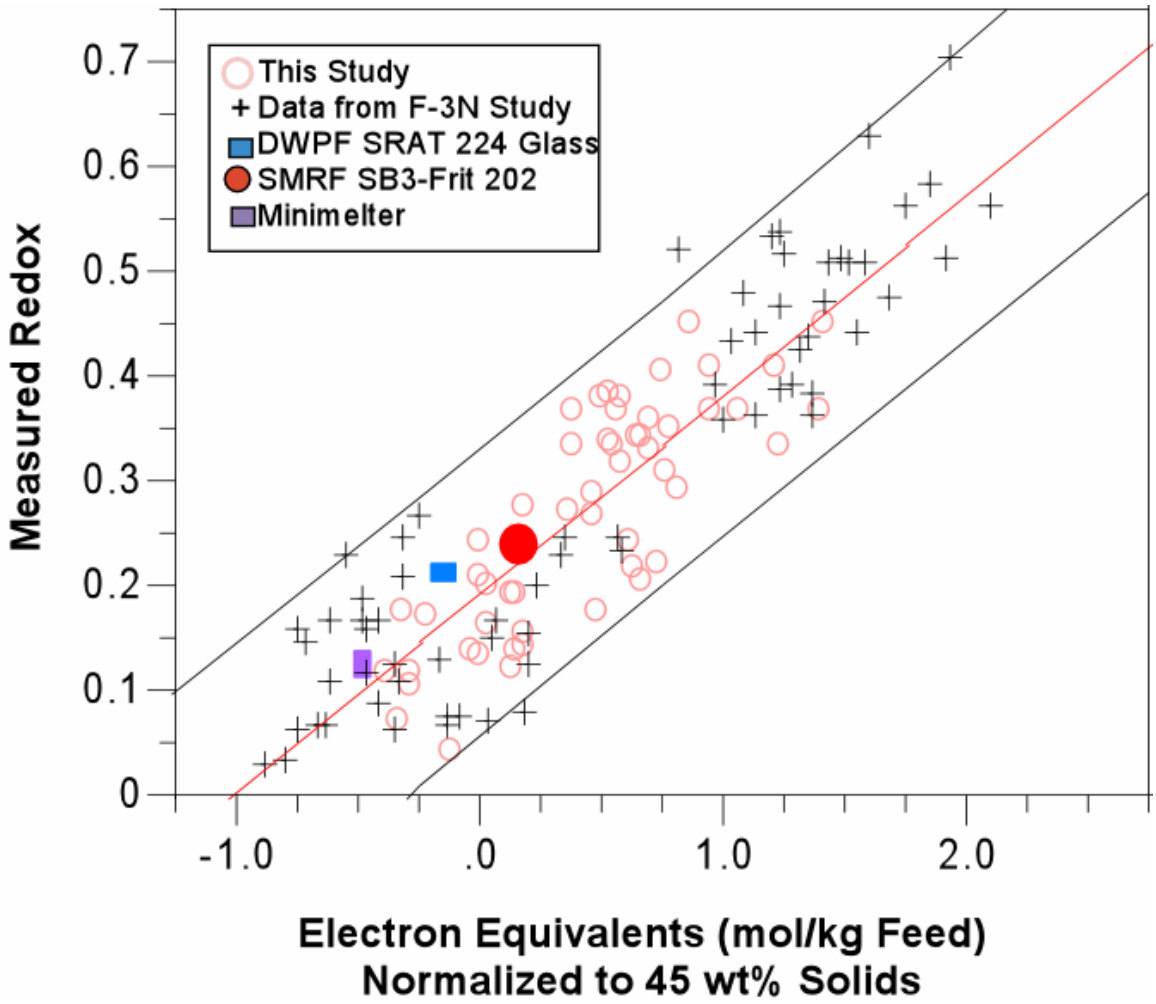

Figure 22. Melter glass REDOX data correlated to Electron Equivalents using SRAT data

Figure 23 shows the SME Electron Equivalents plotted versus the SRAT Electron Equivalents. With only five data points, the scatter does not define a line well. The best-fit line is, however, shown. The general trend is that the SME ξ value is about 0.3 mol/kg higher than calculated from the SRAT ξ.

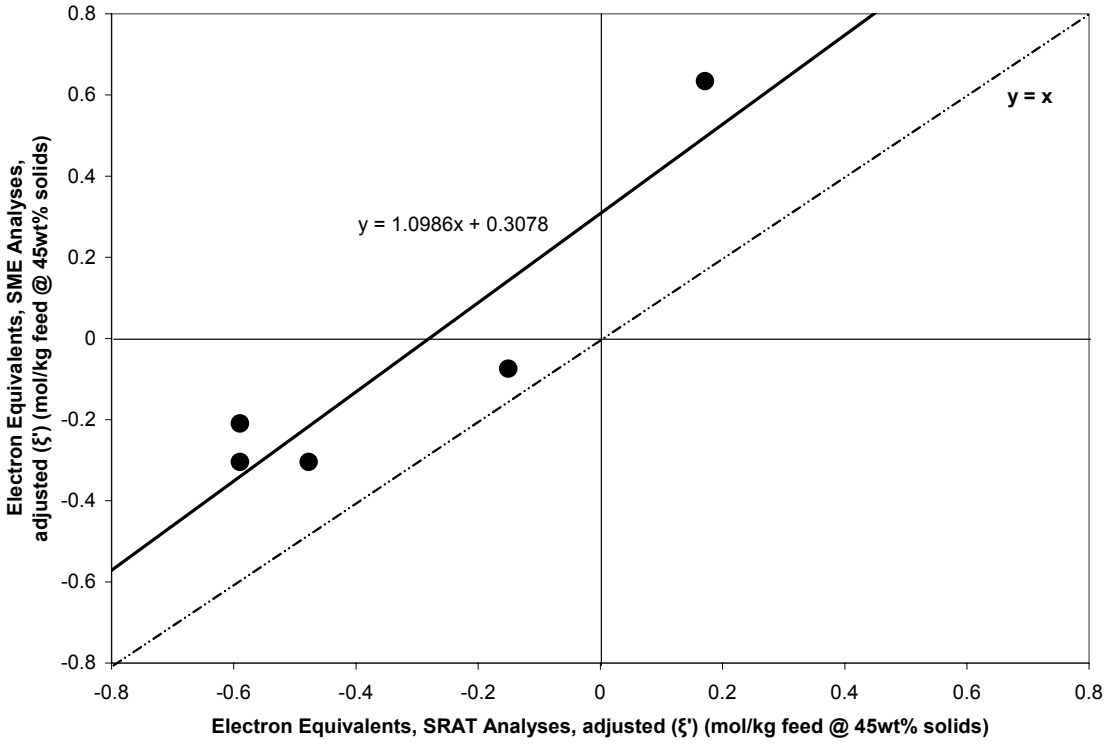

Figure 23. Correlation of Electron Equivalents based on SRAT and SME analyses.

5.0 VALIDATION DATA

The criteria used to determine acceptable "Model Data" as outlined in Section 2.2.2 were loosened when examining "Validation Data" since these data were not used for model development. There were no restrictions on the melter feed from which the "Validation Data" were produced other than that the feed must be either simulated or actual high-level waste. The details on the preparation of these feeds were often unavailable. Furthermore, the restriction on the visual appearance of the validation glasses was relaxed as this information was often also unavailable. Many of the validation iron REDOX measurements discussed in Sections 5.1, 5.2 and 5.5 were obtained using techniques other than the Baumann method [27].

5.1 Historical Data – Other Sources

Most of the data discussed below is taken from the 1997 REDOX report [15]. That report contained extensive discussion of what data were chosen to be used for model validation. The variance of formate and nitrate concentration measurements and REDOX measurements is also discussed. This extensive discussion will not be repeated herein. For many of the historic data Mn values were not available, and oxalate and coal were not reductants that were present in the feeds. These terms were assumed to be zero.

For model validation purposes, glass produced from the IDMS melter at SRTC was compared to the Electron Equivalents model predictions. Most of the IDMS REDOX values fell near those used in the development of the new correlation.

Several Pacific Northwest National Laboratory (PNNL) crucible data sets and a pilot-scale melter data set were also used to validate the REDOX prediction model. These slurries were prepared via addition of both formate and sucrose as reductants. Nitrate and nitrite were the primary oxidants found in these experiments. The iron REDOX measurements for these glasses again agreed well with model predictions except for extremely reduced conditions.

Crucible and small scale melter REDOX data from West Valley Nuclear Services (WVNS) were also examined. However, unlike in the DWPF flowsheet, sugar was used as the primary reductant instead of formate. Moreover, even with oxidant and reductant concentrations that far exceeded those used in DWPF, the Electron Equivalents model was shown to fit most of the data well when the following modification was made to the Electron Equivalents model for the reduction obtained by sugar:

Equation 25

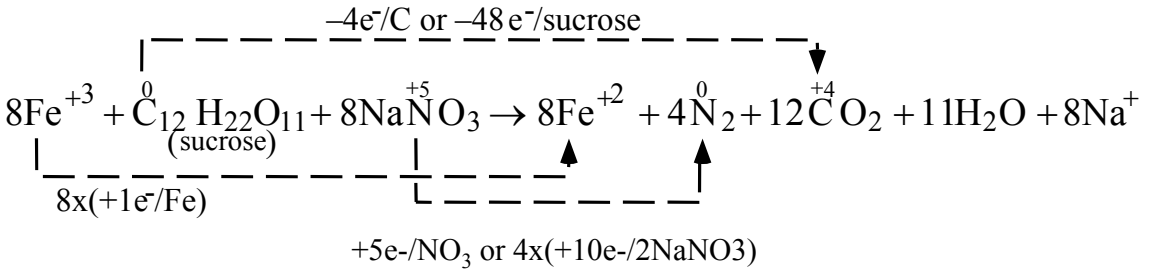

Which converts Equation 24 to Equation 26 below:

$$\frac{Fe^{2+}}{\Sigma Fe} = g\left(2[F] + 4[C] + 4[S] + 4[O_T] - 5[N] - 2[Mn]\right)\frac{45}{T}$$

where g = indicates a function
[F] = formate (mol/kg feed)
[C] = coal (carbon) (mol/kg feed)
[S] = sugar (carbon) (mol/kg feed)
$[O_T]$ = $oxalate_{total}$ (soluble and insoluble) (mol/kg feed)
[N] = nitrate + nitrite (mol/kg feed)
[Mn] = manganese (mol/kg feed)
T = Total solids (wt%)

The Electron Equivalents term, ξ, is then:

$$\xi\begin{pmatrix} mol/kg\ feed \\ @45\,wt\%\,solids \end{pmatrix} = \left(2[F] + 4[C] + 4[S] + 4[\mathrm{O_T}] - 5[N] - 2[Mn]\right)\frac{45}{T}$$

Data from runs of the Scale Glass Melter (SGM) at SRTC were also examined as a validation data source. These data were also found to agree well with the Electron Equivalents correlation.

5.2 Validation of REDOX Prediction Using IDMS Process and PNNL Quartz Crucible and Pilot-Scale Ceramic Melter (PSCM) Data

The Integrated DWPF Melter System (IDMS) was a one-ninth scale (of DWPF) facility used to test various aspects of DWPF operation. Melter feed slurry and glass samples were collected from various IDMS campaigns. The IDMS data used for comparison to the model are given in Table X. The glass samples were actual samples of glass poured from the melter, whereas the vitrified feed samples were the result of crucible vitrifications of the melter feed slurry. Standard deviations are given where multiple analyses were available. The manganese values for these runs were not available and were not incorporated during the validation discussed below.

Quartz crucible and pilot-scale melter runs were performed at Pacific Northwest National Laboratory (PNNL) [50]. These tests used both formate and sugar as reductants, while nitrate and nitrite provided the oxidant. For the quartz crucible data, samples of dried feed were vitrified in an inert atmosphere. Upon reaching the desired temperature of approximately 1200°C, the resulting glass samples were quenched in air and the iron REDOX state measured by colorimetric titration [51]. The feed compositions and measured REDOX ratios for both the quartz crucible and Pilot-Scale Ceramic Melter (PSCM) [52] are provided in Table XI.

Note that the values for formate, nitrate, and sugar for the crucible data are different than those used in the 1997 report. Two sets of feed composition data were reported in the original reference [50]. One was the as-batched (initial slurry) concentrations, while the other was for a refluxed and then dried feed. Both data sets were expressed as mol/L of final melter feed. The 1997 report used the as-batched concentrations, but the refluxed/dried feed data showed that significant formate was lost, while nitrite was converted to nitrate and some nitrogen was lost, most likely as NO_x. Therefore, the refluxed/dried feed data were deemed more representative of the "feed" to the crucible. The refluxed/dried feed data were checked versus "Sample Chemistry" data reported in Table 4.4 of the reference [50]. These results agreed quite well, and the data from Table 4.4 were sufficient to allow the normalization to 45 wt% solids to be performed.

Table X IDMS Process REDOX Data

Campaign	Formate (M)	Nitrate (M)	Vitrified Feed $Fe^{2+}/\Sigma Fe$ Mean	Vitrified Feed $Fe^{2+}/\Sigma Fe$ Std. Dev.	Glass $Fe^{2+}/\Sigma Fe$ Mean	Glass $Fe^{2+}/\Sigma Fe$ Std. Dev.	Electron Equivalents (mol/kg*)
PHA-1	1.22	0.469	NA	NA	0.132	NA	-0.647
PHA-2	1.29	0.713	0.186	0.085	0.165	0.053	-0.725
PHA-3	1.39	0.767	0.315	0.252	0.162	0.047	-0.779
HG-1	1.70	0.705	NA	NA	0.106	0.030	-0.0887
HG-3	1.91	0.541	0.046	NA	0.071	0.025	0.8175
BLEND-1	1.00	0.639	0.052	0.009	NA	NA	-0.887
HAN-1	0.386	0.554	NA	NA	0.084	NA	-1.4721

* normalized to 45 wt% total solids

Table XI PNNL Quartz Crucible and PSCM REDOX Data

Test	Run ID	Formate (M)	Nitrate (M)	Nitrite (M)	Sucrose (M, as carbon)	$Fe^{2+}/\Sigma Fe$	Electron Equivalents (mol/kg*)
Quartz Crucible [(a)]	Formic Acid	0.856	0.446	0.01	0	0.039	-0.388
"	No Formic Acid	0	0.354	0.552	0	0.015	-3.30
"	Nitric Acid + Sugar	0	4.25	1.56	16.3	0.59	26.7
PSCM-22 [(b)]	No Sugar	0.21	0.17	0.0	—	0.015	-0.317
PSCM-22	3.5 g/L Sugar	0.21	0.17	0.0	0.13	0.15	0.066
PSCM-23	3.5 g/L Sugar	0.50	0.61	0.0	0.36	0.055	-0.449

[(a)] Data normalized to 45 wt% total solids

[(b)] Data assumed to be at 45 wt% total solids

The data points from the tables are overlain on the Electron Equivalents REDOX model shown in Figure 19 in Figure 24. Of the ten IDMS data points, two lie outside the 95% confidence interval when the error bounds on the IDMS data are considered. One data point outside does not have error bounds, while the remaining seven points overlap the confidence interval.

The three PNNL PSCM and one PNNL crucible data points shown in Figure 24 also fall within the confidence interval. One crucible data point was at about ξ=-3.5, which is very oxidizing, and one was at ξ=26.6, which put it far to the right and very reducing. Both of these data points are outside the range of the model. Note that the model based only on formic and nitrate species predicts that $Fe^{2+}/\Sigma Fe = 0.99$ when $\xi = 4.18$.

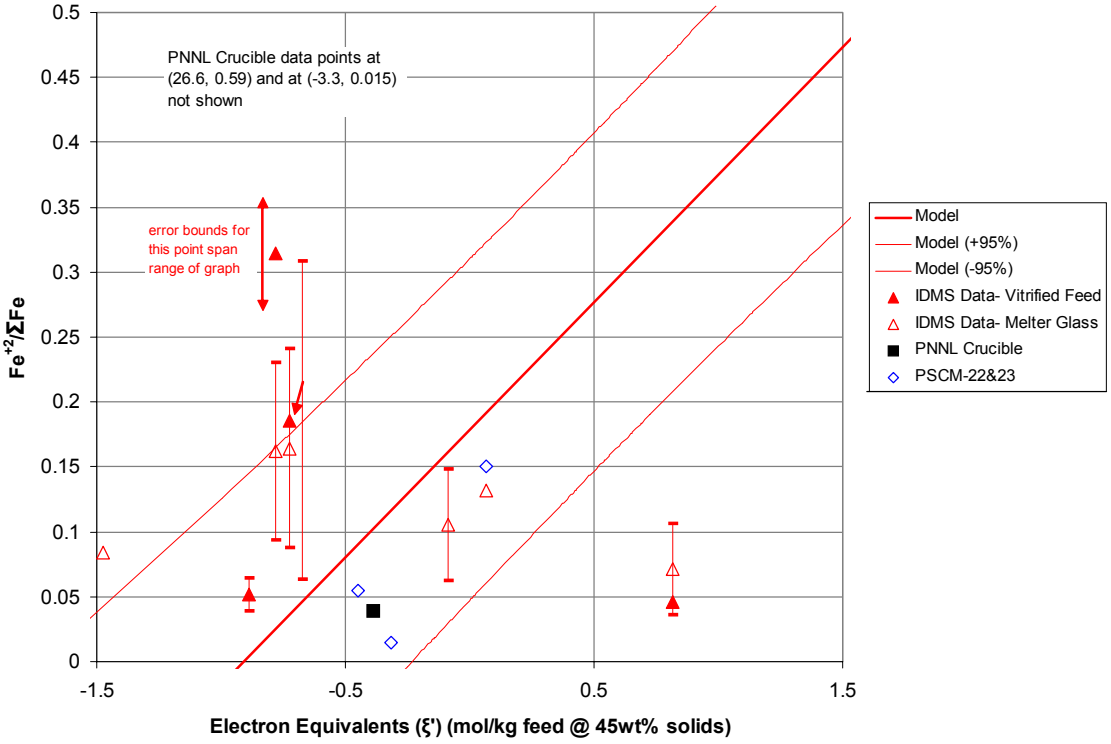

Figure 24. Comparison of IDMS and PNNL data with the Electron Equivalents REDOX model.

5.3 Validation of REDOX Prediction Using Additional PNNL Crucible Data

Crucible studies of the effect of formate and nitrate on glass REDOX adjustment were performed by PNNL in 1996 [53]. These studies were performed on feeds that were very similar to the DWPF, since at that time the Hanford Waste Vitrification Project (HWVP) process was similar to the DWPF process. Nineteen crucible melts were made with varying amounts of nitrate and formate. The starting sludge was heated to 95°C, held for 10 minutes, then formic acid was added over a short time interval, followed by refluxing for two hours. The reported data, reproduced in Table XII, were expressed as the molar concentrations of nitrate and formate in the initial batching into the sludge. Formate sludge and final melter feed (formated sludge + frit) total solids values were given, so the concentrations of formate and nitrate in the melter feed could be calculated. A loss factor of 35% was applied to the formate to account for the losses during the formating process. This value was determined from the average of formate losses from Tables 48 and 49 from the report on the HWVP runs in the IDMS [54]. Additional data reported by Farnsworth in reference 53 are also shown in Table XII. These additional data were adjusted for formate loss assuming losses similar to those used for the other data. The sludge-to-melter feed ratios were also assumed to be similar to those used for the other data.

These data are overlain on the Electron Equivalents REDOX model in Figure 25. Most of the data, except for those at very oxidizing conditions, match the model well. If data on the actual formate losses had been available, the data may have compared even better.

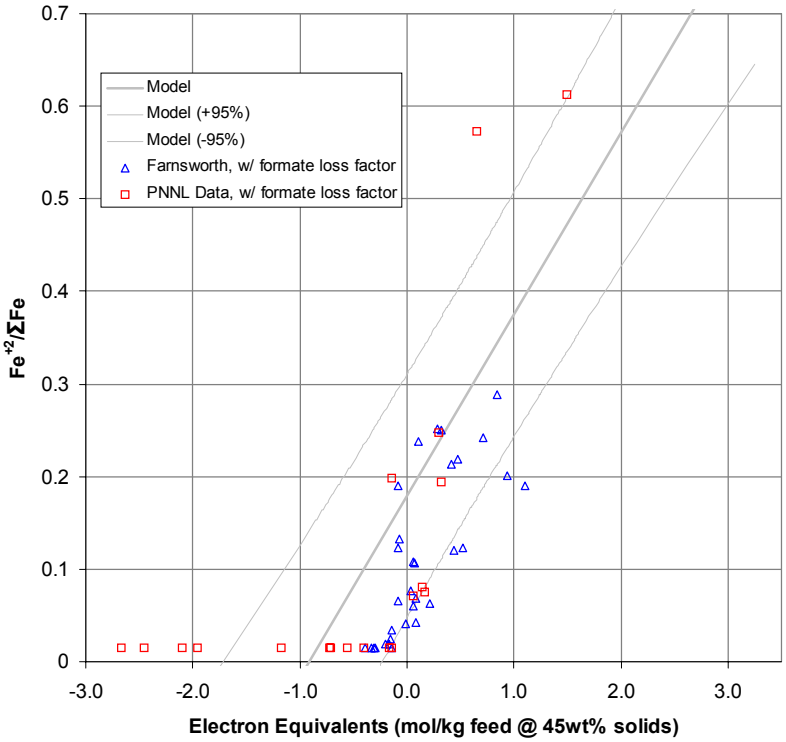

Figure 25. PNNL HWVP formated feed REDOX data compared to the Electron Equivalents REDOX model.

Table XII PNNL Data from Formating of HWVP Simulated Sludges

Comment	Run	Melter Feed Total Solids (wt%)	Sludge Total Solids (wt%)	Est. Melter Feed Density (kg/L)	Est. Sludge Density (kg/L)	Mass Frit / Mass Sludge	Sludge Formate (M)	Sludge Nitrate (M)	Calc. Melter Feed Formate (M)	Calc. Melter Feed Nitrate (M)	Feed Formate (mol/kg)	Feed Nitrate (mol/kg)	Fe^{2+}/ ΣFe	Electron Equivalents (mol/kg norm. to 45% solids)	Electron Equivalents, w/ 35% formate loss factor (mol/kg norm. to 45% solids)
PNNL-11044 Data	Run 1	35.77	14.90	1.26	1.09	0.32	0.47	0.460	0.412	0.403	0.326	0.319	0.015	-1.186	-1.171
	Run 2	36.43	15.86	1.27	1.10	0.32	0.67	0.740	0.587	0.648	0.462	0.510	0.015	-2.010	-1.951
	Run 3	35.31	14.32	1.26	1.08	0.32	0.34	0.130	0.298	0.114	0.237	0.090	0.015	0.027	-0.145
	Run 4	35.36	15.22	1.26	1.09	0.31	0.35	0.690	0.308	0.607	0.245	0.482	0.015	-2.446	-2.093
	Run 5	36.00	15.50	1.27	1.09	0.32	0.32	0.130	0.281	0.114	0.222	0.090	0.015	-0.009	-0.162
	Run 6	36.64	14.46	1.27	1.09	0.35	0.69	0.130	0.599	0.113	0.471	0.089	0.076	0.612	0.169
	Run 7	35.91	15.92	1.26	1.10	0.31	0.67	0.880	0.589	0.774	0.466	0.612	0.015	-2.667	-2.454
	Run 8	35.06	15.54	1.26	1.09	0.30	0.66	0.130	0.583	0.115	0.464	0.091	0.080	0.605	0.146
	Run 9	36.84	16.12	1.27	1.10	0.33	0.35	0.870	0.306	0.760	0.240	0.597	0.015	-3.059	-2.672
Sludge to melter feed solids ratio assumed to be same as Runs 1-10	Run 10	36.08	15.11	1.27	1.09	0.33	0.48	0.330	0.420	0.289	0.331	0.228	0.015	-0.594	-0.709
	Run 11	35.94	15.30	1.27	1.09	0.32	0.50	0.340	0.438	0.298	0.346	0.236	0.015	-0.607	-0.727
	Run 11	35.94	15.30	1.27	1.09	0.32	0.69	0.340	0.605	0.298	0.478	0.236	0.015	-0.278	-0.556
	Run 11	35.94	15.30	1.27	1.09	0.32	1.15	0.340	1.008	0.298	0.797	0.236	0.199	0.520	-0.142
	Run 12	35.94	15.30	1.27	1.09	0.32	1.17	0.420	1.025	0.368	0.811	0.291	0.015	0.208	-0.401
	Run 12	35.94	15.30	1.27	1.09	0.32	1.95	0.420	1.709	0.368	1.351	0.291	0.248	1.561	0.301
	Run 12	35.94	15.30	1.27	1.09	0.32	3.28	0.420	2.875	0.368	2.272	0.291	0.612	3.869	1.499
	Run 13	35.94	15.30	1.27	1.09	0.32	0.53	0.120	0.465	0.105	0.367	0.083	0.071	0.399	0.062
	Run 13	35.94	15.30	1.27	1.09	0.32	0.82	0.120	0.719	0.105	0.568	0.083	0.194	0.902	0.323
	Run 13	35.94	15.30	1.27	1.09	0.32	1.19	0.120	1.043	0.105	0.824	0.083	0.573	1.544	0.656
Farnsworth, in PNNL-11044	NCAW-84	45.00	NA	1.36	NA	NA	0.30	0.140	0.263	0.123	0.194	0.090	0.020	-0.065	-0.200
Sludge to melter feed solids ratio assumed to be same as Runs 1-10	NCAW-84	45.00	↓	1.36	↓	↓	0.52	0.140	0.456	0.123	0.336	0.090	0.041	0.219	-0.015
	NCAW-84	45.00		1.36			1.04	0.140	0.912	0.123	0.671	0.090	0.214	0.891	0.421
	NCAW-86	45.00		1.36			0.26	0.170	0.228	0.149	0.168	0.110	0.015	-0.213	-0.330
	NCAW-86	45.00		1.36			0.56	0.170	0.491	0.149	0.361	0.110	0.190	0.174	-0.079
	NCAW-86	45.00		1.36			0.78	0.170	0.684	0.149	0.503	0.110	0.238	0.458	0.106
	Hi Fe	45.00		1.36			0.22	0.110	0.193	0.096	0.142	0.071	0.020	-0.071	-0.170
	Hi Fe	45.00		1.36			0.52	0.110	0.456	0.096	0.336	0.071	0.069	0.316	0.081
	Hi Fe	45.00		1.36			0.95	0.110	0.833	0.096	0.613	0.071	0.120	0.871	0.442
	Hi Fe	45.00		1.36			1.74	0.110	1.525	0.096	1.123	0.071	0.190	1.891	1.105
	Lo Fe	45.00		1.36			0.52	0.230	0.456	0.202	0.336	0.148	0.015	-0.071	-0.306

Comment	Run	Melter Feed Total Solids (wt%)	Sludge Total Solids (wt%)	Est. Melter Feed Density (kg/L)	Est. Sludge Density (kg/L)	Mass Frit / Mass Sludge	Sludge Formate (M)	Sludge Nitrate (M)	Calc. Melter Feed Formate (M)	Calc. Melter Feed Nitrate (M)	Feed Formate (mol/kg)	Feed Nitrate (mol/kg)	Fe^{2+}/ ΣFe	Electron Equivalents (mol/kg norm. to 45% solids)	Electron Equivalents, w/ 35% formate loss factor (mol/kg norm. to 45% solids)
Farnsworth, in PNNL-11044	Lo Fe	45.00		1.36		0.00	0.78	0.230	0.684	0.202	0.503	0.148	0.124	0.265	-0.088
	Lo Fe	45.00		1.36		0.00	0.95	0.230	0.833	0.202	0.613	0.148	0.108	0.484	0.055
	Lo Fe	45.00		1.36		0.00	1.74	0.230	1.525	0.202	1.123	0.148	0.242	1.504	0.718
	Hi Al	45.00		1.36		0.00	0.26	0.160	0.228	0.140	0.168	0.103	0.015	-0.181	-0.298
	Hi Al	45.00		1.36		0.00	0.52	0.160	0.456	0.140	0.336	0.103	0.066	0.155	-0.080
	Hi Al	45.00		1.36		0.00	0.69	0.160	0.605	0.140	0.445	0.103	0.060	0.374	0.063
	Hi Al	45.00		1.36		0.00	0.87	0.160	0.763	0.140	0.562	0.103	0.063	0.607	0.214
	Hi Al	45.00		1.36		0.00	1.74	0.160	1.525	0.140	1.123	0.103	0.201	1.730	0.944
	Lo Al	45.00		1.36		0.00	0.22	0.100	0.193	0.088	0.142	0.065	0.034	-0.039	-0.138
	Lo Al	45.00		1.36		0.00	0.43	0.100	0.377	0.088	0.278	0.065	0.077	0.232	0.038
	Lo Al	45.00		1.36		0.00	0.95	0.100	0.833	0.088	0.613	0.065	0.219	0.904	0.474
	Hi Na	45.00		1.36		0.00	0.26	0.190	0.228	0.167	0.168	0.123	0.015	-0.278	-0.395
	Hi Na	45.00		1.36		0.00	0.65	0.190	0.570	0.167	0.420	0.123	0.132	0.226	-0.068
	Hi Na	45.00		1.36		0.00	1.11	0.190	0.973	0.167	0.716	0.123	0.250	0.820	0.318
	Hi Na	45.00		1.36		0.00	1.74	0.190	1.525	0.167	1.123	0.123	0.289	1.633	0.847
	Lo Na	45.00		1.36		0.00	0.26	0.110	0.228	0.096	0.168	0.071	0.015	-0.019	-0.137
	Lo Na	45.00		1.36		0.00	0.52	0.110	0.456	0.096	0.336	0.071	0.042	0.316	0.081
	Lo Na	45.00		1.36		0.00	1.04	0.110	0.912	0.096	0.671	0.071	0.124	0.988	0.518
	Hi Zr	45.00		1.36		0.00	0.17	0.090	0.149	0.079	0.110	0.058	0.024	-0.071	-0.148
	Hi Zr	45.00		1.36		0.00	0.43	0.090	0.377	0.079	0.278	0.058	0.106	0.265	0.070
	Hi Zr	45.00		1.36		0.00	0.69	0.090	0.605	0.079	0.445	0.058	0.251	0.600	0.289

5.4 Validation of REDOX Prediction Using West Valley Nuclear Services Data

Table XIII provides a summary of WVNS data for REDOX prediction in crucible melts [3] and data from the operation of a $1/10^{th}$ scale test melter [55]. This melter was a 1/10th scale prototype of the joule-heated, ceramic-lined melter used to vitrify wastes stored at the West Valley Demonstration Project (WVDP). Tests were run by doping simulated waste slurries with varying amounts of nitric acid to simulate WVDP flowsheet levels of nitrate, and sucrose was used as a reductant. These slurries were fed to the test melter where the material was vitrified at approximately the same temperatures as in DWPF. The REDOX ratios provided in Table XIII are determined using a different method than those for DWPF; the method used provides indicators of the reduced and oxidized iron species [51]. The measured density and solids information are unavailable for these data; however, the weight percent total solids is given as "approximately 40 to 50 % solids" [51] for the initial slurry feed. To bound the feed data, the molar concentrations were computed at 40% solids (assuming a density of 1.30 kg/l) and 50% solids (assuming a density of 1.40 kg/l). All data were then normalized to 45 wt% solids.

Table XIII Summary of WVNS Crucible and Melter Data

Crucible		Assuming 40 wt% Total Solids		Assuming 50 wt% Total Solids		Assuming 40 wt% Total Solids Electron Equivalents (mol/kg)	Assuming 50 wt% Total Solids Electron Equivalents (mol/kg)
Run ID	$Fe^{+2}/\sum Fe$	Carbon (mol/kg)	Nitrate (mol/kg)	Carbon (mol/kg)	Nitrate (mol/kg)		
WVNS-A-1	0.010	2.366	2.141	1.893	1.713	-1.242	-0.994
WVNS-A-2	0.231	2.760	2.141	2.208	1.713	0.335	0.268
WVNS-A-3	0.448	3.155	2.141	2.524	1.713	1.913	1.530
WVNS-A-4	0.543	3.943	2.141	3.155	1.713	5.067	4.054
WVNS-B-1	0.010	1.972	1.960	1.577	1.568	-1.912	-1.530
WVNS-B-2	0.259	2.366	1.960	1.893	1.568	-0.335	-0.268
WVNS-B-3	0.425	2.760	1.960	2.208	1.568	1.243	0.994
WVNS-C-1	0.020	1.183	1.143	0.946	0.915	-0.984	-0.787
WVNS-C-2	0.383	1.577	1.143	1.262	0.915	0.593	0.475
WVNS-D-1	0.010	0.000	0.000	0.000	0.000	0.000	0.000
WVNS-D-2	0.457	0.394	0.000	0.315	0.000	1.577	1.262
WVNS-D-3	0.533	1.183	0.000	0.946	0.000	4.732	3.785

Melter				
Run ID	$Fe^{+2}/\sum Fe$	Carbon (mol/kg)	Nitrate (mol/kg)	Electron Equivalents (mol/kg)
1-SVS4	0.038	1.683	1.561	-1.076
2-SVS3	0.061	1.582	1.201	0.325
3-SVS9	0.107	1.787	1.509	-0.397
4-SVS8	0.130	1.496	1.285	-0.439
5-SVS8	0.281	2.242	1.343	2.253
6-SVS8	0.367	2.332	1.285	2.905
7-SVS8	0.401	2.310	1.209	3.198

These data are overlain on the Electron Equivalents REDOX model in Figure 26. All but three of the crucible data points (ranges) lie within the 95% confidence interval. One at Electron Equivalents equal to zero is just below the interval; the A-4 and D-3 points are much further towards oxidizing than the model would predict, but the Electron Equivalents values (+4-5) are well outside the range of the model correlation. Four of the WVNS melter data points are within the confidence interval, one is near it, and the three at the higher Electron Equivalents values are much further to the right of the "Model Data". These data show that the Electron Equivalents model handles sugar as a reductant quite well.

Figure 27 shows that the oxidant and reductant concentrations, expressed in terms of Electron Equivalents, are much higher for the WVNS data than for any of the other data examined. Given that the WVNS data are outside the range of the current model range, the agreement shown in Figure 26 is much better than might be expected.

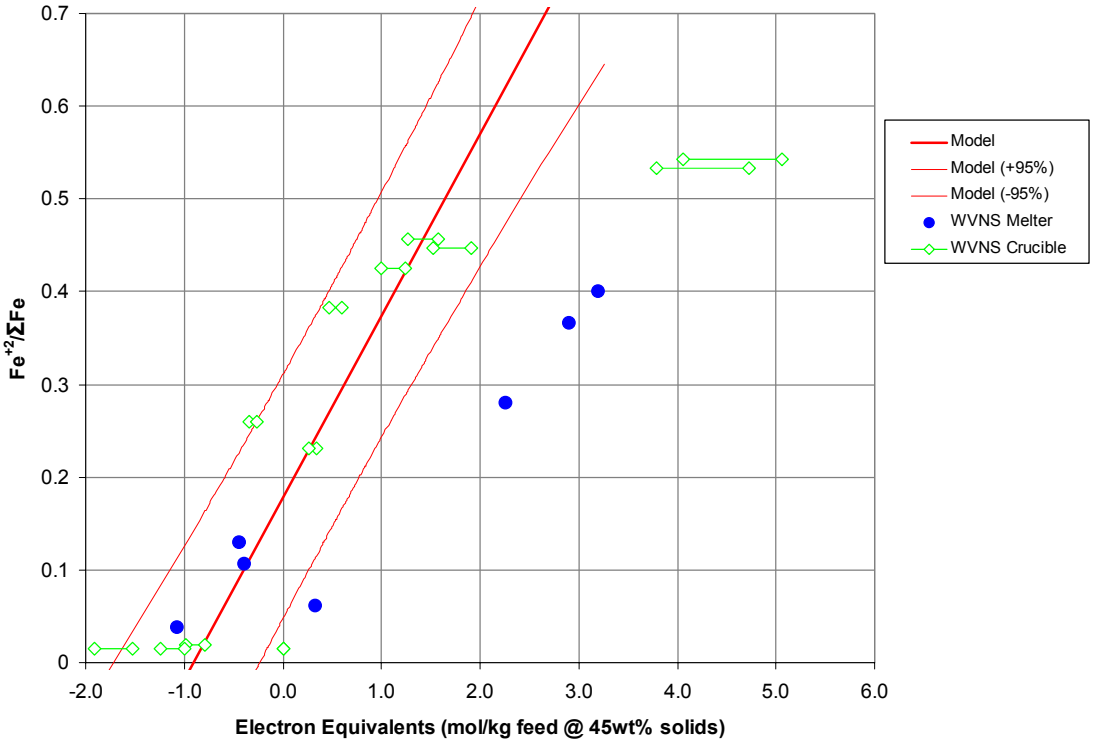

Figure 26. Comparison of WVNS crucible and melter data with the Electron Equivalents REDOX model.

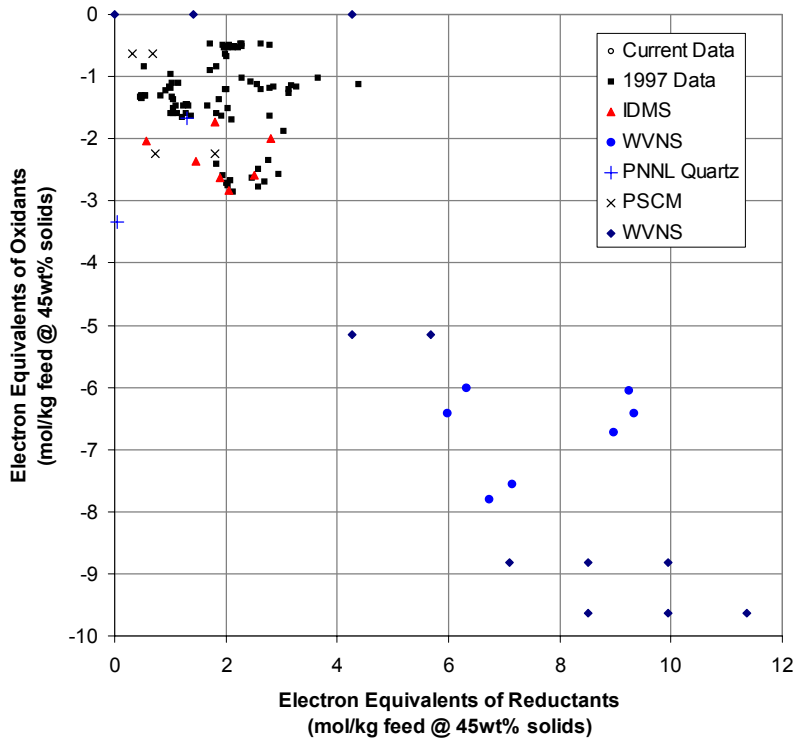

Figure 27. Oxidant and reductant ranges for Model and Validation Data.

Figure 28 shows a plot of measured versus predicted REDOX that was presented in the 1997 REDOX report. For this plot, two times the moles of carbon from sugar were substituted for moles of formate in the {[F]-3[N]}REDOX equation. When these same data are plotted as shown in Figure 29 using the Electron Equivalents model, the data are fit much better than with the {[F]-3[N]} since the relationship is actually {[Carbon]-2.5[N]}, or in the case of sugar {2[Sugar]-2.5[N]}.

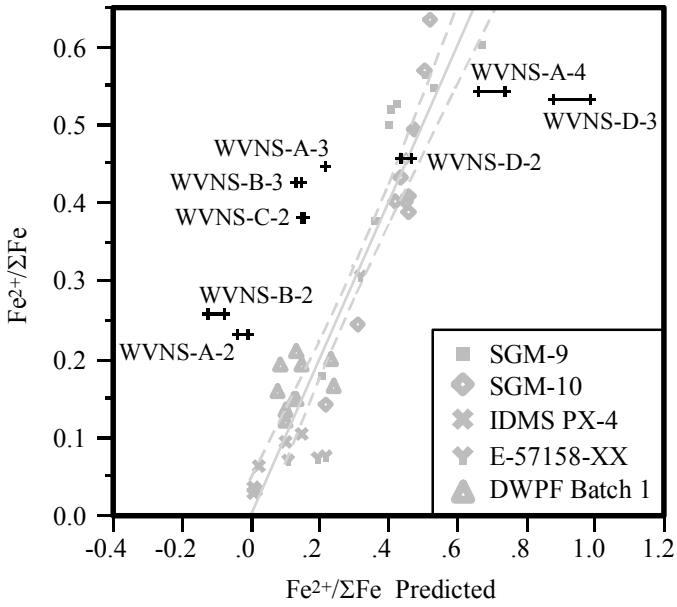

Figure 28. WVNS crucible data predicted by {[F]-3[N]} model from 1997 [15].

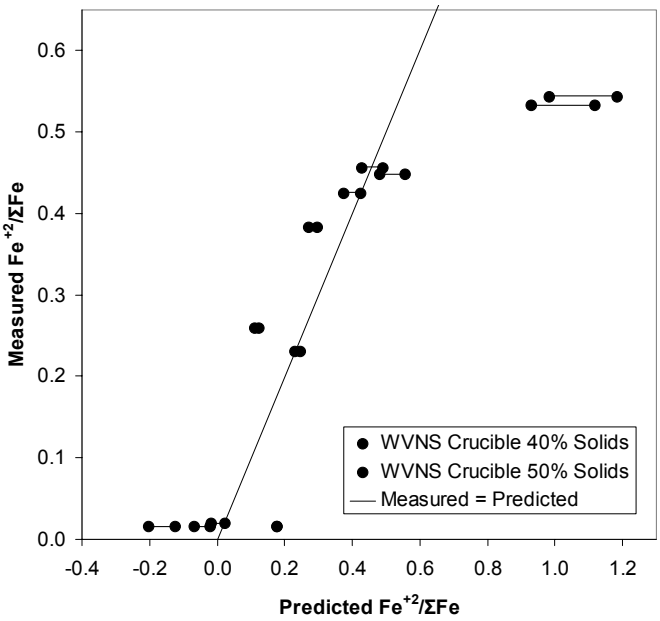

Figure 29. WVNS crucible data predicted by the current Electron Equivalents model.

5.5 Validation of REDOX Prediction Using SRTC Scale Glass Melter (SGM) Tests

The SRTC Scale Glass Melter (SGM) system was used to demonstrate many DWPF design and operational concepts. This joule-heated melter was a 2/3 linear scale version of that in DWPF. The sixth and seventh SGM Runs (SGM-6 and SGM-7) were used to investigate the DWPF coupled flowsheet using simulated sludge and Precipitate Hydrolysis Aqueous (PHA) [56]. Minor changes were made to the SGM-6 feed for SGM-7 with the resulting organic content of the feed being higher than SGM-6. As a result, this feed was much more reducing in the melter than that for SGM-6.

The SGM data are summarized in Table XIV. The nitrate concentrations reported for SGM-6 were actually 100 times smaller than given in this table. The report stated that both feeds were made with essentially the same recipe, so the resulting nitrate concentrations should have been similar. Moreover, during this time period, ion chromatography measurements that were performed were often reported as the concentration of a 100X dilution rather than the back-corrected (as-received) concentration. The carbon content of this feed was a combination of formate from the formic acid adjustment and organics from the PHA. The exact quantities of the formate and organics in these feeds were not given in the report, so it was assumed that all of the organic carbon was formate. Figure 30 shows these data with the Electron Equivalents data. These data are also predicted reasonably well by the model without the inclusion of the manganese data.

Table XIV Summary of SGM REDOX Data

Feed Sample ID	Total Solids (wt%)	Estimated Density (kg/L)	Nitrate (mg/L)	Total Organic Carbon (mg/L)	Glass Sample ID	Nitrate (mol/kg)	Carbon (mol/kg)	$Fe^{2+}/\Sigma Fe$	Electron Equivalents (mol/kg feed norm. to 45 wt% total solids)
2/24/87B	46.37	1.373	25600	11100	TNX6-3A	0.301	0.673	0.047	-0.153
2/24/87B	46.12	1.370	22500	4100	TNX6-3B-27	0.265	0.249	0.09	-0.806
2/25/87	46.15	1.371	23100	18400	TNX6-3B-27	0.272	1.118	0.134	0.854
2/26/87	45.58	1.364	23800	12900	TNX6-4A	0.281	0.787	0.09	0.165
2/27/87	46.15	1.370	20900	10200	TNX6-4B	0.246	0.620	0.133	0.009
2/28/87	43.34	1.340	22200	14100	TNX6-5B	0.267	0.876	0.455	0.432
3/2/87	41.61	1.322	24800	13500	TNX6-6A	0.303	0.850	0.052	0.203
3/3/87	41.90	1.325	24300	16800	TNX6-6B	0.296	1.056	0.122	0.679
5/14/87	44.52	1.353	21326	18480	CAN-7-1	0.254	1.137	0.335	1.014
5/15/87	44.85	1.356	21064	22335	CAN-7-2B	0.250	1.371	0.413	1.494
5/16/87	44.64	1.354	21948	17845	CAN-7-3	0.261	1.097	0.466	0.894
5/17/87	44.30	1.350	19508	17410	CAN-7-4	0.233	1.073	0.495	0.997
5/18/87	43.49	1.342	16474	18305	CAN-7-4#2	0.198	1.136	0.503	1.326
5/21/87	49.07	1.403	26235	19050	CAN-7-4#3	0.302	1.130	0.451	0.690
5/27/87	47.01	1.380	22347	23890	CAN-7-5#4	0.261	1.441	0.472	1.509
5/29/87	46.84	1.378	24863	20520	CAN-7-5	0.291	1.240	0.508	0.984
5/30/87	47.37	1.384	24297	21100	CAN-7-5	0.283	1.269	0.517	1.067
5/31/87	47.10	1.381	23152	21715	CAN-7-5#7	0.270	1.309	0.505	1.210

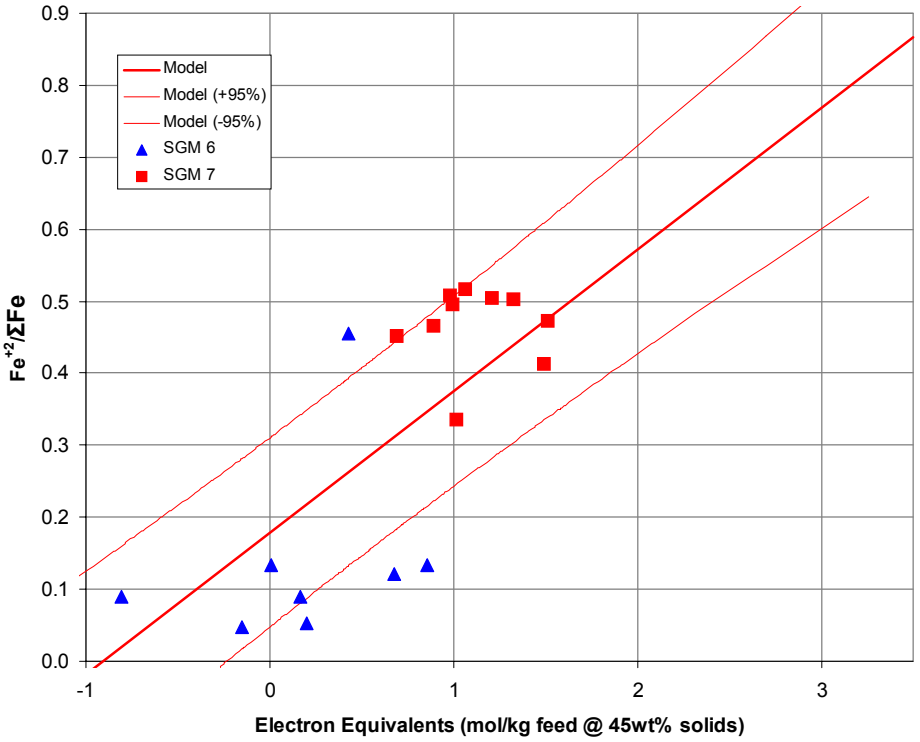

Figure 30. SGM data compared to the Electron Equivalents model.

6.0 CONCLUSIONS

- The acceptable iron REDOX ratio for DWPF melts should remain defined as $0.09 \leq Fe^{2+}/\Sigma Fe \leq 0.33$ as indicated in previous studies. Controlling the DWPF melter at a REDuction/OXidation (REDOX) equilibrium of $Fe^{+2}/\Sigma Fe \leq 0.33$ prevents the potential for conversion of $NiO \rightarrow Ni°$, $RuO_2 \rightarrow Ru°$, and $2SO_4^{=} \rightarrow S_2 + 4O_2$ during vitrification so that metallic and sulfide rich species do not form and accumulate on the floor of the melter. Control of foaming is achieved by having 66-100% of the MnO_2 or Mn_2O_3 species converted to MnO during SRAT refluxing. While 100% of the Mn^{+3} converts to Mn^{+2} at a $Fe^{+2}/\Sigma Fe \geq 0.33$, about 99% is converted at $Fe^{+2}/\Sigma Fe \sim 0.09$. This lower limit will prevent foaming from deoxygenation of manganic species in the melter.

- During crucible vitrifications, SME products and/or melter feeds must be stirred after settling during drying or a refractory frit layer forms on the top 1mm of the surface which traps gasses in the melt.

- Glasses used in modeling must be produced from refluxed melter feed material to ensure conversion to nitrate and formate species. Vitrified material must be

visibly (10X) black and homogeneous; that is, it must contain no brown discoloration due to metallic copper and/or no crystalline or other metallic material as these species make both reliable REDOX ratio and cation measurements difficult–if not impossible. The iron REDOX ratio (i.e., $Fe^{2+}/\Sigma Fe$) is measured using the Baumann colorimetric technique which was recommended for use in DWPF and SRTC in 1989 [57] and must be greater than or equal to the SRTC detection limit of $Fe^{2+}/\Sigma Fe \leq 0.03$. Both REDOX and feed chemistry measurements must be available for the same sample. Measured or as-made total solids information must available. Use of other REDOX measurement techniques has been shown to give less reliable measurements [57].

- Stabilization of alkali-ferric iron and alkali-manganic complexes (as suggested in the literature) over their reduced counterparts in alkali-rich melts was not found to be statistically significant in this study.

- The role of manganese and its distribution between soluble and insoluble melter feed components is complex. Manganese can complex with formate as soluble $Mn(COOH)_2$ in the SRAT supernate, as insoluble MnO_2 in the SRAT insoluble solids, or as insoluble manganous oxalate in the SRAT insoluble solids. The role as $Mn(COOH)_2$ is pH dependent, e.g. $Mn(COOH)_2$ is stable at near neutral pH while aqueous Mn^{+2} is soluble at lower SRAT pH values. Therefore, a measurement of the soluble Mn in the SRAT supernate is insufficient to determine if 66% of the Mn^{+4} has been reduced to Mn^{+2} when the SRAT/SME pH values fluctuate and oxalate is present.

- Due to the complex role of manganese in the presence and absence of oxalate, a decision was made to include the effects of manganese during REDOX modeling.

- Aged SME products made with Frit 320 and Frit 202 contained complex oxalate phases, e.g. manganous oxalate ($C_2MnO4 \bullet 2H_2O$), sodium oxalate ($Na_2C_2O_4$) and calcium oxalate, ($C_2CaO_4 \bullet H_2O$) along with $NaNO_3$.

- As long as the DWPF glass REDOX is controlled at a REDOX ratio of ≤0.33 $Fe^{+2}/\Sigma Fe$ then there will be sufficient oxygen available in the melter plenum to combust carbon (coal) and any other organics to CO_2.

- A REDOX model was developed that generalized the product and reactant species from the 4-stages of the DWPF cold cap reaction model so that the impact on melt REDOX could be represented by

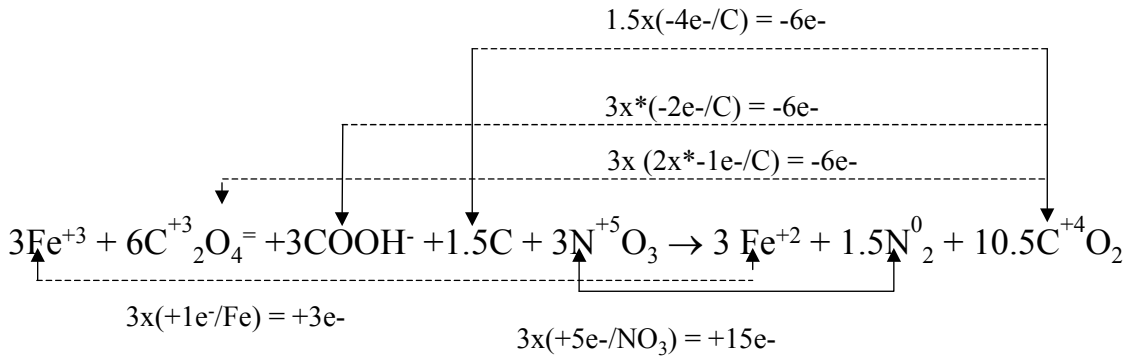

The generalized cold cap reaction assumes that Fe^{3+} enters the melter as Fe_2O_3 and that $COOH^-$ and NO_3^- both enter as properly formated and nitrated sodium compounds. The formated and nitrated salts react with glass formers such as SiO_2 to form Fe^{+2} and Na_2SiO_3 components in the glass and liberate CO_2, N_2 and H_2O vapors to the melter plenum. The remaining organics, oxalate and coal, are destroyed and form CO_2 and water after oxalate undergoes a disproportionation to $COOH^-$. The manganese term, the reduction of Mn^{+4} to Mn^{+2}, is not shown in the above equation for brevity but is included in the Electron Equivalents model.

- Reduction is defined as making an atom or molecule less positive by electron transfer. Oxidation is defined as making an atom or molecule more positive by electron transfer. Therefore, the number of moles of electrons transferred for each REDuction/OXidation reaction can be summed and an Electron Equivalents term for each organic and oxidant species defined. In the REDuction/OXidation equilibrium between nitrate and formate salts, one mole of nitrate gains 5 electrons when it is reduced to N_2 while one mole of carbon in formate loses 2 electrons during oxidation to CO_2. Thus the Electron Equivalents term for formate is 2 while the term for nitrate is 5. In a similar manner, one mole of carbon in coal loses 4 electrons during oxidation to CO_2 so its electron equivalent term is 4. For sugar, one mole of carbon in sugar loses 4 electrons during oxidation to CO_2. For manganese, one mole of Mn^{+4} gains 2 electrons. The pertinent Electron Equivalents terms are 4 for sugar and 2 for manganese.

- Theoretically, one mole of carbon in oxalate should lose 1 electron during oxidation to CO_2 or one mole of oxalate should transfer 2 electrons during oxidation to CO_2 since there are 2 moles of carbon in one mole of oxalate. Therefore, the Electron Equivalents term for oxalate should be 2. However, REDOX modeling indicated that oxalate was twice as effective a reductant as would be anticipated from the simple electron transfer model applied to the other organic species, e.g. the Electron Equivalents term should be 4. Data from SRAT processing indicated that 8-37% of the oxalate salts converts to oxalic acid and then disproportionate to formic acid and CO_2. Therefore, it was assumed that disproportionation also occurs in the cold cap when the liquid slurry impacts the melt pool surface. Since only half of the oxalate is acting as a reductant, the reduction potential of oxalate is doubled.

- The water content of a melter feed alters the species concentrations of the reductants and oxidants and can influence the equilibrium oxygen fugacity (f_{O_2}) in a melter during vitrification. Since the effects of water on oxygen fugacity are small relative to the impact of dilution on feed concentrations, the molar concentrations are transformed to a 45% solids basis as done in previous REDOX modeling. That is, the prediction model for REDOX takes the form:

$$\xi\left(\begin{array}{c} mol/kg\ feed \\ @45\ wt\%\ solids \end{array}\right) = f\left(2[F]+4[C]+4[\mathrm{O_T}]-5[N]-2[Mn]\right)\frac{45}{T}$$

  where T is the total solids in wt% and the other terms are described below.

- The overall relationship between the REDOX ratio and the Electron Equivalents can be expressed as:

$$\frac{Fe^{2+}}{\Sigma Fe} = f\left[\left(2[F]+4[C]+4[\mathrm{O_T}]-5[N]-2[Mn]\right)\frac{45}{T}\right] = f[\xi]$$

  where f = indicates a function
  [F] = formate (mol/kg feed)
  [C] = coal (carbon) (mol/kg feed)
  [O_T] = $oxalate_{total}$ (soluble and insoluble) (mol/kg feed)
  [N] = nitrate + nitrite (mol/kg feed)
  [Mn] = manganese (mol/kg feed)
  T = total solids (wt%)

  and ξ (mol/kg feed)= $\left(2[F]+4[C]+4[\mathrm{O_T}]-5[N]-2[Mn]\right)\frac{45}{T}$ = Electron Equivalents

  In the presence of sugar the Electron Equivalents term becomes

  ξ (mol/kg feed) = $\left(2[F]+4[C]+4[S]+4[\mathrm{O_T}]-5[N]-2[Mn]\right)\frac{45}{T}$

- The REDOX data generated in this study were fit along with the 1997 Model data as a linear function of ξ:

  $\frac{Fe^{2+}}{\Sigma Fe} = b + m\xi$ or $\frac{Fe^{2+}}{\Sigma Fe} = 0.1942 + 0.1910\xi$ with an $R^2 = 0.80$ and a RMSE = 0.0690.

- The $\frac{Fe^{2+}}{\Sigma Fe}$ predictions from the Electron Equivalents model were fitted to measured REDOX data generated from the DWPF melter from SME Batch 224, to data generated by the SRTC mini-melter and to data from the SRTC Slurry-fed Melt Rate Furnace (SMRF). All the data from these melters fell within the 95% confidence bands of the Electron Equivalents REDOX model developed in this study.

- Validation data from SRS pilot scale melters, Pacific Northwest Laboratory testing, and West Valley Nuclear Fuel Services testing agreed with the Electron Equivalents model which has an {[F]-2.5[N]} dependency better than the {[F]-3[N]} DWPF REDOX model.

7.0 LESSONS LEARNED

The following were lessons learned during experimentation:

- The floating of the coal caused a lot of reduction to occur on or near the surface of the vitrified samples and it was difficult to get a representative glass pool sample without surface inhomogeneities. These surface effects were caused by the limited amount of feed available for the multiple crucible runs. This caused poorly reproducible replicates of the measured REDOX ratio from each crucible. The presence of metallic iron, noble metals, and nickel sulfide were confirmed by X-ray diffraction on the surfaces of the vitrified samples where the coal particles had "floated" during vitrification since there is little convective transfer in the crucible compared to a melter. Sample inhomogeneity was more perverse with the SRAT feeds containing coarser coal particles than the finer coal particles.

- Duplicate REDOX analyses were not performed as in previous REDOX modeling studies. Triplicate SME analyses were not performed as in previous REDOX modeling studies due to limited resources. Therefore, inherent experimental variability could not be averaged out as done in previous REDOX modeling studies.

- A minimal amount of vitrified SRAT product was used (40-60g). This made <1/2 inch of glass in the 100mL sealed crucible tests. These small amounts were necessary because the SRAT feed stock was limited and 8 permutations of frit type and waste loading were being tested per SRAT composition. A deeper "melt pool" of glass in every crucible would have eliminated or minimized the floating coal and crystallite problem even if it meant doing fewer permutations of frit type and waste loading.

- Single SRAT product chemistries were used instead of reanalysis of each of the 185 simulated SME products being measured in triplicate as done in previous REDOX studies. The SRAT product concentrations were "adjusted" for the amount of frit added to each simulated SME product. Use of the SRAT concentrations made the modeling effort very sensitive to sub-sampling errors during transfers from the SRAT vessel to the SRTC aliquots and transfer errors from the SRTC aliquots to the crucibles. In general, all the targeted waste loadings were biased high. The high waste loadings produced glass ceramics that did not give consistent redox measurements.

- Leaving the sealed crucibles at 1150°C for 3 hours did not alter the measured REDOX from those reacted for only 1 hour.

APPENDIX A

1997 Model Data from Brown, Jantzen, and Pickett [15]

Samples of melter feed slurries were collected from Scale Glass Melter (SGM), Integrated DWPF Melter System (IDMS), and DWPF campaigns and vitrified in sealed crucibles [23,24,25]. The formate and nitrate concentrations for each slurry were converted (when solids measurements were available) to normalized molar form by 1) multiplying the measured concentrations (which were in parts per million or ppm) by a factor of (45%/measured total percent solids for the slurry)† and 2) converting the resulting concentrations to molar (ppm formate/45010 mg per mole and ppm nitrate/62000 mg per mole).†† Iron REDOX (i.e., Fe^{2+} and ΣFe) analyses were performed by the Analytical Development Section (ADS) on the samples vitrified in sealed crucibles.

Melter feed was doped with varying amounts of oxidants and reductants and then vitrified in crucibles. The data presented in Appendix A were collected by Ramsey, et al. [23,24] and consisted of 27 melter feed slurries and corresponding REDOX ratio determinations.‡ For each feed, ADS performed triplicate analyses for formate and nitrate ion concentrations. Then either one or two sets of iron REDOX measurements were made. The REDOX, formate, and nitrate analyses were not all performed on the same sample; therefore, these results could not be paired, and the appropriate means were used to represent melter feed samples.

The melter feed slurries represented in Appendices B, C, and D were prepared by doping properly formated simulated DWPF and IDMS melter feeds with varying quantities of formate, nitrate, and copper–as many as five samples of each of these feeds were prepared. Up to three of these slurry samples were analyzed for formate, nitrate, and copper concentrations, and the remaining one or two samples were vitrified in sealed crucibles for measurement of iron REDOX. Table A1 summarizes the results from these studies.

The moments (i.e., means and standard deviations) in Table A1 for the measured formate and nitrate concentrations and the computed REDOX ratios were estimated using SAS Institute's JMP® software. To examine the possible error structures for this information, the standard deviations were plotted as functions of the means in Reference [15]. The plots did not suggest that the errors were relative. This result was considered surprising for formate and nitrate; however, at the concentrations considered in these studies, the errors were considered absolute.

---

† If multiple measurements of total solids were available, the mean was used for conversion. The data provided by Ramsey were formulated to be 45% total solids and no conversions were made.

†† The measured formate and nitrate concentrations were multiplied by 100 to compensate for the 1:100 dilution with deionized water that took place prior to submission for analysis. It was assumed that these samples were initially diluted and then analyzed omitting the need for including the slurry density into the conversion.

‡ The first ten sets are from the SGM-9 campaign, the next 11 are from SGM-10, and the remaining six are from IDMS PX-4 operation.

The data presented in Appendix C were collected by R. F. Schumacher and consisted of observations made on a series of IDMS PX-4 Slurry Mix Evaporator (SME) feed slurries (i.e., E-57158-18, -20, -22, -26, and -27) and Scale Glass Melter (SGM-9) feed material (i.e., E-57158-24) [26]. These feed samples underwent controlled additions of formic acid and copper. (No nitrate was added to these samples.) This study resulted in 16 groups (three for series E-57158-24, six for series -26, and seven for series -27) of data useful for iron REDOX ratio prediction.† Each group was analyzed thrice for formate and nitrate concentrations and two additional samples were vitrified (some of which were split for replication purposes). The resulting two or four samples for each group had analyses performed for copper concentration and iron REDOX ratio. The appearance of the vitrified material in the crucible was also reported.

The final set of SRTC crucible data is provided in Appendix D. These 14 sets of glasses were generated from a study in which simulated DWPF Waste Qualification Run Batch 1 melter feed was doped with varying levels of formate, nitrate, and copper to determine the effect of formate and nitrate feed concentrations on the precipitation of copper based on 1994 DWPF flowsheet operation [25]. For each slurry, the formate and nitrate concentrations were measured twice and the copper concentration once. The slurries were then vitrified in sealed crucibles and the REDOX analyses were performed in duplicate (where only the computed REDOX ratios are available).

For modeling purposes, each set of formate, nitrate, and REDOX measurements were averaged providing single observations. For Schumacher's data from Appendix C, series E-57158-27 consisted of mostly black glass, while series E-57158-24 and -26 had mostly brown/black glass with metallic copper precipitates. These data were subsequently used to determine the impact of REDOX on the precipitation of copper. Similarly, sets 17-20 of the DWPF Batch 1 glasses in Appendix D were not used in modeling since they visually exhibited the brown streaking indicative of copper precipitates. These omissions should not effect the ability to control REDOX in DWPF since there already exists a constraint on total copper in glass to prevent these glasses from being produced.

† The E-57158-18, -20, and -22 series of data were omitted from modeling since these glasses were primarily intended to determine the maximum concentration of copper in DWPF glasses at very oxidized conditions. The resulting REDOX ratios for these glasses were below the REDOX ratio detection limit and thus would badly skew any resulting model despite how these values were handled.

Moments (i.e., Means and Standard Deviations) by Sample for Model Crucible Data
(Highlighted Rows are Omitted Due to Copper Precipitation)

		Mn(mg/kg) *	$Fe^{2+}/\Sigma Fe$			Formate (M)			Nitrate (M)	
Sample ID	**Comment**		**N**	**Mean**	**StDev**	**N**	**Mean**	**StDev**	**Mean**	**StDev**
S9-L-F300	Single REDOX Measurement	5000*	1	0.566	.	3	2.103	0.041	0.322	0.015
S9-L-F3000		5000*	2	0.6035	0.0092	3	2.662	0.275	0.288	0.016
S9-L-F800		5000*	2	0.5505	0.0516	3	2.176	0.032	0.309	0.008
S9-L-N100	No REDOX measurements	5000*	.	.	.	3	1.788	0.211	0.59	0.066
S9-L-N1000		5000*	2	0.1805	0.0332	3	1.889	0.097	0.656	0.034
S9-L-N50		5000*	2	0.5235	0.0177	3	1.577	0.365	0.273	0.06
S9-L-N500		5000*	2	0.377	0.0226	3	1.96	0.095	0.472	0.032
S9-L-P1500		5000*	2	0.495	0.0226	3	2.004	0.102	0.328	0.015
S9-L-P3000		5000*	2	0.502	0.0283	3	1.553	0.317	0.274	0.046
S9-L-P200		5000*	2	0.5285	0.0134	3	1.766	0.026	0.316	0.012
S10-L-F1500		6000*	2	0.635	0.1018	3	1.569	0.466	0.111	0.031
S10-L-F300		6000*	2	0.4935	0.0318	3	1.445	0.064	0.135	0.01
S10-L-F800		6000*	2	0.5695	0.0856	3	1.531	0.018	0.127	0.002
S10-L-N100		6000*	2	0.403	0.0552	3	1.349	0.015	0.174	0.006
S10-L-N1000		6000*	2	0.1405	0.0163	3	1.333	0.083	0.447	0.011
S10-L-N500		6000*	2	0.243	0.0085	3	1.386	0.048	0.335	0.013
S10-L-P200		6000*	2	0.3885	0.0064	3	1.418	0.037	0.144	0.001
S10-L-N50	Single REDOX Measurement	6000*	1	0.434	.	3	1.318	0.14	0.141	0.013
S10-L-P1500		6000*	2	0.403	0.0537	3	1.312	0.153	0.127	0.012
S10-L-P3000		6000*	2	0.4565	0.0163	3	1.33	0.204	0.13	0.01
S10-L-P500		6000*	2	0.41	0.0269	3	1.381	0.045	0.14	0.002
I-L-P1500	Single REDOX Measurement	4600*f*	1	0.033	.	3	1.323	0.093	0.711	0.051
I-L-P200	1 Above DL/1 Below DL	4600*f*	2	0.025	0.0141	3	1.390	0.077	0.745	0.047
I-L-P3000	Single REDOX Measurement	4600*f*	1	0.063	.	3	1.302	0.095	0.694	0.051
I-L-P500	1 Above DL/1 Below DL	4600*f*	2	0.0225	0.0106	3	1.42	0.014	0.759	0.032
I-L-PF1500		4600*f*	2	0.104	0.0382	3	1.775	0.04	0.695	0.03
I-L-5/8		4600*f*	2	0.0945	0.0445	3	1.665	0.089	0.713	0.042
SERIES 26 (AR)	REDOX Values Below DL	5000‡	2	0.015	.	3	0.313	0.009	0.354	0.003
(.14,1000)	1 Black Used/2 Brown Omitted	5000‡	1	0.071	.	3	1.098	0.07	0.37	0.024
(.14,2000)	Brown Glass	5000‡	2	0.249	0.1471	3	1.734	0.063	0.338	0.013
(.14,3000)	Brown Glass	5000‡	2	0.2935	0.0035	3	2.374	0.011	0.336	0.018
(.14,4000)	Brown Glass	5000‡	2	0.6	0.1428	3	3.207	0.093	0.333	0.017
(.14,6000)	Brown Glass	5000‡	2	0.512	0.0099	3	4.509	0.245	0.32	0.028
SERIES 27 (AR)	REDOX Values Below DL	5000‡	4	0.015	.	3	0.324	0.003	0.36	0.007
(.17,250)	1 Above DL/1 Below DL	5000‡	2	0.0425	0.0389	3	0.457	0.095	0.294	0.064
(.17,500)	REDOX Values Below DL	5000‡	2	0.015	.	3	0.586	0.15	0.28	0.067
(.17,750)		5000‡	2	0.0725	0.0064	3	0.725	0.047	0.272	0.021
(.17,1000)	Brown Glass	5000‡	2	0.109	0.0368	3	0.939	0.044	0.316	0.025
(.17,1500)	Brown Glass	5000‡	2	0.245	0.0212	3	1.19	0.094	0.301	0.019
(.17,0)	REDOX Values Below DL	5000‡	2	0.015	.	3	0.369	0.009	0.348	0.007
SERIES 24 (AR)			2	0.3075	0.0346	1	1.155	.	0.245	.
(.14,1000)	Brown Glass		2	0.457	0.0	1	2.011	.	0.257	.
(.14,3000)	Brown Glass		2	0.431	0.0212	1	3.022	.	0.209	.
Batch 1-9		4900**	2	0.165	0.1202	2	1.325	0.078	0.41	0.0
Batch 1-10		4900**	2	0.2	0.0424	2	1.255	0.021	0.4	0.042
Batch 1-11		4900**	2	0.195	0.0495	2	0.71	0.042	0.415	0.021
Batch 1-12		4900**	2	0.16	0.0141	2	0.715	0.007	0.42	0.014
Batch 1-13		4900**	2	0.15	0.0849	2	0.915	0.021	0.42	0.028
Batch 1-14		4900**	2	0.21	0.0566	2	0.855	0.035	0.395	0.007
Batch 1-15		4900**	2	0.15	0.0566	2	0.865	0.007	0.41	0.028
Batch 1-16		4900**	2	0.195	0.1061	2	0.66	0.057	0.315	0.021
Batch 1-17	Brown Glass	4900**	2	0.155	0.0778	2	1.085	0.021	0.41	0.028
Batch 1-18	Brown Glass	4900**	2	0.1	0.0849	2	1.08	0.028	0.4	0.028
Batch 1-19	Brown Glass	4900**	2	0.215	0.1061	2	1.04	0.014	0.39	0.028
Batch 1-20	Brown Glass	4900**	2	0.155	0.0778	2	1.075	0.021	0.405	0.007
Batch 1-21		4900**	2	0.135	0.0354	2	0.77	0.071	0.41	0.057
Batch 1-22		4900**	2	0.12	0.0707	2	0.725	0.049	0.395	0.049
JMP® Moments*	All Crucible Data									
	Model Crucible Data									

Sources for Manganese Data:

* Manganese data for the historic SGM-9 (S9) and SGM-10 (S-10) melter feeds in the table above were found in Reference 46 as wt% elemental Mn in calcine. The calcine elemental wt% was converted to MnO in the final glass. This was converted to Mn in the feed in mg/kg using the following relationship

$$Mn_{feed}\ (mg/kg) = 2702 + 1165\ MnO_{glass}$$

which was developed from the data in the current study.

f Manganese oxide (MnO) data for IDMS PHA Run#3 glasses were found in Table 8.0.3 of Reference 48 and converted using the relationship Mn_{feed} (mg/kg) = 2702 + 1165 MnO_{glass}

‡ Manganese oxide (MnO) data for the Series 26 and Series 27 glasses (PX-4 feed) were found in Table 2 of Reference 26 and converted using the relationship Mn_{feed} (mg/kg) = 2702 + 1165 MnO_{glass}

† Manganese oxide (MnO) data for the Series 24 glasses (PX-4 feed) were found in data tables provided by R.F. Schumacher and converted using the relationship Mn_{feed} (mg/kg) = 2702 + 1165 MnO_{glass}

** Manganese oxide (MnO) data for the Batch 1 glasses were found in Table 2 of Reference 58 and converted using the relationship Mn_{feed} (mg/kg) = 2702 + 1165 MnO_{glass}

Appendix B
Molar Formate and Nitrate and Iron REDOX Ratio for Crucible Data Analyzed by W. G. Ramsey

Sample ID	$Fe^{2+}/\Sigma Fe$	Formate (ppm)	Normalized Formate (M)†	Nitrate (ppm)	Normalized Nitrate (M)†
S9-L-F300-A	0.566	95300	2.1173	20100	0.3242
S9-L-F300-B	.	96100	2.1351	20800	0.3355
S9-L-F300-C	.	92600	2.0573	18900	0.3048
S9-L-F3000-A	0.597	134000	2.9771	19000	0.3065
S9-L-F3000-B	0.61	111400	2.4750	17200	0.2774
S9-L-F3000-C	.	114000	2.5328	17400	0.2806
S9-L-F800-A	0.587	97000	2.1551	19300	0.3113
S9-L-F800-B	0.514	99600	2.2128	19600	0.3161
S9-L-F800-C	.	97200	2.1595	18600	0.3000
S9-L-N100-A	.	70800	1.5730	32200	0.5194
S9-L-N100-B	.	89800	1.9951	40300	0.6500
S9-L-N100-C	.	80800	1.7952	37300	0.6016
S9-L-N1000-A	0.157	89700	1.9929	43100	0.6952
S9-L-N1000-B	0.204	84400	1.8751	39500	0.6371
S9-L-N1000-C	.	81000	1.7996	39500	0.6371
S9-L-N50-A	0.511	85200	1.8929	19900	0.3210
S9-L-N50-B	.	53000	1.1775	12800	0.2065
S9-L-N50-C	0.536	74700	1.6596	18100	0.2919
S9-L-N500-A	0.361	93000	2.0662	31400	0.5065
S9-L-N500-B	0.393	84800	1.8840	27600	0.4452
S9-L-N500-C	.	86800	1.9285	28700	0.4629
S9-L-P1500-A	0.479	95500	2.1218	21300	0.3435
S9-L-P1500-B	0.511	87300	1.9396	19500	0.3145
S9-L-P1500-C	.	87800	1.9507	20200	0.3258
S9-L-P3000-A	0.522	55800	1.2397	14100	0.2274
S9-L-P3000-B	0.482	69600	1.5463	17100	0.2758
S9-L-P3000-C	.	84300	1.8729	19800	0.3194
S9-L-P200-A	0.519	78200	1.7374	19000	0.3065
S9-L-P200-B	0.538	79900	1.7752	20400	0.3290
S9-L-P200-C	.	80400	1.7863	19400	0.3129
S10-L-F1500-A	0.563	85400	1.8974	8080	0.1303
S10-L-F1500-B	0.707	79900	1.7752	7940	0.1281
S10-L-F1500-C	.	46600	1.0353	4640	0.0748
S10-L-F300-A	0.516	67700	1.5041	8860	0.1429
S10-L-F300-B	0.471	65400	1.4530	8630	0.1392
S10-L-F300-C	.	62000	1.3775	7680	0.1239
S10-L-F800-A	0.509	69100	1.5352	7950	0.1282
S10-L-F800-B	0.63	69600	1.5463	7930	0.1279
S10-L-F800-C	.	68000	1.5108	7770	0.1253
S10-L-N100-A	0.442	60500	1.3441	10800	0.1742
S10-L-N100-B	0.364	61500	1.3664	11200	0.1806

† The total solids for these analyses were assumed to be 45%; that is, no normalization was performed.

Sample ID	$Fe^{2+}/\Sigma Fe$	Formate (ppm)	Normalized Formate (M)†	Nitrate (ppm)	Normalized Nitrate (M)†
S10-L-N100-C	.	60200	1.3375	10400	0.1677
S10-L-N1000-A	0.129	64300	1.4286	28500	0.4597
S10-L-N1000-B	0.152	58300	1.2953	27600	0.4452
S10-L-N1000-C	.	57400	1.2753	27100	0.4371
S10-L-N500-A	0.237	61300	1.3619	20300	0.3274
S10-L-N500-B	0.249	61000	1.3553	20400	0.3290
S10-L-N500-C	.	64900	1.4419	21700	0.3500
S10-L-P200-A	0.393	61900	1.3752	8960	0.1445
S10-L-P200-B	0.384	64700	1.4375	8970	0.1447
S10-L-P200-C	.	64900	1.4419	8840	0.1426
S10-L-N50-A	.	61300	1.3619	8730	0.1408
S10-L-N50-B	0.434	52300	1.1620	7970	0.1285
S10-L-N50-C	.	64400	1.4308	9600	0.1548
S10-L-P1500-A	0.441	62500	1.3886	8150	0.1315
S10-L-P1500-B	0.365	63500	1.4108	8410	0.1356
S10-L-P1500-C	.	51100	1.1353	7020	0.1132
S10-L-P3000-A	0.445	69400	1.5419	8540	0.1377
S10-L-P3000-B	0.468	59100	1.3130	8230	0.1327
S10-L-P3000-C	.	51100	1.1353	7400	0.1194
S10-L-P500-A	0.391	60100	1.3353	8820	0.1423
S10-L-P500-B	0.429	62300	1.3841	8630	0.1392
S10-L-P500-C	.	64100	1.4241	8600	0.1387
I-L-P1500-A	.	54700	1.2153	40500	0.6532
I-L-P1500-B	0.033	61800	1.3730	46200	0.7452
I-L-P1500-C	.	62100	1.3797	45600	0.7355
I-L-P200-A	0.035	59600	1.3242	43500	0.7016
I-L-P200-B	BDL††	61700	1.3708	45700	0.7371
I-L-P200-C	.	66400	1.4752	49300	0.7952
I-L-P3000-A	0.063	55700	1.2375	40600	0.6548
I-L-P3000-B	.	56600	1.2575	41900	0.6758
I-L-P3000-C	.	63500	1.4108	46600	0.7516
I-L-P500-A	0.03	64600	1.4352	48000	0.7742
I-L-P500-B	BDL††	63300	1.4064	44800	0.7226
I-L-P500-C	.	63900	1.4197	48400	0.7806
I-L-PF1500-A	0.077	78800	1.7507	42000	0.6774
I-L-PF1500-B	0.131	82000	1.8218	45200	0.7290
I-L-PF1500-C	.	78900	1.7529	42000	0.6774
I-L-PF5/8-A	0.063	78900	1.7529	46700	0.7532
I-L-PF5/8-B	0.126	75000	1.6663	44400	0.7161
I-L-PF5/8-C	.	70900	1.5752	41500	0.6694

†† The computed REDOX values below the detection limit (0.03) were reassigned a value of 0.15.

APPENDIX C

Molar Formate, and Nitrate, Iron REDOX Ratio, Element Cu Wt%, and Appearance of Glass for Data Collected by R. F. Schumacher†

† Values in parentheses next to the first of each group represent the amount of formic acid (in µl) that was doped into the feed. The "as received" values for formate and nitrate are 15374 mg/L and 13371 mg/L, respectively for 36.66 total weight percent solids (i.e., not normalized). These can be found in LIMS database, numbers 200023806 and 200023807 for "SMRU 6396 SLURRY".

Table C-1. IDMS PX-4 Melter Feed at Three Differing Copper Concentrations (NB#E-57158-18, ADS#2-8289_)

NB#	ADS#	Copper (Wt%)	Formate (ppm)	Formate (M)	Nitrate (ppm)	Nitrate (M)	% Solids	$Fe^{2+}/\Sigma Fe$	Description
1	2		21180	0.471	28549	0.460			
2	3	0.281					46.00	0.015	Black
3	4	0.299					44.30	0.002	Black
4	5		24778	0.550	28275	0.456			
5	6	0.755					48.31	0.003	Black
6	7	0.486						0.011	Black
7	8		31547	0.701	29248	0.472			
8	9	1.673						0.023	Black
9	900	1.032					50.60	0.017	Black

Table C-2. IDMS PX-4 Melter Feed As Received Copper with Format Additions (NB#E-57158-20, ADS#2-834__)

NB#	ADS#	Copper (Wt%)	Formate (ppm)	Formate (M)	Nitrate (ppm)	Nitrate (M)	% Solids	$Fe^{2+}/\Sigma Fe$	Description
1	19		18123	0.403	26172	0.422			
2		0.290						0.016	Black
3		0.288						0.003	Black
4	20		21659	0.481	25123	0.405			
5		0.275						0.006	Black
6		0.276						0.004	Black
7	21		28908	0.642	25018	0.404			
8		0.264						0.003	Black
9		0.278						0.005	Black
10	22		35288	0.784	23575	0.380			
11		0.245						0.006	Black
12		0.273						0.008	Black
13	23		53071	1.179	23824	0.384			
14		0.277						0.012	Black
15		0.297						0.005	Black
16	24		86446	1.921	23619	0.381			
17		0.271						0.006	Black
18		0.204						0.014	Black

Table C-3. IDMS PX-4 Melter Feed at 2X Copper with Formate Additions
(NB#E-57158-22, ADS#2-838__)

NB#	ADS#	Copper (Wt%)	Formate (ppm)	Formate (M)	Nitrate (ppm)	Nitrate (M)	% Solids	$Fe^{2+}/\Sigma Fe$	Description
1	23		18913	0.420	27371	0.441			
2	10	0.296					37.80	0.003	Black
3	11	0.292					38.30	0.005	Black
4	24		37421	0.831	27749	0.448			
5	12	0.565					38.48	0.003	Black
6	13	0.812					38.97	0.003	Black
7	25		46643	1.036	26933	0.434			
8	14	0.584					39.24	0.007	Black
9	15	0.775					46.87	0.004	Black
10	26		70331	1.563	25822	0.416			
11	16	0.800					39.01	0.006	Black
12	18	0.597					39.11	0.010	Black
13	27		110672	2.459	24228	0.391			
14	19	0.560					39.14	0.012	Black
15	20	0.570					38.78	0.014	Black
16	28		120116	2.669	22699	0.366			
17	21	0.604					39.32	0.014	Black
18	22	0.574					39.58	0.014	Black

Table C-4. SGM-9 Plus Formic Acid
(NB#E-57158-24, ADS#842_)

NB#	ADS#	Copper (Wt%)	Formate (ppm)	Formate (M)	Nitrate (ppm)	Nitrate (M)	% Solids	$Fe^{2+}/\Sigma Fe$	Description
1	84280		73453	1.632	21464	0.346			
2	84281	0.298					63.20	0.283	Black
3	84282	0.286					64.00	0.332	Black
10	84283		127913	2.842	22507	0.363			
11	84284	0.498					48.40	0.457	Metal&Brown
12	84285	0.566					66.90	0.457	Metal&Brown
16	84286		192254	4.271	18302	0.295			
17	84287	0.464					78.40	0.446	≈Brown
18	84288	0.401					68.40	0.416	≈Brown

Table C-5. IDMS PX-4 SME Material Plus Copper Formate and Formic Acid
(NB#E-57158-18, ADS#2-8289_)

NB#	ADS#	Copper (Wt%)	Formate (ppm)	Formate (M)	Nitrate (ppm)	Nitrate (M)	% Solids	$Fe^{2+}/\Sigma Fe$	Description
W-1,2000	84335	0.666						0.088	Brown/Black
W-2	84336	0.581						0.065	Black
2A	339		149900	3.330	37000	0.597			
2B	340		112900	2.508	28900	0.466			
2C	341		115900	2.575	29100	0.469			
W-3,3000	84337	0.586						0.147	Brown/Black
W-4	84338	0.557						0.300	Brown
4A	342		156900	3.486	27200	0.439			
4B	343		156500	3.477	28200	0.455			
4C	344		166300	3.695	30000	0.484			

Table C-6. IDMS PX-4 SME Material Plus .14 Copper Formate and Formic Acid
(NB#E-57158-26, ADS#2-848__)

NB#	ADS#	Copper (Wt%)	Formate (ppm)	Formate (M)	Nitrate (ppm)	Nitrate (M)	% Solids	$Fe^{2+}/\Sigma Fe$	Description
As Rec 1a	61		13800	0.307	22200	0.358			
1b	62		14600	0.324	21800	0.352			
1c	63		13900	0.309	21800	0.352			
2	79	0.286						0.022	Black
3	80	0.294						0.008	Black
1000λ 4a	64		50900	1.131	24600	0.397			
4b	65		51600	1.146	22300	0.360			
4c	66		45800	1.018	21900	0.353			
5	81	0.555						0.071	Black
6	82	0.600						0.091	Black+Brown
6a	8522 0	0.538						0.113	Black+Brown
2000λ 7a	67		81300	1.806	21800	0.352			
7b	68		76800	1.706	20200	0.326			
7c	69		76100	1.691	20800	0.335			
8	83	0.547						0.145	Bl+Brn+Met
9	84	0.536						0.353	Black+Brown
3000λ 10a	70		106400	2.364	21200	0.342			
10b	71		106800	2.373	19500	0.315			
10c	72		107400	2.386	21700	0.350			
11	85	0.458						0.296	Black+Brown
12	86	0.578						0.291	Black+Brown
4000λ 13a	73		139500	3.099	19600	0.316			
13b	74		146500	3.255	21700	0.350			
13c	75		147000	3.266	20600	0.332			

NB#	ADS#	Copper (Wt%)	Formate (ppm)	Formate (M)	Nitrate (ppm)	Nitrate (M)	% Solids	$Fe^{2+}/\Sigma Fe$	Description
14	87	0.242						0.701	Brn+Bl+Met
15	88	0.575						0.499	Brn+Bl+Met
6000λ 16a			205600	4.568	19600	0.316			
16b			212400	4.719	21700	0.350			
16c			190800	4.239	18300	0.295			
17	89	0.549						0.505	Brn+Bl
18	90	0.332						0.519	Brn+Bl+Met

Table C-7. IDMS PX-4 SME Material Plus .17 Copper Formate and Formic Acid (NB#E-57158-27, ADS#2-857__)

NB#	ADS#	Copper (Wt%)	Formate (ppm)	Formate (M)	Nitrate (ppm)	Nitrate (M)	% Solids	$Fe^{2+}/\Sigma Fe$	Description
As Rec. 1a	10		14500	0.322	22700	0.366			
1b	11		14700	0.327	22500	0.363			
1c	12		14600	0.324	21800	0.352			
2	31	0.262						0.019	Blk Gray top
2A	45	0.219						0.002	Blk Gloss
3	32	0.256						0.018	Blk Gray Top
3A	46	0.288						0.004	Blk Gloss
250λ 4a	13		16300	0.362	14000	0.226			
4b	14		24800	0.551	21900	0.353			
4c	15		20600	0.458	18700	0.302			
5	33	0.622						0.004	Blk Gloss
6	34	1.147						0.070	Blk Gloss
500λ 7a	16		30400	0.675	19900	0.321			
7b	17		30200	0.671	19600	0.316			
7c	18		18600	0.413	12500	0.202			
8	35	0.688						0.023	Blk Gloss
9	36	0.537						0.009	Blk Gloss
750λ 10a	19		34900	0.775	18400	0.297			
10b	20		30700	0.682	16100	0.260			
10c	21		32300	0.718	16100	0.260			
11	37	0.681						0.068	Blk Gloss
12	38	0.689						0.077	Blk Gloss
1000λ 13a	22		44500	0.989	21300	0.344			
13b	23		41600	0.924	18900	0.305			
13c	24		40700	0.904	18500	0.298			
14	39	0.506						0.083	Blk +Brwn
15	40	0.607						0.135	Blk + Brwn
1500λ 16A	25		58300	1.295	18900	0.305			
16b	26		52300	1.162	19700	0.318			
16c	27		50100	1.113	17400	0.281			
17	41	0.698						0.230	Brwn + Blk
18	42	0.574						0.260	Brwn + Blk
0 Formic 19a	28		16900	0.375	21900	0.353			
Cu 19b	29		16800	0.373	21800	0.352			
19c	30		16100	0.358	21100	0.340			
20	43	0.652						0.018	Blk Gloss
21	44	0.651						0.009	Blk Gloss

APPENDIX D

Molar Formate and Nitrate, and Iron REDOX Ratio for DWPF Crucible Data Analyzed by W. G. Ramsey, et al.†

† Ramsey, W. G., Askew, N. M., and Schumacher, R. F. "Prediction of Copper Precipitation in the DWPF Melter from the Melter Feed Formate and Nitrate Content," WSRC-TR-92-385, Rev. 0, November 30, 1994.

Sample ID	$Fe^{2+}/\Sigma Fe$	Normalized Formate (M)†	Normalized Nitrate (M)†	Copper (Wt%) ††	Description
Batch 1-9A	0.25	1.38	0.41	0.34	Black Glass
Batch 1-9B	0.08	1.27	0.41		Black Glass
Batch 1-10A	0.23	1.27	0.37	0.31	Black Glass
Batch 1-10B	0.17	1.24	0.43		Black Glass
Batch 1-11A	0.23	0.74	0.4	0.39	Black Glass
Batch 1-11B	0.16	0.68	0.43		Black Glass
Batch 1-12A	0.17	0.72	0.41	0.38	Black Glass
Batch 1-12B	0.15	0.71	0.43		Black Glass
Batch 1-13A	0.21	0.9	0.4	0.39	Black Glass
Batch 1-13B	0.09	0.93	0.44		Black Glass
Batch 1-14A	0.25	0.88	0.39	0.4	Black Glass
Batch 1-14B	0.17	0.83	0.4		Black Glass
Batch 1-15A	0.11	0.87	0.39	0.45	Black Glass
Batch 1-15B	0.19	0.86	0.43		Black Glass
Batch 1-16A	0.27	0.7	0.3	0.44	Black Glass
Batch 1-16B	0.12	0.62	0.33		Black Glass
Batch 1-17A	0.21	1.07	0.39	0.5	Brown Glass
Batch 1-17B	0.1	1.1	0.43		Brown Glass
Batch 1-18A	0.04	1.06	0.38	0.48	Brown Glass
Batch 1-18B	0.16	1.1	0.42		Brown Glass
Batch 1-19A	0.29	1.05	0.37	0.53	Brown Glass
Batch 1-19B	0.14	1.03	0.41		Brown Glass
Batch 1-20A	0.21	1.09	0.4	0.5	Brown Glass
Batch 1-20B	0.1	1.06	0.41		Brown Glass
Batch 1-21A	0.16	0.72	0.37	0.51	Black Glass
Batch 1-21B	0.11	0.82	0.45		Black Glass
Batch 1-22A	0.17	0.69	0.36	0.49	Black Glass
Batch 1-22B	0.07	0.76	0.43		Black Glass

† The total solids for these analyses were assumed to be 45%; that is, no normalization was performed.

†† Only a single copper analysis was performed for each glass sample in this series.

APPENDIX E

Adjustments to Current REDOX data For Variation in Waste Loading

Analysis of Error in Measurement of Boron for SRTC Mobile Lab Boron Measurements for Batch 1 Simulants

The analysis below shows that the total variance estimate is 0.041465, which gives a standard deviation of 0.204. The 95% confidence interval for the mean is then 1.96*0.204=0.399. The mean B value measured was 7.955 wt% as B_2O_3.

As a percentage, the 95% confidence interval on B_2O_3 is then 0.399/7.955, or 5.02%.

Blk (SP)	Sub Blk (SP)	Analytical Block	B (wt%)	B_2O_3 (wt%)
1	1	1-1	2.6452	8.517
1	1	1-1	2.46	7.921
1	1	1-1	2.52	8.114
1	2	1-2	2.50	8.050
1	2	1-2	2.43	7.824
1	2	1-2	2.42	7.792
2	1	2-1	2.52	8.114
2	1	2-1	2.42	7.792
2	1	2-1	2.45	7.889
2	2	2-2	2.48	7.985
2	2	2-2	2.44	7.857
2	2	2-2	2.44	7.857
3	1	3-1	2.57	8.275
3	1	3-1	2.44	7.857
3	1	3-1	2.51	8.082
3	2	3-2	2.45	7.889
3	2	3-2	2.48	7.985
3	2	3-2	2.49	8.018
4	1	4-1	2.53	8.146
4	1	4-1	2.42	7.792
4	1	4-1	2.34	7.535
4	2	4-2	2.51	8.082
4	2	4-2	2.38	7.663
4	2	4-2	2.45	7.889

Response B_2O_3 (wt%)
Summary of Fit

RSquare	0.305087
RSquare Adj	0.001062
Root Mean Square Error	0.203631
Mean of Response	7.955192
Observations (or Sum Wgts)	24

Analysis of Variance

Source	DF	Sum of Squares	Mean Square	F Ratio
Model	7	0.29127229	0.041610	1.0035
Error	16	0.66344681	0.041465	Prob > F
C. Total	23	0.95471910		0.4642

Parameter Estimates

Term	Estimate	Std Error	t Ratio	Prob>|t|
Intercept	7.9551923	0.041566	191.39	<.0001
Analytical Block[1-1]	0.2289349	0.109973	2.08	0.0538
Analytical Block[1-2]	-0.066437	0.109973	-0.60	0.5542
Analytical Block[2-1]	-0.023505	0.109973	-0.21	0.8335
Analytical Block[2-2]	-0.055704	0.109973	-0.51	0.6194
Analytical Block[3-1]	0.1160237	0.109973	1.06	0.3071
Analytical Block[3-2]	0.0086937	0.109973	0.08	0.9380
Analytical Block[4-1]	-0.130835	0.109973	-1.19	0.2515

Expected Mean Squares

The Mean Square per row by the Variance Component per column

EMS	Intercept	Analytical Block&Random
Intercept	0	0
Analytical Block&Random	0	3

plus 1.0 times Residual Error Variance

Variance Component Estimates

Component	Var Comp Est	Percent of Total
Analytical Block&Random	0.000048	0.116
Residual	0.041465	99.884
Total	0.041514	100.000

These estimates based on equating Mean Squares to Expected Value.

Test Denominator Synthesis

Source	MS Den	DF Den	Denom MS Synthesis
Analytical Block&Random	0.04147	16	Residual

Tests wrt Random Effects

Source	SS	MS Num	DF Num	F Ratio	Prob > F
Analytical Block&Random	0.29127	0.04161	7	1.0035	0.4642

Error in Waste Loading from Error in Boron Measurement

$$loading_{waste} = 1 - \frac{X_{measured\ in\ glass}}{X_{frit}} = \frac{Y_{measured\ in\ glass}}{Y_{waste}};$$

waste loading expressed as value from 0-1.
where X = concentration of a frit-only species (B or Li) as oxide
Y = concentration of a waste only component (Fe) as oxide

The waste loading written in terms of symbols is:

$$L = 1 - \frac{X_G}{X_F}$$

The variance of L due to the variance of X_G is:

$$Var(L) = \frac{1}{X_F^2} Var(X_G)$$
$$= \frac{1}{X_F^2}\left(\frac{0.0502}{2}\right)^2 X_G^2$$

If X_G = 5.6 wt% and X_F ~ 8.0 wt%, then

$$L = 1 - \frac{0.056}{0.08} = 0.30\ (30\%\ waste\ loading)$$

$$Var(L) = \frac{1}{0.08^2}\left(\frac{0.0502}{2}\right)^2 0.056^2 = 0.00306$$

$$std.dev.\ \sigma = \sqrt{Var} = 0.0175$$

$$2\sigma = 0.035$$

$$uncertainty\ in\ L = \frac{0.035}{0.3} = 0.117 = 11.7\%$$

This is the uncertainty in the waste loading at 30% waste loading. For the other waste loadings, the uncertainties expressed as percentages are different, as shown below.

X_G	L	Uncertainty (%)
0.06	0.25	15%
0.056	0.30	11.7%
0.052	0.35	8.3%
0.048	0.40	7.3%

For different glass and frit concentrations, the error in the calculated waste loading will also be different. However, the value of 11.7 is near the average % uncertainty and so has been used throughout the analyses in this report since it is only an estimate.

Adjustment to Calculated SME Data for Samples with Measured Waste Loadings Outside the ±11.7% Interval Defined by the Boron Analysis Uncertainty

Samples of SRAT sludge were mixed with calculated amounts of frit and then vitrified. The amount of frit to use for a particular waste loading was based on analytical data for the SRAT sample that was taken from samples during the SRAT runs.

The samples of SRAT sludge received were sub-samples of the SRAT products. If these samples of SRAT sludges received were either enriched or depleted in undissolved solids, the ratios of soluble components (nitrate, formate, soluble oxalate) to undissolved components (undissolved oxalate, Mn oxalate, coal) would be changed. The change in these concentrations would then change the Electron Equivalents term since it is dependent on these concentrations.

The concentrations in the SRAT material actually received could be enriched in solids if the sub-sample was taken with some solids settled, whereas it could be depleted if the sample were somewhat decanted. These same biases could be introduced again when sub-sampling the sub-sample to make up each crucible melt.

The uncertainty of the boron analyses was estimated to be ±5%, which translated to an uncertainty of ±11.7% in the waste loading at a 30 wt% target loading. For glasses with calculated boron waste loadings greater than ±11.7% from the target, the following adjustments were made. These adjustments were used for the data reported as “Electron Equivalents, adjusted” and designated by ξ'.

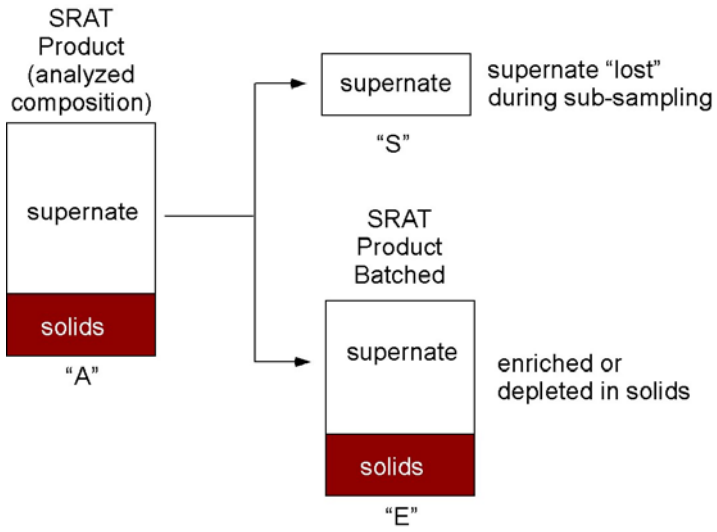

For glasses where the waste loading measured was outside the bounds considered above, the correction of the SRAT product batched was done to get to within an approximate 95% confidence band on the waste loading. I.e., if the target loading was 35%, the measured loading was 42.3%, then the SRAT product batched was adjusted so that the waste loading was 39.1%, which put it within the approximate 95% uncertainty interval. These intervals are shown below.

Target Waste Loading (%)	Waste Loading Approximate 95% Uncertainty Interval
25	22.1-27.9
30	26.5-33.5
35	30.9-39.1
40	35.3-44.7

The known quantities for the SRAT analyzed composition are:

t_A total solids fraction (wt%/100)
i_A undissolved solids fraction
s_A soluble solids fraction
$q_A = \frac{t_A - i_A}{1 - i_A}$ solids fraction in supernate
C_A calcine factor $= \frac{g\ oxides}{g\ solids}$

f_{Ai} sludge concentration of soluble anion (g/L)
g_{Ai} sludge concentration of undissolved anion
m_{Ai} sludge concentration of soluble cation

f_{Si} supernate concentration of soluble anion (g/L)
g_{Si} supernate concentration of undissolved anion
m_{Si} supernate concentration of soluble cation

W_A initial mass of sludge sample

If the sample is enriched in undissolved solids, then supernate was "lost". If the sample was depleted in undissolved solids, this situation can be mathematically treated as though supernate was added.

Mass of a soluble anion: $F_{Ai} = f_{Ai}\ W_A$
Mass of an undissolved anion: $G_{Ai} = g_{Ai}\ W_A$
Total undissolved solids: $I_A = i_A\ W_A$
Total soluble solids: $S_A = s_A\ W_A$

Total solids: $T_A = t_A W_A$

In the sample received (E):

Undissolved solids: $I_E = i_E W_E = i_A W_A$ (all undissolved to E)
Soluble solids: $S_E = s_E W_E = s_A W_A - s_S W_S$ (initial – supernate lost)

Supernate lost: $W_S = \frac{S_S}{s_S}$ and $s_S = q_A$

so then: $W_S = \frac{S_S}{q_A}$ ← S_S is then guessed to give make the calculated waste loading equal the measured waste loading (using equations to follow).

Solids mass in E: $T_E = S_E + I_E$
Total mass of E: $W_E = T_E + H_E$ where H_E is the mass of water in E
$H_E = H_A - H_S$
$H_S = W_S - S_S$

Undissolved anions in E: $g_{Ei} W_E = g_{Ai} W_A$

Soluble anions in E: $f_{Ei} W_E = \frac{S_E}{S_A} f_{Ai} W_A$

The fraction to E is the ratio of the mass of supernate lost to the mass of supernate in A.

Concentration of undissolved anion in E: $g_{Ei} = \frac{g_{Ai} W_A}{W_E}$

Concentration of soluble anion in E: $f_{Ei} = \frac{f_{Ai} W_A S_E}{W_E S_A}$

Note: the sum of the supernate solids in the original sample should equal the soluble solids content:

$$\frac{\sum_i f_{Si} + \sum_j g_{Sj} + \sum_k m_{Sk}}{\rho_S} \left(\frac{g}{kg} \right) \approx s_A = s_S$$

An estimated supernate calcine factor is then:

$$C_S = \frac{\sum_i f_{Si}\phi_i + \sum_j g_{Sj}\phi_j + \sum_k m_{Sk}}{\sum_i f_{Si} + \sum_j g_{Sj} + \sum_k m_{Sk}} = \frac{\textit{supernate solids as oxides}}{\textit{supernate solids}}$$

where Φ_i is the calcine factor for component i.

This equation assumes that the anions supply the oxygen to the cations to form the oxides. This estimate could also be done by the following equation where the cations are just converted to oxides:

$$C_S = \frac{\sum_k m_{Sk}\phi_k}{\sum_i f_{Si} + \sum_j g_{Sj} + \sum_k m_{Sk}}$$

The actual SRAT calcine factor (for E) is then:

$$C_E = C_S\, S_E + C_I\, I_E$$
$$C_I = C_A - C_S$$

The frit required for the actual SRAT sample E is:

$$F_E = \frac{W_E}{W_A} F_A$$

The actual waste loading is then:

$$L = \frac{C_E W_E}{C_E W_E + F_E}$$

By changing S_S, the L calculated above is compared to the actual L measured until they are equal.

APPENDIX F
Total Solids Versus Density Correlation Data

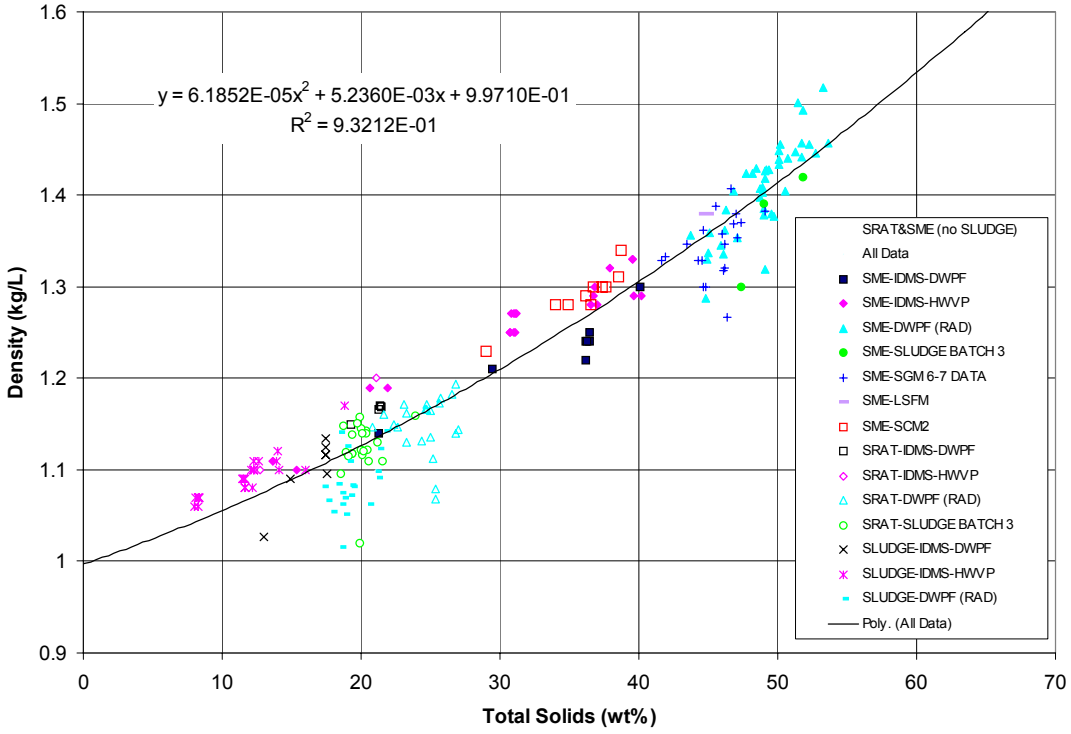

DWPF Data:

Source: spreadsheet from Carol Jantzen (from Pete Patel)

DWPF BATCH	Location	Total Solids (wt%)	Density (kg/L)	DWPF BATCH	Location	Total Solids (wt%)	Density (kg/L)
46	SME	52.70	1.445	avg 46-93	SRAT	22.37	1.150
49	SME	50.77	1.440	avg 94-207	SRAT	20.83	1.146
52	SME	49.11	1.418	SRAT 208	SRAT	26.84	1.193
60	SME	45.03	1.337	SRAT 209	SRAT	25.34	1.079
65	SME	48.99	1.385	SRAT 210	SRAT	21.62	1.161
70	SME	49.56	1.380	SRAT 211	SRAT	25.03	1.164
75	SME	50.58	1.405	SRAT 212	SRAT	22.60	1.147
80	SME	49.09	1.426	SRAT 213	SRAT	24.36	1.132
85	SME	48.97	1.378	SRAT 214	SRAT	24.62	1.166
90	SME	46.27	1.383	SRAT 215	SRAT	24.97	1.135
93	SME	43.70	1.356	SRAT 216	SRAT	26.85	1.140
96	SME	48.87	1.408	SRAT 217	SRAT	25.66	1.173
100	SME	48.74	1.407	SRAT 218	SRAT	25.17	1.113
110	SME	50.08	1.449	SRAT 219	SRAT	25.38	1.068
120	SME	48.95	1.403	SRAT 220	SRAT	26.96	1.144
130	SME	46.20	1.361	SRAT 221	SRAT	24.69	1.172
140	SME	51.75	1.457	SRAT 222	SRAT	23.31	1.162
150	SME	49.35	1.428	SRAT 223	SRAT	23.13	1.172
160	SME	52.26	1.456	SRAT 224	SRAT	23.25	1.131
170	SME	53.25	1.517	SRAT 225	SRAT	26.54	1.183
180	SME	53.60	1.457	SRAT 226	SRAT	24.74	1.166
190	SME	48.48	1.429	SRAT 227	SRAT	25.74	1.178

DWPF BATCH	Location	Total Solids (wt%)	Density (kg/L)	DWPF BATCH	Location	Total Solids (wt%)	Density (kg/L)
200	SME	49.14	1.428	SRAT 208	SLUDGE	21.15	1.092
207	SME	50.20	1.455	SRAT 209	SLUDGE	19.24	1.084
208	SME	51.43	1.501	SRAT 210	SLUDGE	18.43	1.142
209	SME	46.10	1.336	SRAT 211	SLUDGE	21.70	1.142
210	SME	44.95	1.330	SRAT 212	SLUDGE	21.30	1.123
211	SME	44.79	1.287	SRAT 213	SLUDGE	18.57	1.075
212	SME	49.08	1.319	SRAT 214	SLUDGE	18.75	1.069
213	SME	45.91	1.345	SRAT 215	SLUDGE	17.87	1.054
214	SME	47.11	1.353	SRAT 216	SLUDGE	19.22	1.072
215	SME	45.08	1.359	SRAT 217	SLUDGE	19.35	1.081
216	SME	48.17	1.424	SRAT 218	SLUDGE	17.57	1.066
217	SME	50.08	1.439	SRAT 219	SLUDGE	18.29	1.085
218	SME	48.73	1.398	SRAT 220	SLUDGE	19.13	1.110
219	SME	49.71	1.377	SRAT 221	SLUDGE	18.82	1.051
220	SME	51.75	1.442	SRAT 222	SLUDGE	21.08	1.098
221	SME	50.10	1.433	SRAT 223	SLUDGE	18.52	1.016
222	SME	51.85	1.492	SRAT 224	SLUDGE	17.28	1.082
223	SME	46.78	1.405	SRAT 225	SLUDGE	18.90	1.126
224	SME	47.70	1.424	SRAT 226	SLUDGE	18.56	1.063
225	SME	51.27	1.447	SRAT 227	SLUDGE	20.53	1.062

LSFM & SCM Melter Data:

Run	Location	Total Solids (wt%)	Density (kg/L)	Reference
LSFM-8	SME	44.80	1.38	DPST-83-915
SCM-2	SME	38.70	1.34	DPST-84-659
SCM-2	SME	36.20	1.29	
SCM-2	SME	37.40	1.30	
SCM-2	SME	37.60	1.30	
SCM-2	SME	36.70	1.30	
SCM-2	SME	38.50	1.31	
SCM-2	SME	36.50	1.28	
SCM-2	SME	34.90	1.28	
SCM-2	SME	29.00	1.23	
SCM-2	SME	34.00	1.28	

Scale Glass Melter (SGM) Data:

From WSRC-RP-97-34 Rev. 0			
Run	Sample Type	Total Solids (wt%)	Density (kg/L)
SGM6	SME	46.37	1.267
SGM6	SME	46.12	1.318
SGM6	SME	46.16	1.346
SGM6	SME	45.59	1.388
SGM6	SME	46.15	1.320
SGM6	SME	43.35	1.112
SGM6	SME	41.62	1.328
SGM6	SME	41.90	1.333
SGM6	SME	44.66	1.300
SGM7	SME	44.53	1.329
SGM7	SME	44.86	1.300
SGM7	SME	44.64	1.362
SGM7	SME	44.30	1.328
SGM7	SME	43.50	1.347
SGM7	SME	49.08	1.382
SGM7	SME	47.01	1.379
SGM7	SME	46.84	1.368
SGM7	SME	47.38	1.370
SGM7	SME	47.10	1.354
SGM7	SME	46.65	1.407
SGM7	SME	45.99	1.357

Integrated DWPF Melter System Data

Run	Location	Total Solids (wt%)	Density (kg/L)	Source
PX6	SLUDGE	12.98	1.03	PX6 Run Report WSRC-TR-94-0556, Rev. 0
PX6	SLUDGE	17.43	1.12	PX6 Run Report WSRC-TR-94-0556, Rev. 0
PX6	SLUDGE	17.43	1.13	PX6 Run Report WSRC-TR-94-0556, Rev. 0
PX6	SLUDGE	17.54	1.10	PX6 Run Report WSRC-TR-94-0556, Rev. 0
PX6	SLUDGE	17.46	1.12	PX6 Run Report WSRC-TR-94-0556, Rev. 0
PX6	SLUDGE	17.47	1.12	PX6 Run Report WSRC-TR-94-0556, Rev. 0
PX6	SRAT	19.30	1.15	PX6 Run Report WSRC-TR-94-0556, Rev. 0
PX6	SRAT	21.46	1.17	PX6 Run Report WSRC-TR-94-0556, Rev. 0
PX6	SRAT	21.30	1.17	PX6 Run Report WSRC-TR-94-0556, Rev. 0
PX6	SRAT	21.38	1.17	PX6 Run Report WSRC-TR-94-0556, Rev. 0
PX6	SME	36.14	1.22	PX6 Run Report WSRC-TR-94-0556, Rev. 0
PX6	SME	36.17	1.24	PX6 Run Report WSRC-TR-94-0556, Rev. 0
PX6	SME	36.44	1.25	PX6 Run Report WSRC-TR-94-0556, Rev. 0
PX6	SME	36.47	1.24	PX6 Run Report WSRC-TR-94-0556, Rev. 0
PX6	SME	36.31	1.24	PX6 Run Report WSRC-TR-94-0556, Rev. 0

Run	Location	Total Solids (wt%)	Density (kg/L)	Source
PX6	SME	40.05	1.30	PX6 Run Report WSRC-TR-94-0556, Rev. 0
HM1	SLUDGE	14.89	1.09	WSRC-RP-93-593, Rev. 0
BL3	SME	21.26	1.14	WSRC-RP-93-593, Rev. 0
HM1	SME	29.44	1.21	WSRC-RP-93-593, Rev. 0
HWVP2	SME	37.92	1.32	WSRC-TR-92-0403, Rev. 1
HWVP2	SME	20.67	1.19	WSRC-TR-92-0403, Rev. 1
HWVP2	SME	21.92	1.19	WSRC-TR-92-0403, Rev. 1
HWVP2	SRAT	21.11	1.20	WSRC-TR-92-0403, Rev. 1
HWVP2	SLUDGE	18.78	1.17	WSRC-TR-92-0403, Rev. 1
HWVP1	SME	13.61	1.11	WSRC-TR-92-0403, Rev. 1
HWVP1	SME	15.34	1.10	WSRC-TR-92-0403, Rev. 1
HWVP1	SRAT	12.74	1.10	WSRC-TR-92-0403, Rev. 1
HWVP1	SLUDGE	11.60	1.08	WSRC-TR-92-0403, Rev. 1
HWVP LAB SCALE	SLUDGE	12.24	1.11	WSRC-TR-92-0403, Rev. 1
HWVP	SLUDGE	8.23	1.07	WSRC-TR-92-0403, Rev. 1
HWVP	SLUDGE	8.12	1.07	WSRC-TR-92-0403, Rev. 1
HWVP	SLUDGE	8.34	1.07	WSRC-TR-92-0403, Rev. 1
HWVP	SLUDGE	8.24	1.07	WSRC-TR-92-0403, Rev. 1
HWVP	SLUDGE	8.24	1.06	WSRC-TR-92-0403, Rev. 1
HWVP	SLUDGE	7.98	1.06	WSRC-TR-92-0403, Rev. 1
HWVP	SLUDGE	11.59	1.09	WSRC-TR-92-0403, Rev. 1
HWVP	SLUDGE	11.51	1.09	WSRC-TR-92-0403, Rev. 1
HWVP	SLUDGE	11.47	1.09	WSRC-TR-92-0403, Rev. 1
HWVP	SLUDGE	11.61	1.09	WSRC-TR-92-0403, Rev. 1
HWVP	SLUDGE	14.03	1.12	WSRC-TR-92-0403, Rev. 1
HWVP	SLUDGE	13.92	1.11	WSRC-TR-92-0403, Rev. 1
HWVP	SLUDGE	14.05	1.10	WSRC-TR-92-0403, Rev. 1
HWVP	SLUDGE	16.03	1.10	WSRC-TR-92-0403, Rev. 1
HWVP	SLUDGE	11.60	1.08	WSRC-TR-92-0403, Rev. 1
HWVP	SLUDGE	12.14	1.08	WSRC-TR-92-0403, Rev. 1
HWVP	SLUDGE	12.28	1.10	WSRC-TR-92-0403, Rev. 1
HWVP	SLUDGE	12.27	1.10	WSRC-TR-92-0403, Rev. 1
HWVP	SLUDGE	12.24	1.10	WSRC-TR-92-0403, Rev. 1
HWVP	SLUDGE	12.13	1.10	WSRC-TR-92-0403, Rev. 1
HWVP	SLUDGE	12.66	1.11	WSRC-TR-92-0403, Rev. 1
HWVP	SME	31.02	1.25	WSRC-TR-92-0403, Rev. 1
HWVP	SME	30.77	1.25	WSRC-TR-92-0403, Rev. 1
HWVP	SME	30.76	1.25	WSRC-TR-92-0403, Rev. 1
HWVP	SME	31.07	1.25	WSRC-TR-92-0403, Rev. 1
HWVP	SME	31.04	1.27	WSRC-TR-92-0403, Rev. 1
HWVP	SME	30.81	1.27	WSRC-TR-92-0403, Rev. 1
HWVP	SME	31.05	1.27	WSRC-TR-92-0403, Rev. 1
HWVP	SME	31.14	1.27	WSRC-TR-92-0403, Rev. 1
HWVP	SME	39.54	1.33	WSRC-TR-92-0403, Rev. 1
HWVP	SME	39.58	1.33	WSRC-TR-92-0403, Rev. 1
HWVP	SME	39.63	1.29	WSRC-TR-92-0403, Rev. 1
HWVP	SME	40.22	1.29	WSRC-TR-92-0403, Rev. 1
HWVP	SME	36.56	1.28	WSRC-TR-92-0403, Rev. 1
HWVP	SME	36.85	1.30	WSRC-TR-92-0403, Rev. 1
HWVP	SME	36.97	1.28	WSRC-TR-92-0403, Rev. 1
HWVP	SME	36.75	1.29	WSRC-TR-92-0403, Rev. 1

Sludge Batch 3 Studies SRTC Data

Run	Location	Total Solids (wt%)	Density (kg/L)
SB3-21	SME	51.8	1.420
SB3-22	SME	49	1.390
SB3-23	SME	47.4	1.300
SB3-1	SRAT	18.5	1.095
SB3-2	SRAT	18.7	1.148
SB3-3	SRAT	19.95	1.158
SB3-4	SRAT	18.9	1.119
SB3-5	SRAT	23.95	1.159
SB3-6	SRAT	21.55	1.109
SB3-7	SRAT	19.4	1.118
SB3-8	SRAT	19.35	1.117
SB3-9	SRAT	20.11	1.116
SB3-10	SRAT	19.98	1.122
SB3-11	SRAT	20.36	1.143
SB3-12	SRAT	20.52	1.110
SB3-13	SRAT	20.45	1.122
SB3-14	SRAT	20	1.145
SB3-15	SRAT	20.35	1.140
SB3-16	SRAT	19.7	1.151
SB3-17	SRAT	19.4	1.138
SB3-18	SRAT	19.05	1.115
SB3-19	SRAT	21.2	1.130
SB3-20	SRAT	20.1	1.140
SB3-23	SRAT	19.9	1.020
SB3-24	SRAT	20.2	1.120

REFERENCES

1 B.A. Hamm, R.E. Eibling, M.A. Ebra, T. Motyka, and H.D. Martin, **"High-Level Insoluble Waste Preparation for Vitrification,"** Sci. Basis for Nuclear Waste Management, VIII, C. M. Jantzen, et al. (Eds.), Materials Research Society, Pittsburgh, PA 793-799 (1985).

2 H.D. Schreiber, and A.L. Hockman, **"Redox Chemistry in Candidate Glasses for Nuclear Waste Immobilization,"** Journal of the American Ceramic Society , Vol. 70, No. 8, pp. 591-594 (1987).

3 D.S. Goldman and D.W. Brite, **"Redox Characterization of Simulated Nuclear Waste Glass,"** *J. Am. Ceram. Soc.*, **69** [5], pp. 411-413, (1986).

4 V. Jain, **"Redox Forecasting in the West Valley Vitrification System,"** Ceramic Transactions, Vol. 29, Advances in the Fusion and Processing of Glass, eds., A. K. Varsheya, D. F. Bickford, and P. P. Bihuniak, pp. 523-533, (1983).

5 A.S. Choi, **"Maximum Total Organic Carbon Limit for DWPF Melter Feed,"** WSRC-TR-95-0119, Rev. 0 (March 13, 1995).

6 D.F. Bickford, and A.S. Choi, **"Control of High Level Radioactive Waste-Glass Melter-Part 5: Modeling of Complex Redox Effects,"** Proceedings of the Fifth International Symposium on Ceramics in Nuclear and Hazardous Waste Management (Eds. G.G. Wicks, D.F. Bickford, and L.R. Bunnell, Ceramic Transactions Vol. 23, American Ceramic Society, Westerville, OH, 267-279 (1991).

7 C.M. Jantzen, J.B. Pickett, K.G. Brown, T.B. Edwards, D.C. Beam, **"Process/Product Models for the Defense Waste Processing Facility (DWPF): Part I. Predicting Glass Durability from Composition Using a Thermodynamic Hydration Energy Reaction MOdel (THERMO),"** US DOE Report WSRC-TR-93-0672, 464p. (September, 1995).

8 C.M. Jantzen and M.J. Plodinec, **"Composition and Redox Control of Waste Glasses: Recommendation for Process Control Limit,"** U.S. DOE Report DPST-86-773, E.I. duPont deNemours & Co., Savannah River Laboratory, Aiken, SC (November, 1986).

9 M.J. Plodinec, **"Foaming During Vitrification of SRP Waste,"** U.S. DOE Report DPST-86-213, E.I. duPont deNemours & Co., Savannah River Laboratory, Aiken, SC (January, 1986).

10 L.M. Lee and L.L. Kilpatrick, **"A Precipitation Process for Supernate Decontamination,"** USERDA Report DP-1639, E. I. du Pont de Nemours & Co., Inc., Savannah River Laboratory (1982).

11 S.R. Young, J. Morrison, S.L. Adamson, M.A. Baich, J.C. Marek, and R.A. Jacobs, **"Campaign Report: Precipitate Hydrolysis Experimental Facility, Runs 25-36,"** WSRC-RP-89-538, rev. 0 (February 2, 1990).

12 D.F. Bickford and C.M. Jantzen, **"Inhibitor Limits for Washed Precipitate Based on Glass Quality and Solubility Limits,"** DPST-86-546 (1986).

13 C.W. Hsu, **"Defense Waste Processing Facility Nitric Acid Requirement for Treating Sludge,"** U.S. DOE Report WSRC-RP-92-1056, Savannah River Technology Center, Westinghouse Savannah River Co., Aiken, SC (September, 1992).

14 J.C. Marek and R.E. Eibling, **"Draft Calculational Algorithms for Nitric Acid Flowsheet,"** SRTC-PTD-92-0050 (September 29, 1992).

15 K.G. Brown, C.M. Jantzen, and J.B. Pickett, **"The Effects of Formate and Nitrate on Reduction/Oxidation (Redox) Process Control for the Defense Waste Processing Facility (DWPF),"** WSRC-RP-97-34 (February, 1997).

16 C.M. Jantzen, R.F. Swingle, F.G. Smith, **"Impact of Tank 19 Zeolite Mound on DWPF Vitrification of SB3,"** U.S. DOE Report WSRC-TR-2002-00288, Westinghouse Savannah River Co., Aiken, SC (April, 2003).

17 C.C. Herman, T.L. Fellinger, N.E. Bibler, and D.C. Koopman, "**Scoping SRAT Runs with Simulated Sludge Batch 3**", SRT-GPD-2002-00044 (April 12, 2002).

18 M.G. Bronikowski, M.C. Thompson, F.R. Graham, T.L. Fellinger, W.R. Wilmarth, and D.T. Hobbs, "**Technical Task and Quality Assurance Plan for Assessing Downstream Effects of Plutonium/Gadolinium in Sludge Washing and SRAT**", WSRC-RP-2002-00178 (March 6, 2002).

19 N.E. Bibler, D.K. Peeler, and T.B. Edwards**, "An Assessment of the Impacts of Adding Am/Cm and Pu/Gd Waste Streams to Sludge Batch 3 (SB3) on DWPF H2 Generation Rates and Glass Properties",** WSRC-TR-2002-00145 (March 22, 2002).

20 A.Q. Goslen, **"Estimated Sodium Oxalate in the Tank Farm"** (March 22, 1984).

21 Fowler, J.R., **"Estimate of Maximum Amount of Reducing Agents and Sand in SRP Waste for DWPF TDS,"** (September 9, 1980).

22 J.A. Stone, J.A. Kelley, T.S. McMillan**, "Sampling and Analyses of SRP High-Level Waste Sludges,"** DP-1399 (August, 1976).

23 W.G. Ramsey, C.M. Jantzen, and D.F. Bickford, **"Redox Analyses of SRS Melter**

Feed Slurry; Interactions Between Formate, Nitrate, and Phenol Based Dopants," Proceedings of the 5th International Symposium on Ceramics in Nuclear Waste Management, G.G. Wicks, D.F. Bickford, and R. Bunnell (Eds.), American Ceramic Society, Westerville, OH, 259-266 (1991).

24 W.G. Ramsey, T.D. Taylor, K.M. Wiemers, C.M. Jantzen, N.D. Hutson, and D.F. Bickford, **"Effects of Formate and Nitrate Content on Savannah River and Hanford Waste Glass Redox"** Proceedings of the Advances in the Fusion and Processing of Glass, III, New Orleans, LA, D.F. Bickford, et.al. (Eds.) Am. Ceramic Society, Westerville, OH, 535-543 (1993).

25 W.G. Ramsey, N.M. Askew, and R.F. Schumacher, **"Prediction of Copper Precipitation in the DWPF Melter from the Melter Feed Formate and Nitrate Content,"** WSRC-TR-92-385, Rev. 0 (November 30, 1994).

26 W.G. Ramsey, and R.F. Schumacher, **"Effects of Formate and Nitrate Concentration on Waste Glass Redox at High Copper Concentration."** WSRC-TR-92-484, October 23, 1992.

27 E.W. Baumann, **"Colorimetric Determination of Iron(II) and Iron(III) in Glass,"** Analyst, 117, 913-916 (1992).

28 D.R. Best, **"Determining Fe+2/Fe+3 and Fe+2/Fetotal Using the HP8452A Diode Array Spectrometer,"** Procedure Manual L28, Procedure 1.8 Rev. 2 (March 14, 2001).

29 W.H. Manring, and G.M. Diken, **"A Practical Approach to Evaluating Redox Phenomena Involved in the Melting-Fining of Soda Lime Glasses,"** J. Non-Crystalline Solids, **38&39**, pp. 813-818, 1980.

30 D.S. Candela, **"Evolution of Aqueous Vapor from Silicate Melts: Effect of Oxygen Fugacity,"** Geochim. Cosmochim. Acta, **50**, 1205-1211, 1986.

31 A.S. Choi, **"Validation of DWPF Melter Off-Gas Combustion Model,"** U.S. DOE Report WSRC-TR-2000-00100, Westinghouse Savannah River Co., Aiken, SC (June 23, 2000).

32 A.S. Choi, **"Prediction of Melter Off-Gas Explosiveness,"** U.S. DOE Report WSRC-TR-90-00346, Westinghouse Savannah River Co., Aiken, SC (January 22, 1992).

33 C.C. Herman, D.C. Koopman, N.E. Bibler, D.R. Best, and M.F. Williman, **"SRAT Processing of Sludge Batch 3 Simulant to Evaluate Impacts of H-Canyon Slurry Containing Precipitated Pu and Gd,"** U.S. DOE Report WSRC-TR-2002-00322, Westinghouse Savannah River Co., Aiken, SC (July 25, 2002).

34 C.C. Herman, T.B. Edwards, D.C. Koopman, D.R. Best, J.C. George, M.F. Williams, **"Data Summary from Sludge Batch 3 Simulant SRAT Runs to Evaluate Impacts of Noble Metals Mass and Coal Size, Mass, and Treatment,"** SRT-GPD-2002-00121, Rev. 0 (November 1, 2002).

35 C.C. Herman, D.C. Koopman, D.R. Best, M.F. Williams**, "Data Summary from SRAT Runs SB3-19 to SB3-24 to Evaluate Sodium Oxalate Addition Levels and SME Processing,"** SRT-GPD-2002-00200, Rev. 0 (January 27, 2003).

36 C.C. Herman, D.C. Koopman, D.R. Best, and M.F. Williams, **"Sludge Batch 3 Simulant Flowsheet Studies: Phase I SRAT Results,"** U.S. DOE Report WSRC-TR-2003-00088 (March 20, 2003).

37 D.C. Koopman and C.C. Herman**, "Analysis of Initial SB3 Slurry Mix Evaporator Simulations,"** SRTC-GPD-2003-00019 (March 3, 2003).

38 N.E. Bibler, D.K. Peeler, T.B. Edwards, **"An Assessment of the Impacts of Adding Am/Cm and Pu/Gd Waste Streams to Sludge Batch 3 (SB3) on DWPF H_2 Generation,"** U.S. DOE Report WSRC-TR-2002-00145 (March 22, 2002).

39 K.G. Brown, **"Estimating Waste Loading from DWPF SME Analytical Results for Sludge-Only Operation,"** SRTC-GPD-2002-00004 (January 9, 2002).

40 H.S. Waff, **"The Structural Role of Ferric Iron in Silicate Melts,"** Canadian Mineralogist, 15, 198-199 (1977).

41 W.D. Bancroft and R.L. Nugent, **"The Manganese Equilibrium in Glasses,"** J. Phys. Chem. 33, 481-497 (1929).

42 H.D. Schreiber, P.G. Leonhard, R.G. Nofsinger, M.W. Henning, C.W. Schreiber, and S.J. Kozak, **"Oxidation-Reduction Chemistry of NonMetals in a Reference Borosilicate Melt,"** Advances in the Fusion of Glass, D.F. Bickford, W.E. Horsfall, F.E. Wooley, E.N. Boulos, J.N. Lingscheit, F. Harding, F. Olix, W.C. LaCourse, and L.D. Pye (Eds.), Am. Ceram. Soc., Westerville, OH, 29.1-19.14 (1988).

43 C.M. Jantzen, N.E. Bibler, D.C. Beam, and M.A. Pickett, **"Characterization of the Defense Waste Processing Facility (DWPF) Environmental Assessment (EA) Glass Standard Reference Material,"** U.S. DOE Report WSRC-TR-92-346, Rev.1, 92p (February, 1993).

44 C.M. Jantzen, **"Redox Studies and Modeling for DWPF Sludge Batch 3,"** U.S. DOE Reprot WSRC-RP-2002-00341, Rev. 0 (August 2, 2002).

45 D.H.Lindsay, **"Experimental Studies of Oxide Minerals,"** Reviews in Mineralogy, V. 3, p.L-61-L-88 (November, 1976).

46 A.S. Choi, **"Summary of Campaigns SGM-9 and SGM-10 of the DWPF Scale Glass Melter,"** U.S. DOE Report DPST-88-626, E.I. duPont deNemours & Co., Aiken, SC (December 15, 1988).

47 A. Muan and E.F. Osborn**, "Phase Equilibria Among Oxides in Steelmaking,"** Addison-Wesley Publishing Company, Inc., Reading, MA, 236pp. (1965).

48 J.A. Ritter, N.D. Hutson, M.E. Smith, M.K. Andrews, D.H. Miller, and J.R. Zamecnik, **"Integrated DWPF Melter System Campaign Report Coupled Feed Operation,"** U.S. DOE Report WSRC-TR-90-131, Rev. 0, Westinghouse Savannah River Co., Aiken, SC (March 1, 1990).

49 D.C. Koopman, C.C. Herman, N.E. Bibler, **"Sludge Batch 3 Preliminary Acid Requirements Studies with Tank 8 Simulant,**" U.S. DOE Report WSRC-TR-2003-00041, Westinghouse Savannah River Co., Aiken, SC (January 31, 2003).

50 P.A. Smith, J.D. Vienna, and M.D. Merz, **"NCAW Feed Chemistry: Effect of Starting Chemistry on Melter Offgas and Iron Redox,"** U.S. DOE Report PNL-10517, Pacific Northwest Laboratory, Richland, Washington (March 1995).

51 D.R. Jones, W.C. Janshiki, and D.S. Goldman, **"Spectroscopic Determination of Reduced and Total Iron with 1,10-Phenalthroline,"** Anal. Chem., 53, 923-924 (1981).

52 R.W. Goles, R.K. Nakaoka, **"Hanford Waste Vitrification Program Pilot-Scale Ceramic Test Melter 23,"** U.S. DOE Report PNL-7142, UC-721, Pacific Northwest Laboratory, Richland, Washington (1990).

53 K. D. Weimers, **"The Effect of HWVP Feed Nitrate and Carbonate Content on Glass REDOX Adjustment,"** U.S. DOE Report, PNNL-11044, Pacific Northwest National Laboratory, Richland, Washington (March 1996).

54 N. D. Hutson, **"Integrated DWPF Melter System Campaign Report: Hanford Waste Vitrification Plant (HWVP) Process Demonstration,"** U.S. DOE Report WSRC-TR-92-0403, Rev. 1, Westinghouse Savannah River Co., Aiken, SC (June 11, 1993).

55 Bowan, B. W. **"A Redox Forecasting Correlation Developed Using a New One-Tenth Scale Test Melter for Vitrifying Simulated West Valley High-Level Radioactive Wastes,"** M. S. Thesis, Alfred University, Alfred, New York, 1990.

56 P.D. Guidotti, K.R. Crow, A.F. Wiesman, M.R. Baron, A.M. Wehner, J.A. Grifin, J.A. Shuford, J. M. O'Rouke, **"Summary of Campaigns SGM-6 and SGM-7 of the DWPF Scale Glass Melter,"** U.S.DOE Report DPST-87-532, E. I. du Pont de Nemours & Co., Inc. Savannah River Laboratory, Aiken, SC (September 11, 1987).

57 C.M. Jantzen, **"Verification and Standardization of Glass Redox Measurement for DWPF,"** U.S. DOE Report DPST- 89-222, E.I. du Pont de Nemours & Co., Savannah River Laboratory, Aiken, SC (1989).

58 R.F. Schumacher, **"Copper Solubility in DWPF, Batch 1 Waste Glasses- Update Report,"** U.S. DOE Report WSRC-TR-92-449, Rev. 0, Savannah River Technology Center, Westinghouse Savannah River Co., Aiken, SC (September 18, 1992).

DISTRIBUTION:

L. M. Papouchado, 773-A
E. W. Holtzscheiter, 773-A
D.A. Crowley, 773-A
S.L. Marra, 999-W
J. R. Harbour, 773-42A
T.L. Fellinger, 773-A
N.E. Bibler, 773-A
R. C. Tuckfield, 773-42A
T.B. Edwards, 773-42A
D. F. Bickford, 773-A
A. S. Choi, 773-42A
R. F. Schumacher, 999-W
W. E. Daniel, 999-W
M. E. Smith, 773-42A
D. K. Peeler, 999-W
D. P. Lambert, 773-A
A. D. Cozzi, 999-W
J. F. Ortaldo, 704-S
R. E. Edwards, Jr., 703-H
H. H. Elder, 703-H
M.S. Miller, 704-S
J.N. Chen, 704-27S
J. E. Occhipinti, 704-27S
M.A. Rios-Armstrong, 704-27S
J. F. Sproull, 704-30S
D.C. Iverson, 704-30S
STI, 703-43A (4)